# SECTION 2 : DETAILED STUDY OF THE LANDSLIDES AT THE JUNCTION OF SAI SHA ROAD AND TAI MONG TSAI ROAD IN JUNE 1998

**Fugro Scott Wilson Joint Venture**

**This report was originally produced in November 1999**
**as GEO Landslide Study Report No. LSR 13/99**

# FOREWORD

This report presents the findings of a detailed study of a series of landslides that occurred between 9 June 1998 and 24 June 1998 on a temporary cut slope in a Landslip Preventive Measures (LPM) construction site at the junction of Sai Sha Road and Tai Mong Tsai Road, Sai Kung. Debris from the landslides was contained largely within the construction site boundary. No one was injured in the landslides.

The key objectives of the detailed study were to document the facts about the landslides, present relevant background information and establish the probable causes of the failures. The scope of the study was generally limited to site reconnaissance, ground investigation, desk study and analysis. Recommendations for follow-up actions are reported separately.

The report was prepared as part of the 1998 Landslide Investigation Consultancy (LIC), for the Geotechnical Engineering Office (GEO), Civil Engineering Department (CED) under Agreement No. CE 74/97. This is one of a series of reports produced during the consultancy by Fugro Scott Wilson Joint Venture (FSW). The report was written by Mr S Sum and reviewed by Mr Y C Koo. The assistance of the GEO in the preparation of the report is gratefully acknowledged.

Y C Koo
Project Director/Fugro Scott Wilson Joint Venture

CONTENTS

## 1. INTRODUCTION

Between 4:00 p.m. and 6:00 p.m. of 9 June 1998, a landslide occurred on the northern portion of a temporary cut slope within an active construction site, during the course of slope upgrading works under the Landslip Preventive Measures (LPM) Programme, at the junction of Sai Sha Road and Tai Mong Tsai Road (Plate 1 and Figure 1). This landslide involved the full cut slope height of about 18 m. On 10 June 1998, between 4:00 p.m. and 6:00 p.m. a second landslide occurred at the lowest 6 m of the southern portion of the cut slope. This southern landslide extended progressively upslope to almost the full cut slope height of 24 m by 29 June 1998 (Plate 2). Debris from the landslides was deposited at the toe of the slope within the construction site and most of the displaced material remained on the slope. There were no injuries or fatalities as a result of the landslides.

Following the landslides, Fugro Scott Wilson Joint Venture (FSW), the 1998 Landslide Investigation Consultants, commenced a detailed study of the failure for the Geotechnical Engineering Office (GEO). The principal objectives of the detailed study were to document the landslide, present relevant background information and establish the probable causes of the failure.

This report presents the findings of the study which comprised the following key tasks:

(a) desk study, including a review of relevant documentary records relating to the history of the site, examination of aerial photographs and topographic maps of the site,

(b) discussion with the parties responsible for the design and supervision of the LPM works,

(c) topographic survey, geological mapping and detailed observations and measurements at the landslide site,

(d) limited ground investigation field works and laboratory testing,

(e) analysis of rainfall data,

(f) slope stability analysis of the sections that failed, and

(g) diagnosis of the probable causes of the landslides.

## 2. THE SITE

### 2.1 Site Description

The landslides occurred at a temporary soil cut slope within an active LPM construction site for the upgrading of cut slope No. 8SW-A/C8, which was registered in the 1977/78 Catalogue of Slopes.

The toe of the temporary cut slope in the northern and southern portions of the site is at about 13 mPD and 10 mPD respectively. Sai Sha Road is along the eastern boundary of the site (Figure 2). The ground above the temporary cut slope is vegetated quasi-natural terrain, with trees and shrubs, at an average gradient of about 10° to the horizontal. No prominent surface hydrogeological features, such as natural drainage lines, were noted at the crest of the cut slope. A cross section showing the ground profile of the site is presented in Figure 3.

The temporary cut slope was formed by removing a toe berm and excavating into the original cut slope (Section 2.2.5) to provide space for the construction of a gravity retaining wall along the slope toe followed by backfilling above the wall. Slope excavation commenced in March 1998. By the end of April 1998, the chunam surface provided on the southern portion of the slope had been removed.

In the area of the northern landslide, the temporary cut before the failure was about 18 m in height, with the lower 12 m sloping at a gradient of about 50° to the horizontal and the upper 6 m at about 30° to the horizontal. At the time of the failure, 24 nos. temporary soil nails had been installed within the ground that failed (Figure 2).

In the area of the southern landslide, the temporary cut before the failure comprised 3 batters with a total height of about 24 m and an overall gradient of about 42° to the horizontal. Prior to the excavation of the temporary cut, 28 nos. permanent and 80 nos. temporary soil nails were installed within the ground that subsequently failed. The layout of the soil nails is shown in Figure 2.

Prior to the failures, construction of the crest drainage channel was in progress. About 20 m of the crest channel had been completed in the northern portion of the temporary cut where the landslide occurred. No surface drainage channels were provided on the southern portion of the temporary cut at the time of the failure (Figure 2).

## 2.2 Site History and Previous Studies

### 2.2.1 Site Development History

The site development history has been determined from a review of the available aerial photographs and relevant documentation.

The earliest aerial photographs of the site taken between 1924 and 1964 show that the site was a natural hillside with trees and shrubs. The hillside dips to the south-eastern direction towards the shoreline (Figure 3). Tai Mong Tsai Road, located about 50 m south-east of the site, was constructed between 1956 and 1963 by cutting into the toe of the natural hillside along the shoreline. Cut slope No. 8SW-A/C8 was formed between 1964 and 1972 during the construction of Sai Sha Road. There is no evidence of any changes of the cut slope geometry until 1995 when major landslides occurred on the slope (Section 2.2.3).

Prior to the 1995 landslides, the cut slope was covered with chunam. Patches of the chunam surface with a dark tone, which might indicate moisture zones on the slope, could be seen frequently in aerial photographs taken since 1973. Aerial photographs taken in 1981, 1983, 1984, 1986 and 1993 and site photographs taken in 1992 and 1995 show that many

areas of the chunam surface on the slope were resurfaced. It is not certain if these were related to local erosion or instabilities of the slope.

### 2.2.2 Previous Studies

The first recorded inspection on cut slope No. 8SW-A/C8 was carried out in March 1978 by consultants engaged by the Government to prepare the 1977/78 Catalogue of Slopes (Binnie & Partners, 1978). At the time of the inspection, no signs of seepage or distress were noted.

In September 1992, the Design Division of GEO carried out a Stage 1 Study on the cut slope (GEO, 1992). No signs of seepage or distress were noted and no emergency actions were considered necessary.

In mid-1992, the GEO initiated a consultancy agreement entitled "Systematic Inspection of Features in the Territory" (SIFT), to search systematically for features not included in the 1977/78 Catalogue of Slopes and to update information on previously registered features, by studying aerial photographs together with limited site inspections. In March 1994, the SIFT study assigned the cut slope to Class C1, i.e. a slope "formed or substantially modified before 30 June 1978".

In January 1996, the cut slope was inspected by consultants appointed by the Highways Department (HyD) under the project entitled "Roadside Slope Inventory and Inspections". The record of the Engineer Inspection stated that there were past failures on the slope and noted that "routine maintenance not carried out satisfactorily because surface drainage systems not clear, drainage channels cracked/damaged, rigid surface cover cracked/damaged, detrimental vegetation not cleared and weepholes blocked" (FMR, 1996). The Engineer Inspection recommended a stability assessment be undertaken. No signs of seepage were noted during the inspection.

The GEO commenced a consultancy agreement, entitled "Systematic Identification and Registration of Slopes in the Territory" (SIRST), in July 1994 to update the 1977/78 Catalogue of Slopes and to prepare the New Catalogue of Slopes. The GEO's consultants for the SIRST project inspected the slope in February 1997. The SIRST report recorded no signs of seepage on the slope.

### 2.2.3 Past Landslides

During torrential rain associated with Typhoon Helen on 14 August 1995, landslides and significant cracking of the chunam occurred on cut slope No. 8SW-A/C8. The locations of the instabilities are shown in Figure 4. The total volume of the landslide debris was estimated by the GEO (1995) to be about 2,000 $m^3$.

In the northern portion of the cut slope, two landslides occurred. The landslide at about the mid-length of the northern portion measured about 15 m by 15 m on plan and involved the full cut slope height of about 16 m. The other landslide at the north end of the cut slope had a dimension of about 8 m by 8 m on plan and also involved the full cut slope

height of about 10 m. The failure debris buried the footpath along the slope toe and blocked one lane of Sai Sha Road. The chunam surfaces over the ground immediately adjacent to these landslides were severely cracked, broken into slabs and locally severely crushed. This possibly indicates that the slope at these areas was also close to failure (Plate 3 and Figure 4).

The travel angles of the debris of the 1995 landslides, corresponding to the inclination of the line joining the distal end of the debris and the crest of the landslide, were estimated to be about 34° to 38°. These are consistent with those generally observed in rain-induced landslides on cut slopes in Hong Kong (Wong & Ho, 1996).

In the southern portion of the cut slope, the lowest batter, which had a height of about 7.5 m and a gradient of about 50° to the horizontal, subsided and bulged out of the slope.

Based on the recommendations of the GEO, the contractor of HyD carried out urgent repair works which included removal of debris, trimming back of the landslide scars in the northern portion of the slope, provision of reinforced shotcrete surface to the trimmed area and construction of a temporary rockfill berm along the toe of the entire cut slope (Plate 4). Following the completion of the urgent repair works, HyD installed 30 settlement monitoring stations on the slope and monitored from February 1996 to May 1997. The monitoring results did not show any trend of significant ground movements.

### 2.2.4 Design of the LPM Works

Following the major failures in 1995, the cut slope was included in the 1996/97 LPM Programme. A detailed geotechnical assessment, including desk study, ground investigation, stability analysis and design of slope upgrading works, was carried out by the Design Division of the GEO (GEO, 1997). The ground investigation comprised 11 drillholes, 10 trial pits and 4 chunam strips and was carried out in 1996 and 1997 (Figure 5). Eighteen piezometers with Halcrow buckets were installed in the drillholes and monitoring was carried out from October 1996 to July 1997.

The ground investigation revealed that the cut slope comprised principally completely decomposed tuff (CDT). Closely-spaced, sub-vertical, curvilinear relict joints infilled with a soft black, often slickensided, clayey mineral were noted in trial pits and drillholes. In trial pits excavated on the subsided lowest batter of the southern slope, opened sub-vertical relict joints with clay and manganese infillings were observed. Significant rises in piezometric levels of 4.5 m to 8 m and 1.5 m to 2.5 m were recorded in piezometers located at the crest and toe of the cut slope respectively during the heavy rainstorm of 2 July 1997.

Laboratory tests were conducted on undisturbed Mazier and block samples of CDT. The tests included classification tests and index tests, direct shear tests and single and multistage consolidated undrained triaxial compression tests with pore water pressure measurement. A summary of the classification and index test results is presented in Table 1. The triaxial compression test results are presented in the form of $p'$-$q$ plot in Figure 19. Based on these results, general shear strength parameters of $c' = 4$ kPa, $\phi' = 36°$ were adopted for the CDT in the design of the upgrading works.

The geotechnical assessment concluded that the high groundwater level and the presence of weak sub-vertical relict joints could have contributed to the 1995 landslides. The assessment further stated that "these (sub-vertical relict) joints could have also contributed to the 1995 landslip by opening up when the stability of the slope became marginal, thereby cracking chunam surface, and hence increasing infiltration and creating water-filled sub-vertical fissures".

The effect of the sub-vertical relict joints on the stability of the slope was assessed by assuming that a portion of the critical slip surface would pass through a weak and persistent sub-vertical relict joint (about 9 m) with an assumed shear strength of $c' = 0$, $\phi' = 29°$. This assessment concluded that the effect of the sub-vertical joints on the upgraded slope was "insignificant".

The proposed LPM works included the construction of a reinforced concrete retaining wall at the slope toe together with backfilling with rockfill behind the wall up to about two third of the slope height. Permanent soil nails, with 400 mm square concrete nail heads, were to be provided on the upper third of the slope. Raking drains (15 m long) at 5 m horizontal spacing were to be installed along the slope toe. A typical section showing details of the proposed LPM works and the groundwater profile adopted in the design is presented in Figure 6.

To provide space for the construction of the retaining wall, a temporary cut, to be reinforced by means of temporary soil nails with 150 mm square steel plate nail heads, was included in the LPM design (Figures 6). In the contract document, the construction sequence required the top 3 rows of soil nails to be installed and the upper third of the slope to be shotcreted first. Excavation and installation of the subsequent soil nails were to be carried out in stages. The LPM works were programmed to commence in October 1997 with all soil nail and raking drain installation, and slope excavation completed before May 1998.

The design of the LPM works was checked by the Mainland East Division of the GEO in October 1997.

### 2.2.5 Construction of the LPM Works

Construction of the LPM works, which was supervised by the Works Division of the GEO, commenced in October 1997. Following site establishment and preparation works, installation of soil nails commenced in mid-December 1997. In mid-February 1998, the GEO accepted the Contractor's proposal to revise the construction sequence for the southern and northern portions of the slope, originally stipulated in construction drawing No. GCE 3223 issued by the GEO, to that as shown in Figures 7 and 8 respectively. The actual construction sequence however deviated from the agreed one. Based on FSW' s review of site records and discussions with the site supervisory staff, the actual construction sequence adopted is described below.

In the northern portion of the slope, the entire 18 m-high 30° to 50° temporary cut face was first excavated to about 1 m above the level of Sai Sha Road. This was followed by installation of temporary soil nails to the unsupported cut face. At the time of failure, only the top row of the temporary soil nails within the northern landslide area were installed.

Installation of the next row of soil nails was in progress (Figures 2 and 8). Overall, the Contractor had apparently cut some 2.5 m more than intended in this locality.

In the southern portion of the slope, installation of the top 8 rows of soil nails, except for the nail heads, was completed by mid-February 1998. Removal of chunam and excavation of the temporary toe slope commenced in mid-March 1998. At the time of failure, all but the lowest 2 rows of temporary soil nails were installed (except for the soil nail heads) and the temporary excavation was formed to almost its intended profile. The actual construction sequence for the southern portion of the slope is shown in Figure 7.

The progress of the temporary slope excavation and installation of soil nails just prior to the June 1998 landslides are presented in Figure 2. At the time of the landslides, 24 temporary soil nails were installed and 6 open drillholes made within the ground of the northern landslide, whereas 28 permanent and 80 temporary soil nails were installed within the ground of the southern landslide.

## 3. THE LANDSLIDES

### 3.1 Description of the Landslides

FSW commenced geological mapping of the landslides on 7 August 1998, the results of which are described in Sections 3.2 and 4. The sequences of the two landslides and the site conditions prior to and immediately following the landslides were established through FSW' s review of site records and discussions with the site supervisory staff.

On 5 June 1998 a small failure, about 10 m in width and 2 m in height, occurred at the upper part of the northern portion of the exposed cut slope, following some rainfall in early June. The main failure at the northern portion of the cut slope occurred during a heavy rainstorm on 9 June 1998 between 4:00 p.m. and 6:00 p.m. The mode of instability in the northern landslide principally comprised a translational failure in the near surface material. The failure affected the upper part of the slope up to the crest channel, which was noted by the site supervisory staff on 10 June 1998 to be partially blocked by construction debris. At this time tarpaulin sheeting was placed over parts of the upper portion of the cut slope. Heavy surface runoff was observed on the exposed lower part of the slope. Landslide debris, with a total volume of about 900 $m^3$, was deposited onto the working platform at the toe of the slope. The debris comprised very wet and loose, clayey, sandy silt with corestones of up to about 2 m diameter, relatively intact blocks of CDT up to about 10 $m^3$ at the top of the disturbed material, and several deformed soil nail bars.

The extent and profile of the northern landslide, shown in Figures 2 and 9 respectively, were estimated by the Design and Works Divisions of the GEO following removal of the landslide debris during site clearance works. The landslide resulted in a 13 m high and 35 m wide failure scar. The average depth of the landslide was about 3 m and the surface of rupture was generally concave in shape. A general view of the northern landslide is shown in Plate 1.

Between 4:00 p.m. and 6:00 p.m. on 10 June 1998 a small landslide occurred at the southern portion of the slope. During the subsequent rainfalls in June 1998 the landslide

retrogressed up the cut slope progressively. Heavy seepage from the surface was observed at the landslide location. Landslide debris, with a total volume of about 1700 $m^3$, was deposited onto the working platform at the toe of the slope. The debris comprised a mixture of relatively intact blocks of CDT upto about 20 to 30 $m^3$, corestones upto about 2 m diameter, very wet and loose clayey, sandy silt, and many deformed soil nail bars. The extent and profile of the southern landslide, shown in Figures 4, 10, 11, 12 and 13, were determined by the Survey Division of the Civil Engineering Department (CED), prior to the commencement of the site clearance works. The landslide resulted in a 20 m high and 38 m wide scar which was generally concave in shape. A general view of the southern landslide is shown in Plate 2. The average depth of the southern landslide as established in investigation pits (Figures 11 and 12) was about 8 m. The mode of instability in the southern landslide principally comprised a deep-seated rotational failure

The maximum travel distance of the landslide debris for the southern and northern landslides, estimated from photographs of the landslide taken by site staff and from survey plans, was about 6.5 m and 3.5 m from the slope toe respectively. These correspond to travel angles of about 35° and 38° respectively, which are similar to those observed for common rain-induced landslides at cut slopes in Hong Kong (Wong & Ho, 1996). As such, the landslides were not considered to be particularly mobile.

## 3.2 Field Mapping and Observations After the Landslide

The landslides were first brought to the attention of the Landslip Investigation Division of the GEO in early August 1998. FSW first visited the site on 7 August 1998. During site inspections in August 1998, it was noted that urgent repair works comprising slope trimming and shotcreting of the northern landslide location had been completed (Plate 6). Part of the upper portion of the main scarp and the flanks of the southern landslide had been sprayed with shotcrete (Plate 7).

The northern portion of the cut slope, at the time of failure on 9 June 1998, was covered with sheeting on the upper slope area, and a scaffolding platform had been erected for soil nail and raking drain installation. Landslide debris, comprising corestones, collided with and damaged some of the scaffolding. Several temporary soil nails with 150 mm square steel plate heads protruded from the middle portion of the cut slope affected by the landslide. The landslide created a 1 m to 2 m high main scarp. Relatively intact debris, comprising blocks of CDT up to about 10 $m^3$, was located immediately below the main scarp.

In the southern landslide, the crown was located at the upper-most berm, and both the lower and middle batters were affected by the instability. The main scarp (about 1 m to 2 m high) and parts of the flanks of the landslide were shotcreted at the end of June 1998 as part of the urgent repair works. Despite these works, downward movement of the disturbed material still continued. In August 1998, the main scarp was observed to have enlarged to about 4 m high, the upper half of which remained covered with shotcrete (Plates 2 and 7).

In the southern landslide, release planes on the south-facing backscarp included joint sets dipping at 68° to 88° towards the south to south-southeast, and on the east-facing backscarp, a sub-vertical joint set dipping towards east-northeast and east-southeast. Some of the release surfaces were infilled with slickensided kaolin and manganese oxide deposits each

with a thickness of upto about 2 mm (Plate 8). Several open relict joints, some of which were partially infilled with clay and silt deposits, were observed in and below the disturbed material dipping steeply (75° to 85°) into the slope (Plate 9).

In the southern landslide, relatively intact blocks of CDT, including part of the failed lower berm, were noted in the landslide debris. Several deformed soil nail bars (nail heads not yet installed), sections of grout, and plastic grout tubes (originally inserted into the drillholes with the soil nails) protruded from the main scarp, along the flanks of the landslide and within the debris (Plates 8 and 10). The deformed soil nail bars were generally inclined downslope.

Following the instabilities that occurred in June 1998, urgent repair works were completed between July and September 1998. These included the provision of a shotcrete cover to the surface of the unfailed portions of the cut slope and installation of raking drains in the areas adjacent to the landslide locations. According to the site supervisory staff, landslide debris had been removed from the northern landslide. In the portion of slope between the northern and southern landslides, according to the observations of the site staff, hair cracks up to about 1 mm wide were noted in early August at the lower portion of the newly applied shotcrete surface. By late August, the cracks here were noted to have progressively developed to a maximum width of about 10 mm, whereas new cracks were seen at the upper shotcreted surface. In places, the cracks were noted to extend into the soil and were not confined only to the shotcreted surface. In view of the observed distress in this area, a concrete buttress was constructed in September along the toe of this portion of slope, and an additional layer of shotcrete was applied on the surface.

## 4. SUBSURFACE CONDITIONS AT THE SITE

### 4.1 General

The subsurface conditions at the site were inferred using information from desk and field studies. The desk study comprised a review of existing data, including results of the ground investigation carried out in 1996, whilst the field study included geological mapping and limited ground investigation supervised by FSW after the landslides.

Bachy Soletanche carried out the ground investigation for the GEO in 1996 which comprised 11 drillholes, 11 trial pits and four surface strips (Figure 5).

Geological mapping of the site by FSW commenced on 7 August 1998. Ground investigation for this study commenced on 22 August 1998 and comprised 5 investigation pits, 4 surface strips and GCO probe tests (Figure 5).

### 4.2 Geology and Previous Ground Investigations

The geological features observed at the landslide site are shown in Figure 14. Geological sections through the landslides are shown in Figures 15 and 16 for the northern and southern landslides respectively.

An extract of Sheet 8 of the Solid and Superficial Geology of Sai Kung is shown in Figure 17. The rocks at the site were mapped by the Hong Kong Geological Survey (HKGS) as coarse ash crystal tuff of the Tai Mo Shan Formation, part of the Repulse Bay Volcanic Group, according to the 1:20,000-scale geological map (GEO, 1989). A northwest-southeast striking inferred fault (the O Tau fault) is located about 150 m northeast of the site. Lai and Langford (1991) mapped an inferred northeast-southwest trending fault about 200 m off the coast (Figure 17). Photogeological lineaments also trending northwest-southeast and northeast-southwest are present in the area.

The geology at the landslide site, shown in Figure 14, comprises partially weathered, jointed, predominantly coarse ash crystal tuff overlain by residual soil up to about 4 m thick. The partially weathered rock (predominantly PW 0/30) consists of completely to highly decomposed tuff, with corestones of moderately to slightly decomposed tuff. The thickness of completely to highly decomposed tuff based on records of drillholes sunk in 1996 was estimated to be about 10 m to 12 m towards the centre of the slope, and about 15 m to 18 m in the northern and southern portions of the slope respectively. A rockhead depression is inferred along the lower portion of the slope. The depression at the centre of the slope is about 3 m and increases towards the northern and southern portions of the slope to a maximum of about 8 m (Figures 15 and 16). An area of outcropping corestones, indicated as PW 30/50 in Figure 14, is located at the northern portion of the cut slope. The CDT was typically described as soft to firm, reddish to greyish brown to brownish yellow, mottled white and black, clayey sandy silt with occasional fine gravel.

The partially weathered tuff is pervasively jointed. Two persistent, closely-spaced, generally tight to extremely narrow, often slickensided, and steep (64° to 85°) joint sets dipping northwest and north-northeast/south-southwest respectively (i.e. both dipping into the slope), are dominant over the entire site. These two major joint sets are predominantly infilled with thin (generally 1 mm to 2 mm) kaolin and/or thin (about 1 mm) manganese oxide deposits. In addition, sub-horizontal manganese oxide infilled relict joints were observed within investigation pits on the slopes and near the base of excavations for the retaining wall footings along the slope toe. Also an eutaxitic fabric was observed by staff from the Hong Kong Geological Survey in a corestone dipping at 16°-20°/110°-112°. A stereoplot of the measured orientations of the relict joints is presented in Figure 18.

Manganese oxide infilling was observed on many joint planes in all the drillholes except D07 and D08 (located at the toe towards the centre and southern portion of the slope respectively, see Figure 8) and in trial pits TP03 to TP05 (located at the toe towards the southern portion of the slope) during the 1996 ground investigation (Bachy Soletanche, 1997).

## 4.3 Current Investigation

### 4.3.1 Ground Investigation

Five investigation pits (IP1 to IP5) were excavated in the southern landslide location following partial removal of landslide debris (Figure 5). In the upper part of IP1 and IP2, a slip surface dipping steeply (about 75°) was observed at about 7 m to 9 m below the estimated pre-failure ground surface. The slip surface was typically slickensided and undulating, and comprised remoulded moist, soft, slightly sandy, silt and clay (Plate 11). In the middle

portion of IP2, the slip surface was in the form of a shear zone dipping at 35° to 45° and at about 6 m to 7 m below the estimated pre-failure ground surface (Plate 12 and Figures 10 and 11). Within the shear zone, slickensides and sigmoidal S-C fabrics were observed along and between shear planes, indicating downslope movement of the overlying material (Plate 13). Towards the toe of the slope, the slip surface was encountered in IP5 in the form of a shear zone dipping at about 10° to 25° (Figure 12). In several locations the slip surface was observed around the margins of corestones (Plate 14), and occasionally along kaolin-infilled and manganese oxide infilled relict joints dipping out of the slope (Plate 15).

The material above the slip surface typically comprised CDT containing a disturbed fabric (Plate 14) and occasionally destroyed fabric (Plate 16). Localised shear planes (features possibly formed following the initial movement) dipping into (dip/dip direction of 45°-85°/300°-330°), and to a lesser extent, out of the slope (20°-65°/130°-170°) (Plate 17) were also observed above the slip surface. These localised shear planes were occasionally located along kaolin and manganese oxide infilled relict joints and along joints containing clay and silt infilling. Relative displacement along the localised shear planes was estimated to be typically between 10 mm and 200 mm (Plate 18). Open (1 mm to 5 mm) tension cracks were also observed within the slipped mass dipping (45 ° to 85°) into the slope (Plate 18). Some of these cracks were infilled with disturbed loose sandy materials.

The material below the slip surface typically comprised CDT containing an intact to slightly disturbed fabric. An open (12 mm maximum), manganese oxide infilled relict joint was mapped below the slip surface in the upper portion of IP2.

GCO probe tests were carried out at the southern landslide site in August 1998 to try to establish the depth of landslide debris. In general, the probing did not advance to the inferred slip surface of the landslide which was established in the trial pits (Figure 11).

The post-failure ground investigation of the northern landslide included one surface strip along the centre of the re-profiled surface, and examination of the excavation at the toe of the slope during the on-going LPM works. The re-profiled surface was found to comprise generally intact partially weathered rock (PW 0/30) with about 4.5 m residual soil at the crest. This is consistent with the observation by the site supervisory staff that landslide debris had been removed (Section 3.2). Two major (40 mm to 60 mm thick) kaolin veins were mapped by GEO prior to the failure, along the middle and lower portions of the northern re-profiled surface, dipping into the slope to the northwest and southeast at 30° to the horizontal (Figure 14).

Other important geological features of the site also include laterally-extensive (up to 40 m), northeast-striking clay layers within the CDT which dip steeply (50° to 80°) into the slope towards the northwest (Figures 12 and 14). These were particularly noticeable within the excavations at the toe of the landslides, within IP4 and IP5 (where they were estimated to be in excess of 500 mm thick) and across the lowermost batter between the two landslide locations (Plate 19). The clay layers are typically 150 mm to 300 mm thick, with a few joints and fissures, and often contain a laterally discontinuous seam (predominantly 5 mm to 10 mm thick) of buff brown silt and clay along the centre (Plate 20). The clay material on either side of the seam is considered to be completely decomposed, occasionally lapilli-bearing, fine to coarse ash tuff. Although the origin of the seam itself is not fully understood, it may

represent minor intrusive activity. The presence of the clay layers will probably impede groundwater flow and affect the hydrogeological conditions at the landslide site.

CS3, which is located on the shotcreted cut slope face between the northern and southern landslides, revealed minor sub-vertical movements (up to 15 mm displacement) along a clayey seam within a clay layer dipping at 62° into the slope (towards 320°), and along a manganese oxide infilled (1 mm to 2 mm thick) joint within a clay layer dipping at 55° into the slope (towards 320°). Slickensides were observed plunging in the same dip directions as the dip of the seam and joint.

Relict joints infilled with kaolin and manganese oxides were generally observed in the middle and lower portions of the slope and are absent within the residual soil at the top of the slope (Figure 14). Several major (40 mm to 70 mm thick) manganese oxide veins were encountered in IP5 towards the toe of the southern landslide location, dipping steeply (58° to 65°) into the slope towards the northwest.

Slickensides are especially well-developed on polished manganese oxide and kaolin accumulations. The plunge of the slickensides are highly variable across the site (0-85°/010°-350°) with some plunging obliquely relative to the dip direction of the joint plane. The slickensided surfaces are often observed on gently undulating, curved, discontinuous planes partially bounding corestones. They are considered to have been the result of minor, localised movements within the soil and rock mass. This may have been a result of previous slope movements and/or tectonic activity related to the nearby faults.

Angular cobbles of moderately decomposed coarse ash tuff, with a relatively low density, were found in the debris of the southern landslide. Similar rock materials were not commonly encountered on the slope during the ground investigation.

### 4.3.2 Examination of Damaged Soil Nail Bars

Selected deformed soil nail bars found in the landslide debris were examined by a metallurgist to assess the probable mode of damage. After a preliminary examination of the fractured ends of 11 deformed bars, 8 fractured ends which exhibited signs of damage were further examined using a binocular microscope.

The key findings were that bending and plastic deformation were evident in some of the bars (Plate 21), suggesting that these nail bars failed in a ductile manner. None of the bars examined suggested tensile or shear failures.

## 4.4 Laboratory Tests

Laboratory tests were conducted on soil and rock samples retrieved from the ground investigation carried out following the June 1998 landslides. The soil tests included particle size distribution, Atterberg limits tests, direct shear box tests, consolidated undrained triaxial compression tests with pore water pressure measurement and oedometer consolidation tests.

Samples selected for testing included CDT, clay layer, kaolin and manganese oxide infilled relict joints.

The results of particle size distribution and Atterberg limits tests on CDT, clay layer and kaolin veins are summarized in Table 2. The average fines (i.e. clay and silt) content was 61% for CDT, 94% for the clay layer and 95% for the kaolin vein. The average plasticity index of CDT was 16%, and the liquid limit was 53%. For the clay layer and kaolin veins, the average plasticity indices were 20 % and 28% respectively, while the liquid limits were 59% and 79%, respectively. The results indicate that these materials exhibit high plasticity and low permeability. A summary of similar tests on CDT carried out in 1997 for the design of the LPM works is presented in Table 1 for comparison. Tests carried out on CDT under this landslide investigation and that under the LPM programme show similar results.

The permeabilities of intact CDT and clay layer were assessed by oedometer consolidation tests. The ranges of permeabilities of intact CDT and clay layer were found to be $2.6\times10^{-9}$ to $6\times10^{-9}$ m/s and $3.9 \times 10^{-9}$ to $7.8 \times 10^{-9}$ m/s respectively.

The shear strength of intact CDT and clay layers were assessed by triaxial compression tests on specimens prepared from block samples. Results of triaxial compression tests are summarized in Table 3. The results for CDT and those obtained from triaxial compression tests performed on CDT for the LPM design are presented in the form of $p'$-$q$ plots in Figure 19. The shear strength of intact CDT derived from the linear regression of these combined test data was estimated to be $c' = 6.5$ kPa, $\phi' = 33°$, which is typical for materials of a similar nature in Hong Kong. The shear strength of the clay layer derived from linear regression of the test data was estimated to be $c' = 12.2$ kPa, $\phi' = 30°$.

The shear strength of kaolin and manganese oxide infilled relict joints and of the kaolin veins were assessed by direct shear box tests. At the initial stage of the testing programme, standard shear box tests were performed in accordance with BS1377: Part 7: 1990. The test results (i.e. $c' = 26.6$ kPa, $\phi' = 25°$ for kaolin vein and $c' = 15.8$ kPa, $\phi' = 35°$ for relict joint) are considered not representative of the actual strength of the samples tested for the following reasons. Firstly, the volume changes of the specimen during shearing (either contraction or dilation) would have resulted in the kaolin vein or the relict joint becoming out of phase with the plane of shearing in the shear box. Secondly, it was difficult to align the relict joint of the specimen exactly along the plane of shearing in the shear box because the relict joints are often curvilinear.

The setting of the direct shear test was subsequently modified by using gypsum to mount the specimen in the shear box to ensure that shearing would occur essentially along the relict joint. The specimen was soaked in water, consolidated and then sheared as in a standard test. For tests on slickensided relict joints, specimens were prepared in such a way that shearing was to take place along the slickensided direction. The results of the modified direct shear tests are summarised in Table 4 and shown in Figure 20. The results show a considerable scatter, which may be attributed to the variability of shear strength of relict joints. The average, upper bound and lower bound shear strength parameters of slickensided relict joints in CDT, assuming $c' = 0$, were estimated to be $\phi' = 19°$, $30°$ and $10°$ respectively. These were significantly lower than that obtained in previous tests.

Laboratory tests on bulk density, water content, dry density, specific gravity and porosity were performed on medium to slightly decomposed tuff, and slightly decomposed to fresh tuff, respectively. Test results are shown in Table 5. Based on the test results, the characteristics of the rock samples tested were of typical values.

In addition to the soil and rock tests described above, tests were undertaken to determine the chemical composition of the manganese oxide infilling deposited at the relict joint. Details of the composition are tabulated in Table 6.

## 4.5 Groundwater Conditions

The groundwater conditions at the site at the time of the June 1998 landslides were assessed from a review of the available groundwater records, seepage observations and the hydrogeological setting of the site. The information reviewed include the following:

(a) Pre-landslide (i.e. before the 1998 landslides) groundwater monitoring data for piezometers, with Halcrow buckets installed, in 11 vertical drillholes (D01 to D11, see Figure 5 for drillhole locations and Figure 21 for records of groundwater monitoring of D03) over the period October 1996 to November 1997 (GEO, 1997). Significant rises of the main groundwater table up to a maximum of 8 m at the crest, and 2.5 m at the toe of the slope were recorded by Halcrow buckets in association with the rainstorm of 2 July 1997. The groundwater level measurements were undertaken on 9 July 1997, 7 days after the rainstorm, and whilst the peak levels were recorded by the Halcrow buckets, it is uncertain when they occurred. It is also uncertain if there were any delayed responses (Section 2.2.4 and Figure 21).

(b) Pre-landslide observation based on the May 1998 site record photographs that an elevated water table might have formed (possibly above a clay layer) at about mid-height of the temporary cut slope at the location of the southern landslide (Plate 22).

(c) Observations made by LPM site supervisory staff at the northern slope after the 5 June 1998 minor landslide and prior to the 9 June 1998 major landslide that no seepages were noted from the slope faces although there existed numerous erosion gullies. After the major landslide, heavy surface runoff was observed on the lower part of the disturbed material. However, it is uncertain if there were any seepages on the upper part as it was covered by tarpauline sheet at the time of inspection.

(d) Observation that the major landslide in the northern part of the slope occurred between 4:00 p.m. and 6:00 p.m. on 9 June 1998, i.e. immediately following a period of intense rainfall, and that the southern major landslide commenced between 4:00 p.m. and 6:00 p.m. on 10 June 1998, at a time almost 24 hours after a period of intense rainfall, where the disturbed and unstable material continued

to move for a prolonged period thereafter in response to comparatively less severe rainfall.

(e) Observations that the northern landslide involved a relatively thin mantle of disturbed material, whereas the southern landslide involved a deep-seated failure.

(f) Post-landslide (i.e. after the 1998 landslides) groundwater monitoring data for piezometers, with Halcrow buckets installed, in 1 vertical drillhole (D03, Figure 5 for drillhole location and Figure 21 for record of groundwater monitoring) over the period September 1998 to March 1999.

(g) Post-landslide observation recorded in the incident report that heavy seepages were noted from the slope face at the southern landslide location (GEO, 1998).

(h) Post-landslide observation that groundwater was noted to be flowing from the raking drains installed at the northern portion of the slope with a maximum flow rate of 45 ml/s as measured on 16 September 1998.

(i) Post-landslide observation made over the period August 1998 to March 1999 that no seepages were noted from the slope faces and in the inspection pits dug at the landslide site in the course of the post-landslide ground investigation. However, seepages were noted at about 1 m below the existing levels of Sai Sha Road (i.e. about 10 mPD at the southern landslide location and 13mPD at the northern landslide location) along the base of the excavations for the retaining wall construction at the slope toe.

(j) Observation that the area above the slope is a vegetated, very gently sloping (10° to horizontal) natural terrain (Figure 3) which is susceptible to direct infiltration of rain water.

(k) Observation in the middle and lower parts of the slope that there exist a system of clay layers and major kaolin infilled discontinuities which dip steeply into the slope (Section 4.3.1 and Figure 14) and that their presence could possibly impede downslope groundwater flow.

(l) Interpretation that there exists a depression in the rockhead profile at the slope toe which could have promoted concentration of subsurface groundwater flow (Section 4.2, Figures 15 and 16).

(m) Observation that the slope is about 150 m to 200 m from two nearby inferred faults (Figure 17). Previous tectonic activities, as inferred from the slickensided and kaolin and manganese oxide infilled relict joints, suggest the possibility of a subsurface preferential groundwater flow path.

In light of the observations made as described in (d) and (e) above, it would seem reasonable to postulate that the two landslides that occurred in July 1998 are of different types.

The northern landslide, which is relatively shallow (Figure 27) and occurred approximately around the time of peak rainfall intensity (Figure 23), is likely to have been triggered by direct surface infiltration of rain water into the soil mantle associated with the short duration rainfall.

The southern landslide, on the other hand, involves a deep seated failure in the soil mass (Figure 26), which occurred some 24 hours after the peak rainfall period (Figure 23). This apparent delayed response suggests that the landslide might have been associated with a significant rise of the main groundwater table.

The groundwater conditions of the southern landslide at the time of the June 1998 failures were postulated based on the piezometer monitoring records of the 2 July 1997 storms, given that the 9 June 1998 and 2 July 1997 storms were comparable (Section 5). The inferred groundwater level corresponding to the 2 July 1997 rainstorm is shown in Figures 15 and 16. At the time of the current landslides, the complete removal of the chunam cover on the original slope face could have enhanced direct infiltration. It would therefore seem reasonable to expect that the groundwater level at the time of the southern landslide was probably higher than that inferred from groundwater monitoring of the 2 July 1997 rainstorm. Further discussion of the observed significant rise in the main groundwater table is presented in Section 6.

## 5. ANALYSIS OF RAINFALL RECORDS

The nearest GEO automatic raingauge (No. N15) is located at Sung Tsun Primary School in Yau Ma Po, which is about 1.5 km to the southwest of the landslides site. The daily rainfalls recorded by the raingauge for the period of May 1995 to April 1999 are shown in Figure 22. The hourly rainfall records for the 12-hour and 24-hour period preceding the main northern and southern landslides, which were assumed to occur at 5:30 p.m. of 9 June 1998 and 6:00 p.m. of 10 June 1998 respectively, are presented in Figure 23.

Based on the rainfall records, rain was severe from mid-night of 9 June 1998 to the time of the northern landslide. The 12-hour and 24-hour rainfalls preceding the time of the northern landslide were 352.5 mm and 531.5 mm respectively. The maximum 60-minute rainfall was 87.5 mm which was recorded between 5:15 a.m. and 6:15 p.m.

For the southern landslide which occurred on 10 June 1998, the 12-hour and 24-hour rainfalls preceding the landslide (5:00 p.m.) were only 8.5 mm and 59.5 mm respectively. These rainfalls were much less than the rainfall on the previous day (Figure 23). In this respect, the southern landslide can be considered as a delayed failure with respect to the major rainstorm event on 9 June 1998.

The maximum rolling rainfall data recorded at GEO raingauge No. N15 for selected durations before the northern and southern landslides are presented in Tables 7 and 8 respectively. The 24-hour rainfalls ending at 5:00 p.m. on 9 June 1998, with an estimated

return period of 71 years, and at 6:30 p.m. on 9 June 1998, with an estimated return period of 97 years, were the most severe rainfall periods immediately preceding the northern and southern landslides respectively.

Isohyets of rainfall for the 24-hour period to the time of the northern landslide (5:30 p.m. on 9 June 1998) for the whole SAR are shown in Figure 24.

A comparison between the patterns of past heavy rainstorms affecting the landslides site is shown in Figure 25. This demonstrates that the highest 31-day rainfall prior to both the northern and southern landslides were 1058.5 mm and 1114 mm, respectively, which are not the most severe rainstorms compared to the historical records of the 2 July 1997 rainstorm (1288 mm). However, when comparing the shorter durations, it is evident that the rolling rainfall for a period up to 7 days preceding the landslides was the most intense rainfall experienced by the area for the records analysed since the installation of Raingauge No. N15 in 1982.

## 6. THEORETICAL STABILITY ANALYSES

Stability analyses using the rigorous method of Morgenstern & Price (1965) were carried out to assist the diagnosis of the probable triggering factors and causes of the landslides. Representative cross-sections of the southern and northern landslides are presented in Figures 26 and 27 respectively.

The pre-failure ground profile was established through a review of site records and construction drawings. The geometry of the failure surface for the southern landslide was interpreted based on geological mapping of the site, particularly the investigation pits, carried out by FSW after the failure (Section 4.3). The failure surface for the northern landslide was estimated based on records provided by the Design and Works Divisions of GEO, which indicated the probable slip surface established by site inspections during removal of landslide debris.

At the time of the failure, a total of 24 and 108 soil nails had been installed in the slope affected by the northern and southern landslides respectively. In the stability analyses, the stabilising forces provided by these soil nails on the active and passive zones of the slope were estimated using the method described by Watkins & Powell (1992). The bending and shear resistance in soil nails were neglected in the calculations (Jewell & Pedley, 1990).

As discussed in Section 4.5, the observations of the northern landslide being a relatively shallow translational failure and occurred during heavy rainfall suggest that it was likely to have been caused by the development of transient elevated water pressure above the slip surface. In the theoretical stability analyses, the effect of a rise in the water table above the base of the main slip surface, was examined.

On the other hand, the southern landslide which was a deep-seated rotational failure and occurred some 24 hours after the peak rainfall period suggest that it was probably associated with a rise in the main groundwater table. The groundwater level at the time of the landslide was postulated initially based on the 2 July 1997 storms, as both the 9 June 1998 and 2 July 1997 storms were comparable in terms of severity, but a further rise in

groundwater level was probable because of enhanced water ingress following the complete removal of the chunam cover. In the theoretical stability analyses, the effect of a further rise above the inferred 2 July 1997 groundwater level was examined.

The results of the stability analyses indicate that, when strength parameters derived for CDT from linear regression of the combined (GEO and FSW) triaxial test results were used (i.e. $c' = 6.5$ kPa, $\phi' = 33°$), the northern and southern landslides would be predicted if the groundwater levels at these slopes rose respectively to 2.4 m above the slip surface and 1.2 m above the groundwater level corresponding to the 2 July 1997 rainstorm (Figures 28 and 29). If the LPM design shear strength parameters for CDT (i.e. $c' = 4$ kPa, $\phi' = 36°$) were used, landslides would be predicted if the groundwater levels at the northern and southern slopes rose respectively to 2.2 m above the slip surface and 1.3 m above the 2 July 1997 rainstorm groundwater level.

In view of the fact that the CDT, in which the landslides occurred, contains closely-spaced and often slickensided relict joints, infilled with clay and manganese oxide, the strength of the soil mass was likely to have been weaker than that of the intact material without joints. For comparison purposes, shear strength parameters of the soil mass were estimated using the probabilistic method proposed by Koo (1982) for the stability analyses of the southern and northern landslides based on conventional limit equilibrium methods as shown in Figures 30 and 31 respectively. It can be seen that these strength parameters $c' = 5.9$ kPa, $\phi' = 32.3°$ are close to that of the intact CDT ($c' = 6.5$ kPa, $\phi' = 33°$). This is consistent with the observation that slickensided relict joints were generally dipping into the slope (i.e. their effect on slope stability is therefore relatively small) and that the failure surface was only occasionally along relict joints (Section 4.3). However, it cannot be ruled out that the weaker relict joint was a contributory factor to the present landslides, in allowing internal displacement and shearing to take place in the soil mass and providing release surfaces. In this way, the operational strength of the soil mass might have been adversely affected to some extent but this is difficult to quantify.

Given the uncertainties regarding the precise groundwater conditions at the time of the failures, sensitivity analyses were carried out using different groundwater levels for a range of operational strength parameters. The results of the sensitivity analyses, which are summarized in Figures 28 and 29 for the southern and northern landslides respectively, indicate that the groundwater levels at the time of failures at the northern and southern landslides were probably in the range of 1.5 m to 2.5 m above the slip surface and 0.5 m to 1.5 m above the groundwater level corresponding to the 2 July 1997 rainstorm. These inferred groundwater conditions were more severe than that assumed in the LPM design for the temporary cut slope (Figure 27).

## 7. DIAGNOSIS OF PROBABLE CAUSES OF THE LANDSLIDES

The close correlation between the rainfall and the timing of the failures suggests that the landslides were probably triggered by the heavy rainfall of 9 June 1998.

The principal causes of the failures relate to problems encountered during the temporary works stage, which are as follows :

(a) the actual groundwater conditions realised were much more severe than that assumed in the design of the temporary works,

(b) the delay in site works meant that construction extended into the wet season hence exposing the temporary slopes to conditions which were not envisaged and allowed for in the original design and such effects were not subsequently reassessed in construction reviews, and

(c) the contribution of soil nails to slope stability was limited for the northern landslide in that some of the temporary and permanent nail heads were not yet installed.

A further contributory factor to the failures is that the detailing of the temporary soil nail heads was not effective in providing support to the temporary slopes. The relatively small nail heads provided in the design (i.e. 150 mm square steel plate) meant that the available capacity in the passive zone could not have been fully mobilised because the capacity of the nail was limited by the active zone. The relatively low mobility of the debris in the southern landslide during initial failure was probably due to development of forces in the soil nails as they were deformed. As ground movement and cracking developed, the available limited bonding within the active zone of the soil nails probably reduced, resulting in further displacement during subsequent rainfall.

A detailed assessment has been carried out to examine the mass strength of the relict jointed volcanic saprolite in limit equilibrium analysis (Section 6). This suggests that the overall mass strength was not significantly affected by the infilled relict joints based on consideration of the probabilistic distribution of joint orientations and the reduced strength of infilled joints. The stability analyses demonstrate that a mechanism exists involving the development of high groundwater pressure which can explain the slope failures.

The survey plans and LPM site records suggest that the disturbed material in the 1995 instability had been removed during the cut back of the slope by HyD' s urgent repair works in 1995 and during the further cut back by the LPM works in 1997 and 1998. The failure surfaces of the 1998 landslides were found to be about 10 m beyond the inferred 1995 failure surfaces. These suggest that the1998 failures did not involve direct reactivation of the 1995 failures although they are partly coincidental on plan (Figure 4).

The mechanism and mode of the failures suggest that the infilled relict joints probably played a key role in affecting the material behaviour to water ingress. The presence of persistent discontinuities (particularly sub-vertical joints) with weak infill is conducive to locally damming water flow and possible build-up of localised water pressures. Furthermore, the relict joints would also have acted as release surfaces in promoting stress concentration and redistribution, leading to progressive failure and possible local opening up of the soil mass. This in turn would have increased the potential for direct infiltration and possible development of cleft water pressure. The above behaviour probably contributed to the relatively gradual development of the failure process. It is conceivable that the above destabilising process in a relict jointed saprolite could be initiated well before the condition pertaining to total collapse (i.e. a factor of safety of one) given the inherent brittleness of the soil mass.

Although groundwater monitoring data is limited, the available information indicates that the landslide site has a high groundwater regime which has a strong storm response. A significant groundwater response of up to about 8 m rise associated with the 2 July 1997 rainstorm was recorded by piezometers prior to commencement of slope excavation work. The majority of the chunam surface protection on the original slope had been removed as part of the LPM works by the end of April 1998 and the surface protection and drainage provisions for the temporary slopes may not be adequate. Given the severe rainstorm on 9 June 1998, the actual groundwater responses at the failure locations were probably significant.

The significant responses in groundwater levels could be due to the infilled relict joints, particularly the subvertical relict joints, locally damming water flow. The depression in rockhead profile near the toe of the slope was also liable to hinder downslope water flow and channelise subsurface groundwater flow. The topography of the site setting is such that the catchment above the landslides is relatively small. However, the existence of the two nearby inferred faults (Figure 17) and the presence of tectonic activities, as inferred from the slickensided and manganese oxide infilled relict joint planes, suggest the possibility of a subsurface catchment with preferential groundwater flow paths which allow water ingress from a relatively distant source.

The southern landslide was not particularly mobile. The failure initially involved ground deformation which continued to develop with further rainfall. The ground tended to open up as part of the failure process and deteriorated with time. This led to loss of bonding along the active zone of the soil nails but the presence of the soil nails with bending and shear capacity near failure as well as some limited pull-out capacity in the active zone probably contributed to the limited mobility of the failure.

## 8. CONCLUSIONS

It is concluded that the landslides that occurred in June 1998 on the temporary cut slope at the junction of Sai Sha Road and Tai Mong Tsai Road was probably triggered by severe rainfall.

Transient elevated water pressure in the upper part of the slope following direct infiltration into the unprotected slope is likely to have resulted in the northern landslide. Significant elevation in the main groundwater table is likely to have resulted in the southern landslide. The clay or manganese oxide infilled subvertical relict joints in the ground mass probably contributed to the failures by acting as release surfaces and allowing the development of localised water pressure through damming of water flow.

The landslides occurred in a slope with a complex geology, high groundwater regime and a history of failure. The delay in the site works meant that temporary slope construction had to be carried out during the wet season. The actual groundwater conditions realised were much more severe than those assumed in the design of the temporary works which was based on dry-season conditions. In addition, the actual construction sequence adopted did not follow that stipulated in the original design. A further contributory factor to the failures was that the detailing of the small temporary soil nail heads rendered the support provided to the

temporary slopes ineffective because the available capacity in the passive zone of the nails could not be fully mobilised.

## 9. REFERENCES

Bachy Soletanche Group (1997). Ground Investigation Factual Fieldwork Report, Contract No. GE/95/06, Works Order No. GE/95/06.215, Feature No. 8SW-A/C8, j/o Sai Sha Road and Tai Mong Tsai Road, Sai Kung.

Binnie & Partners (1978). Landslide Studies, Phase 1 Re-appraisal, Cut and Natural Slopes & Retaining Walls, Cut Slope Reference No. 8SW-A/C8. 3 p.

Burnett, A.D. & Lai, K.W. (1984). A review of the photogeological lineaments and fault system of Hong Kong. Proceeding of the Conference on Geological Aspects of Site Investigation. Hong Kong, pp 113-131.

Chen P.Y.M. (1994). Methods of Tests for Soils in Hong Kong for Civil Engineering Purposes (Phase 1 Tests). Geotechnical Engineering Office, Hong Kong, 91 p. (GEO Report No. 36).

Cruden, D.M. & Varnes D.J. (1996). Landslide Types and Processes. In: R.L. Schuster and A.K. Turner (eds), Landslides Investigation and Mitigation, Transportation Research Board Special Report 247, National Academy Press, Washington, pp 36-75.

FMR Consultants (1996). Roadside Slope Inventory and Inspections, Slope No. 8SW-A/C8. Engineering Inspection Record, 9 p.

Geotechnical & Concrete Engineering (HK) Ltd (1997). Material Testing Laboratory Report, Contract No. GE/95/07, Works Order No. GE/95/07.96, Feature No. 8SW-A/C8, j/o Sai Sha Road and Tai Mong Tsai Road, Sai Kung.

Geotechnical Control Office (1984). Geotechnical Manual for Slopes (Second Edition). Geotechnical Control Office, Hong Kong, 295 p.

Geotechnical Control Office (1987). Guide to Site Investigation (Geoguide 2). Geotechnical Control Office, Hong Kong, 368 p.

Geotechnical Engineering Office (1988). Guide to Rock and Soil Description (Geoguide 3). Geotechnical Engineering Office, Hong Kong, 189 p.

Geotechnical Engineering Office (1989). Sai Kung : solid and superficial geology. Hong Kong Geological Survey, Map Series HGM 20, Sheet 8, 1:20,000 scale. Geotechnical Engineering Office, Hong Kong, 295 p.

Geotechnical Engineering Office (1992). Stage 1 Study Report, Feature No. 8SW-A/C8. Geotechnical Engineering Office, Hong Kong, 2 p.

Geotechnical Engineering Office (1995). GEO Incident Report No. ME 95/8/11. Geotechnical Engineering Office, Hong Kong, 5 p.

Geotechnical Engineering Office (1996). Report on the Fei Tsui Road Landslide of 13 August 1995 (Volume 2). Geotechnical Engineering Office, Hong Kong, 295 p.

Geotechnical Engineering Office (1997). Stage 3 Study Report, Slope 8SW-A/C8, Junction of Sai Sha Road and Tai Mong Tsai Road, Report No. S3R 152/97.

Geotechnical Engineering Office (1998). Lasndslip Incident Report, Contract No. GE/97/01, Slope No. 8SW-A/C8. Works Division, Geotechnical Engineering Office, Hong Kong, 6 p.

Geotechnical Engineering Office (1999). Soil Testing Report No. 707 for 1998 Landslide Investigation Consultancy, Detailed Study for Slope 8SW-A/C8 at Sai Sha Road. Public Work Central Laboratory, Geotechnical Engineering Office, Hong Kong, 5 Volumes.

Head, K.H. (1982). Manual of Soil Laboratory Testing, Volume 2 : Permeability, Shear Strength and Compressibility Tests. Pentech Press, New York, 747 p.

Irfan, T.Y. (1992b). Mineralogical Assessment and Creep-type Instability at Two Landslip Sites. Geotechnical Engineering Office, Hong Kong, 143 p. (GEO Report No. 13)

Jewell R.A. & Pedley M.J. (1990). Soil Nailing : the role of bending stiffness. Ground Engineering, March, pp. 30-36.

Koo, Y.C. (1982a). Relict joints in completely decomposed volcanics in Hong Kong. Canadian Geotechnical Journal, vol. 19, pp 117-123.

Koo, Y.C. (1982b). The mass strength of jointed residual soils. Canadian Geotechnical Journal, vol. 19, pp 225-231.

Lai, K.W. & Langford, R.L. (1991). Special and temporal characteristics of major faults of Hong Kong. Proceedings of the International Conference on Seismicity in Eastern Asia, Hong Kong.

Morgenstern, N.R. & Price, V.E. (1965). The analysis of the stability of general slip surfaces. Geotechnique, Vol. 15, pp 79-93.

Watkins, A.T. & Powell, G.E. (1992). Soil nailing to existing slopes as landslip preventive works. Hong Kong Engineer, vol. 20, no. 3, pp 20-27.

Wong, H.N. & Ho, K.K.S. (1996). Travel distance of landslide debris. Proceedings of the Seventh International Symposium on Landslide, Trondhiem, Norway, vol. 1, pp 417-422.

# LIST OF TABLES

Table 1 - Summary of Classification and Index Test Results for Completely Decomposed Tuff for the LPM Works

| Material Type | Moisture Content (%) | Density | | Atterberg Limits | | | Specific Gravity | Particle Size Distribution | | | |
|---|---|---|---|---|---|---|---|---|---|---|---|
| | | Bulk ($Mg/m^3$) | Dry ($Mg/m^3$) | LL (%) | PL (%) | PI (%) | | Gravel (%) | Sand (%) | Silt (%) | Clay (%) |
| CDT | 35.9 - 64.0 (45.6) | 1.57 - 1.84 (1.73) | 0.96 - 1.36 (1.19) | 40 - 65 (48) | 19 - 31 (23) | 11 - 34 (24) | 2.66 - 2.71 (2.69) | 0 - 16 (2) | 4 - 64 (18) | 29 - 61 (44) | 6 - 60 (36) |

Legend: CDT Completely Decomposed Tuff
LL Liquid Limit
PL Plastic Limit
PI Plasticity Index

Note: Numbers in bracket are average values.

Table 2 - Classification and Index Test Results

| Material Type | Sample No. | Depth below Ground Level (m) | Sample Type | Particle Size Distribution | | | | Atterberg Limits | | | Moisture Content (%) | Specific Gravity | Density | | Permeability (m/s) |
|---|---|---|---|---|---|---|---|---|---|---|---|---|---|---|---|
| | | | | Gravel (%) | Sand (%) | Silt (%) | Clay (%) | LL (%) | PL (%) | PI (%) | | | Bulk ($Mg/m^3$) | Dry ($Mg/m^3$) | |
| CDT | BS1 | 3 | Block | 2 | 32 | 50 | 16 | 62 | 43 | 19 | 51.4 | 2.60 | 1.38 | 0.91 | -- |
| CDT | BS3 | 2.5 | Block | 2 | 43 | 41 | 14 | 47 | 33 | 14 | 38.5 | 2.69 | 1.68 | 1.21 | $5.95 \times 10^{-9}$ |
| CDT | BS5 | 6.5 | Block | 1 | 29 | 56 | 14 | 52 | 36 | 16 | 46.2 | 2.67 | 1.65 | 1.13 | $3.51 \times 10^{-9}$ |
| CDT | BS6 | 6 | Block | 1 | 38 | 47 | 14 | 51 | 37 | 14 | 45.9 | 2.67 | 1.65 | 1.13 | -- |
| CDT | BS7 | 7 | Block | 4 | 47 | 34 | 15 | -- | -- | -- | 50.1 | 2.69 | 1.69 | 1.13 | $2.61 \times 10^{-9}$ |
| CDT | BS8 | 7 | Block | 1 | 33 | 48 | 18 | -- | -- | -- | -- | -- | -- | -- | -- |
| Clay layer | BS4 | 3.5 | Block | 0 | 6 | 78 | 16 | 59 | 39 | 20 | 52.1 | 2.67 | 1.69 | 1.11 | -- |
| Clay layer | BS9 | 5.5 | Block | 0 | 2 | 81 | 17 | -- | -- | -- | 54.5 | 2.67 | 1.73 | 1.12 | $3.94 \times 10^{-9}$ |
| Clay layer | BS18 | 5 | Block | 1 | 17 | 69 | 13 | 49 | 34 | 15 | 51.8 | 2.69 | 1.68 | 1.11 | $7.79 \times 10^{-9}$ |
| Kaolin Vein | BS13 | 7.5 | Block | 0 | 5 | 82 | 13 | 79 | 51 | 28 | -- | -- | -- | -- | -- |

Legend: LL Liquid Limit
PL Plastic Limit
PI Plasticity Index
CDT Completely Decomposed Tuff

Note: Depths of samples shown in this table refer to the slope profile before the 1995 landslide.

Table 3 - Triaxial Compression Test Results

| Material Type | Sample No. | Sample Type | Depth (m) | Moisture Content before Testing (%) | Dry Density before Testing ($Mg/m^3$) | Specific Gravity | Type of Test | p' (kPa) | q (kPa) |
|---|---|---|---|---|---|---|---|---|---|
| CDT | BS9 | Block | 5.5 | 52.4 | 1.12 | 2.66 | CUM | 76.1 | 47.3 |
| | | | | | | | | 105.4 | 61.6 |
| | | | | | | | | 150.3 | 83.9 |
| CDT | BS11 | Block | 6 | 43.4 | 1.08 | 2.64 | CUM | 102.1 | 68.5 |
| | | | | | | | | 141.4 | 86.7 |
| | | | | | | | | 166.8 | 99.2 |
| CDT | BS12 | Block | 7 | 43.3 | 1.06 | 2.67 | CUM | 64.4 | 48.3 |
| | | | | | | | | 102.2 | 69.8 |
| | | | | | | | | 153.2 | 93.7 |
| Clay Layer | BS9 | Block | 5.5 | 51.9 | 1.13 | 2.67 | CUM | 61.3 | 41.6 |
| | | | | | | | | 93.9 | 58.3 |
| | | | | | | | | 131.9 | 79.0 |
| Clay Layer | BS18 | Block | 5 | 54.2 | 1.10 | 2.69 | CUM | 77.8 | 50.3 |
| | | | | | | | | 120.9 | 71.9 |
| | | | | | | | | 152.6 | 87.1 |

Legend: CDT Completely Decomposed Tuff; LL Liquid Limit; PL Plastic Limit; CUM Consolidated undrained multi stage triaxial compression test

$p' = 1/2(\sigma_1' + \sigma_3')$, where $\sigma_1'$ and $\sigma_3'$ are the major and minor principal effective stresses respectively

$q = 1/2(\sigma_1' - \sigma_3')$

Table 4 - Shear Box Test Results for Relict Joints in Completely Decomposed Tuff

| Material Type | Sample No. | Depth below Ground Level (m) | Sample Type | Vertical Stress at the Beginning of Test (kPa) | Maximum Shear stress (kPa) | Horizontal Displacement at Maximum Shear Stress (mm) | Vertical Displacement at Maximum Shear Stress (mm) | Vertical Stress at Maximum Shear Stress (kPa) |
|---|---|---|---|---|---|---|---|---|
| Slickensided Relict Joint | A0A | 7 | Undisturbed | 13.1 | 2.4 | 3.6 | -0.06 | 13.9 |
| Slickensided Relict Joint | A0B | 7 | Undisturbed | 14.3 | 4.6 | 6.0 | -0.22 | 15.9 |
| Slickensided Relict Joint | A0C | 7 | Undisturbed | 14.3 | 2.7 | 4.6 | -0.25 | 15.5 |
| Slickensided Relict Joint | A0D | 7 | Undisturbed | 14.3 | 5.3 | 2.2 | -0.02 | 14.9 |
| Slickensided Relict Joint | A0E | 7 | Undisturbed | 14.3 | 8.4 | 7.3 | -0.60 | 16.3 |
| Slickensided Relict Joint | BS8 | 7 | Undisturbed | 11.5 | 7.8 | 9.8 | 0.02 | 13.7 |

Notes: (1) Depths of samples shown in this Table refer to the slope profile before the 1995 Landslide.

(2) The tests were carried out in accordance with Rock Characterization Testing & Monitoring published for the Commission on Testing Methods, International Society for Rock Mechanics, 1981 edition.

(3) The size of the shear box was 60 mm x 60 mm.

(4) The shearing rate was 0.08 mm / min.

(5) A positive vertical displacement denotes dilation and a negative vertical displacement denotes compression.

Table 5 - Results of Laboratory Tests on Rock Samples

| Sample No. | Rock Type | Bulk Density ($kg/m^3$) | Water Content (%) | Dry Density ($kg/m^3$) | Specific Gravity | Porosity (%) |
|---|---|---|---|---|---|---|
| RS1 | M/SD Tuff | 2240 | 11.2 | 2020 | 2.65 | 24.6 |
| RS2 | M/SD Tuff | 2030 | 21.1 | 1680 | 2.65 | 38.3 |
| RS3 | M/SD Tuff | 2250 | 11.5 | 2020 | 2.67 | 24.6 |
| RS4 | M/SD Tuff | 2220 | 12.0 | 1980 | 2.65 | 25.8 |
| RS5 | M/SD Tuff | 2320 | 8.5 | 2140 | 2.66 | 19.8 |
| RS6 | M/SD Tuff | 2050 | 19.8 | 1710 | 2.64 | 36.8 |
| RS7 | M/SD Tuff | 2180 | 12.9 | 1930 | 2.66 | 27.7 |
| RS8 | M/SD Tuff | 2050 | 19.9 | 1710 | 2.67 | 36.5 |
| RS9 | SD/Fresh Tuff | 2690 | 0.1 | 2680 | 2.68 | 0.2 |
| RS10 | SD/Fresh Tuff | 2690 | 0.1 | 2690 | 2.69 | 0.3 |
| RS11 | SD/Fresh Tuff | 2630 | 0.8 | 2610 | 2.65 | 2.8 |
| RS12 | SD/Fresh Tuff | 2680 | 0.1 | 2670 | 2.68 | 0.3 |
| RS13 | SD/Fresh Tuff | 2680 | 0 | 2680 | 2.68 | 0.3 |
| RS14 | SD/Fresh Tuff | 2690 | 0.1 | 2690 | 2.68 | 0.3 |
| RS15 | SD/Fresh Tuff | 2680 | 0.1 | 2670 | 2.68 | 0.4 |

Note : The samples tested were corestones exposed after the landslides.

Table 6 - Laboratory Chemical Tests Results for Manganese Oxide Infilling at Relict Joints

| Sample No. | Sample 1 | Sample 2 |
|---|---|---|
| 1. Aluminium oxide content (%) | 5.3 | 6.4 |
| 2. Iron oxide content (%) | 4.7 | 8.6 |
| 3. Manganese oxide content (%) | 6.9 | 20.5 |
| 4. Magnesium oxide content (%) | 0.2 | 0.2 |

Note : The values shown in this table indicate the percentage by weight of the oxide content of the sample.

Table 7 - Maximum Rolling Rainfall at GEO Raingauge No. N15 and Estimated Return Periods for Selected Durations Preceding the Northern Landslide on 9 June 1998

| Duration | Maximum Rolling Rainfall (mm) | End of Period | Estimated Return Period (years) |
|---|---|---|---|
| 5 minutes | 14.0 | 6:15 on 9 June 1998 | 3 |
| 15 minutes | 33.5 | 6:15 on 9 June 1998 | 5 |
| 1 hour | 87.5 | 6:15 on 9 June 1998 | 5 |
| 2 hours | 141.5 | 6:25 on 9 June 1998 | 9 |
| 4 hours | 218.5 | 7:00 on 9 June 1998 | 19 |
| 12 hours | 358.5 | 17:25 on 9 June 1998 | 33 |
| 24 hours | 531.5 | 17:30 on 9 June 1998 | 71 |
| 48 hours | 547.0 | 17:30 on 9 June 1998 | 34 |
| 4 days | 572.5 | 17:30 on 9 June 1998 | 16 |
| 7 days | 625.5 | 17:30 on 9 June 1998 | 15 |
| 15 days | 711.0 | 17:30 on 9 June 1998 | 9 |
| 31 days | 1058.5 | 17:30 on 9 June 1998 | 20 |

Notes :
(1) Return periods were derived from the Gumbel's equation and data published in Table 3 of Lam & Leung (1994).
(2) Maximum rolling rainfall was calculated from 5-minute rainfall data.
(3) The use of 5-minute rainfall data for durations between 2 hours and 31 days results in better data resolution, but may slightly over-estimate the return periods using Lam & Leung (1994)'s data, which is based on hourly rainfall for these durations.

Table 8 - Maximum Rolling Rainfall at GEO Raingauge No. N15 and Estimated Return Periods for Selected Durations Preceding the Southern Landslide on 10 June 1998

| Duration | Maximum Rolling Rainfall (mm) | End of Period | Estimated Return Period (years) |
|---|---|---|---|
| 5 minutes | 14.0 | 6:15 on 9 June 1998 | 3 |
| 15 minutes | 33.5 | 6:15 on 9 June 1998 | 5 |
| 1 hour | 87.5 | 6:15 on 9 June 1998 | 5 |
| 2 hours | 141.5 | 6:25 on 9 June 1998 | 9 |
| 4 hours | 218.5 | 7:00 on 9 June 1998 | 19 |
| 12 hours | 358.5 | 17:25 on 9 June 1998 | 33 |
| 24 hours | 562.0 | 18:30 on 9 June 1998 | 97 |
| 48 hours | 604.0 | 10:45 on 10 June 1998 | 57 |
| 4 days | 622.0 | 11:00 on 10 June 1998 | 25 |
| 7 days | 690.0 | 10:15 on 10 June 1998 | 26 |
| 15 days | 777.5 | 11:00 on 10 June 1998 | 14 |
| 31 days | 1114.0 | 4:25 on 10 June 1998 | 29 |

Notes :
(1) Return periods were derived from the Gumbel's equation and data published in Table 3 of Lam & Leung (1994).
(2) Maximum rolling rainfall was calculated from 5-minute rainfall data.
(3) The use of 5-minute rainfall data for durations between 2 hours and 31 days results in better data resolution, but may slightly over-estimate the return periods using Lam & Leung (1994)'s data, which is based on hourly rainfall for these durations.

LIST OF FIGURES

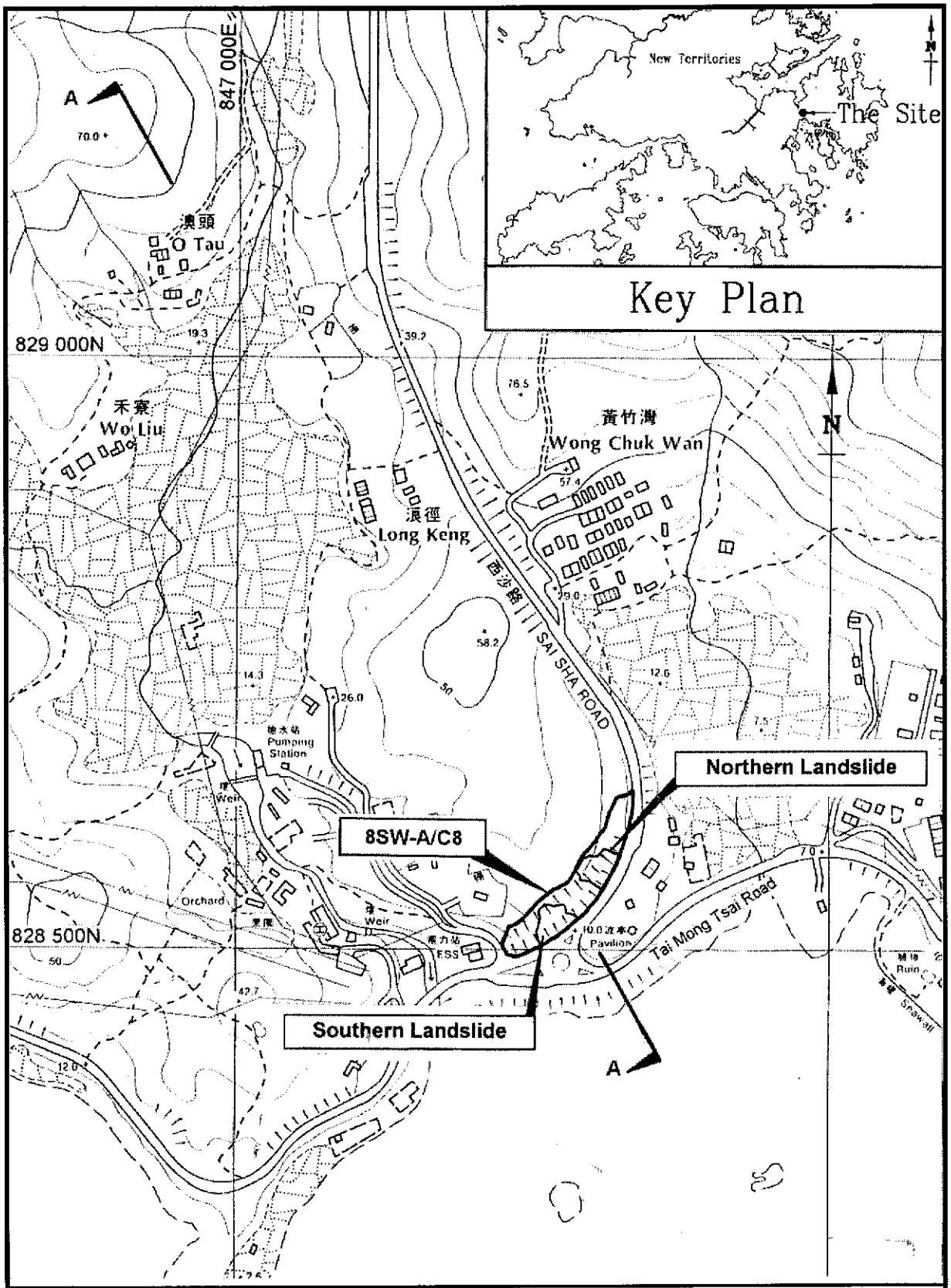


Note: Base Map is extracted from Survey Sheet no. 8SW-A, scale 1 : 5000, dated November 1991.

Figure 1 – Site Location Plan

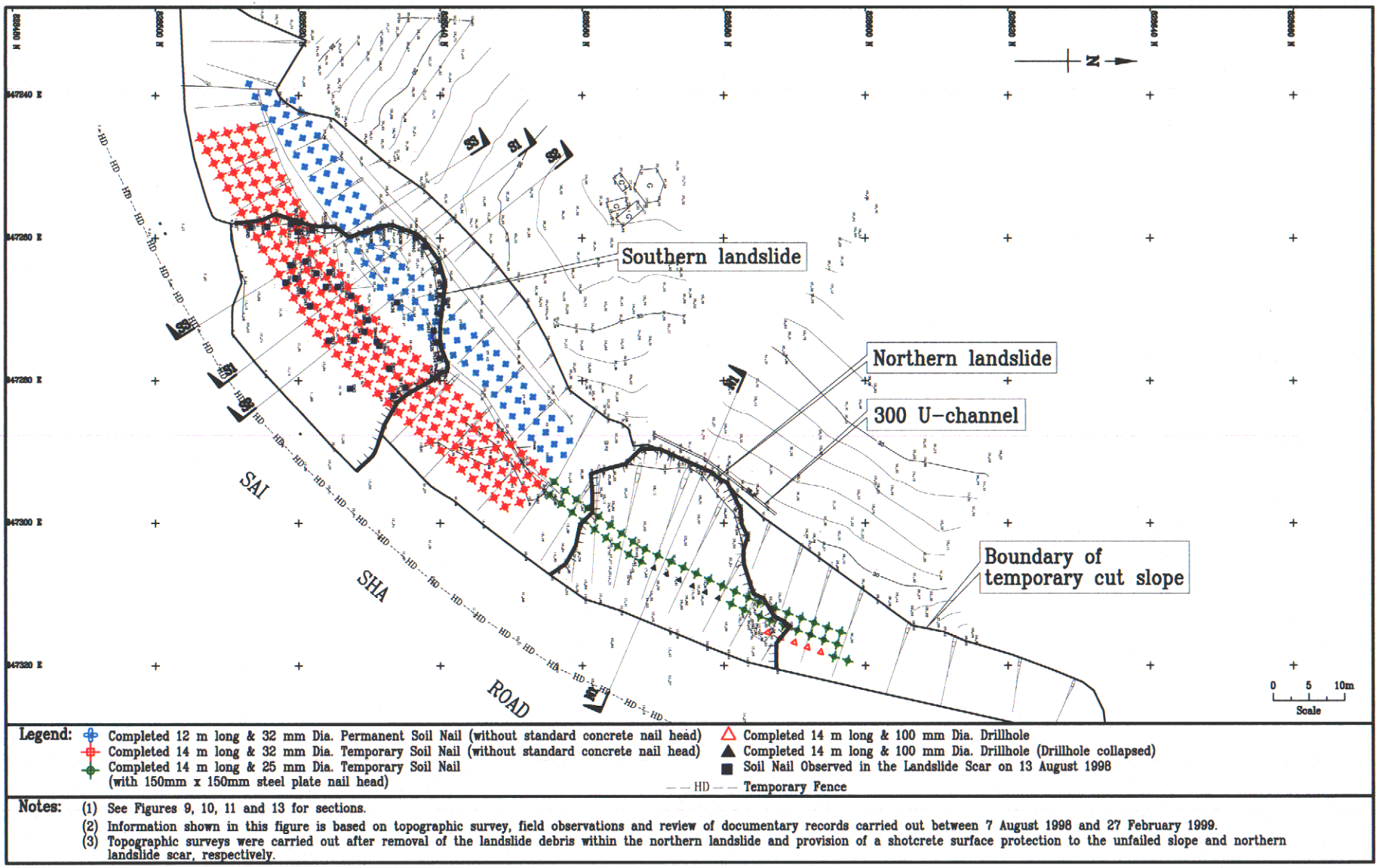


Figure 2 - Plan of the Landslides

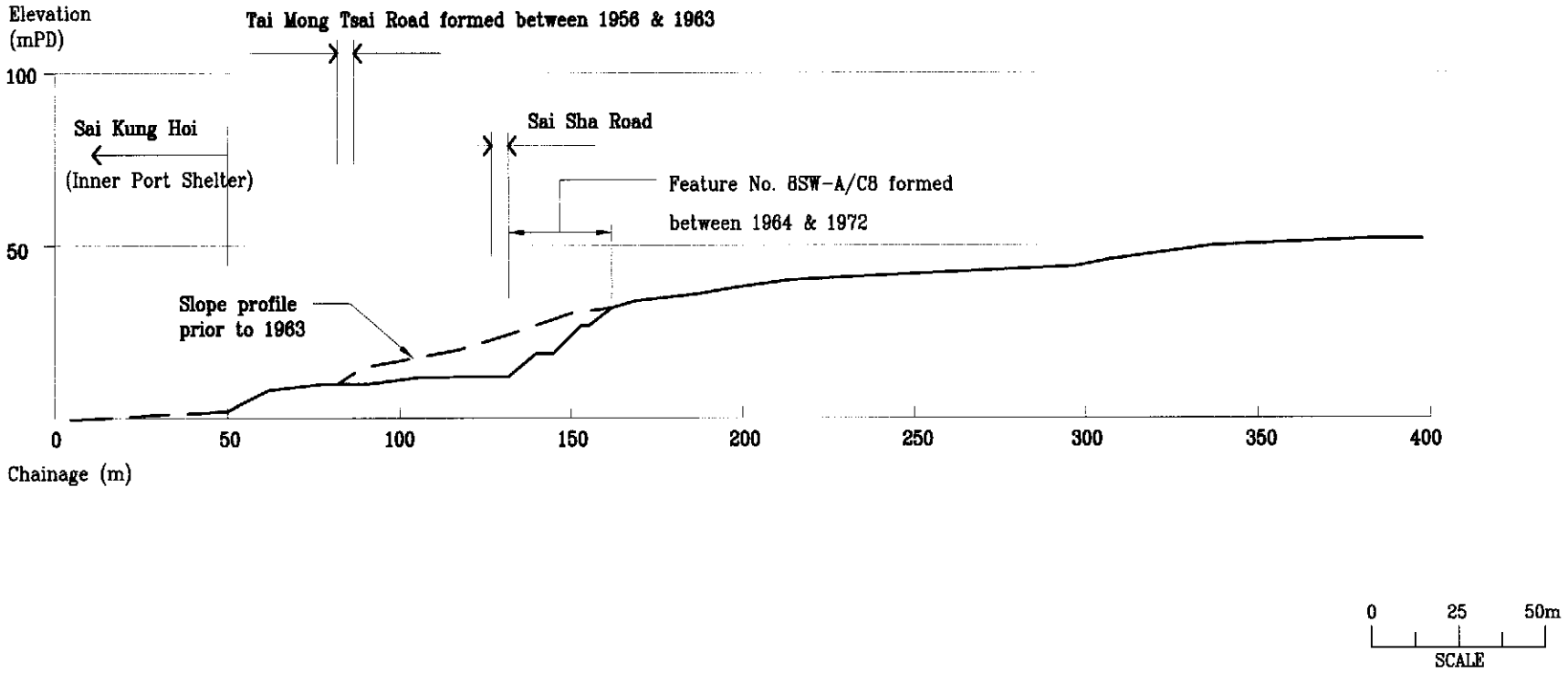


**Notes :** (1) See Figure 1 for location of section.

(2) Information shown in this figure is based on Survey Sheet Nos. 8SW-7A & 8SW-7B (1 : 1000) dated November 1995 and March 1996 respectively and Survey Sheet Nos. C-131-SW-C and C-131-SW-D (1in : 100ft) dated 1963.

Figure 3 - Section A-A Showing the Ground Profile of the Site Area Before and After the Formation of Slope No. 8SW-A/C8

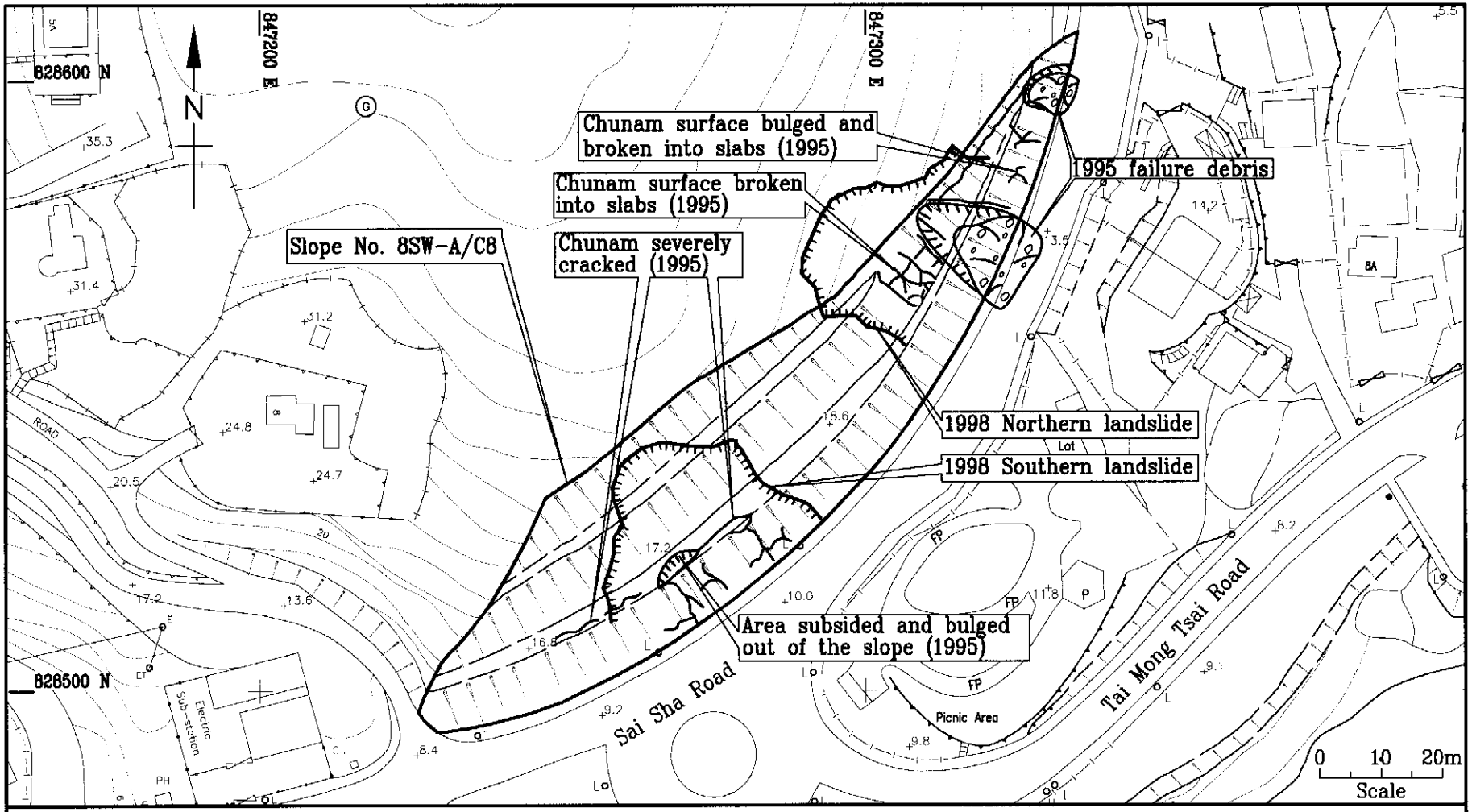


Figure 4 - Locations of 1995 and 1998 Landslides

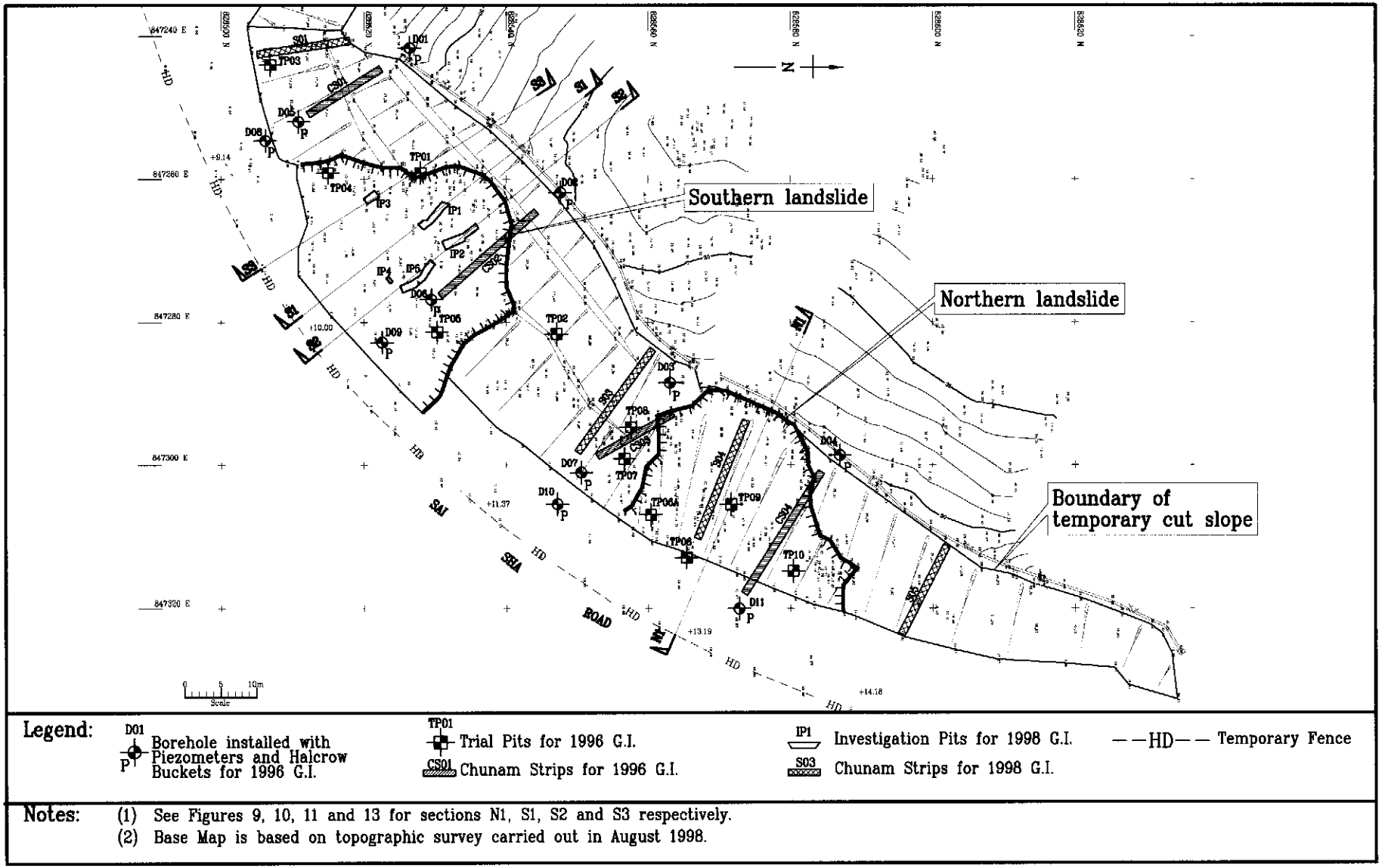


Figure 5 - Plan of Ground Investigation

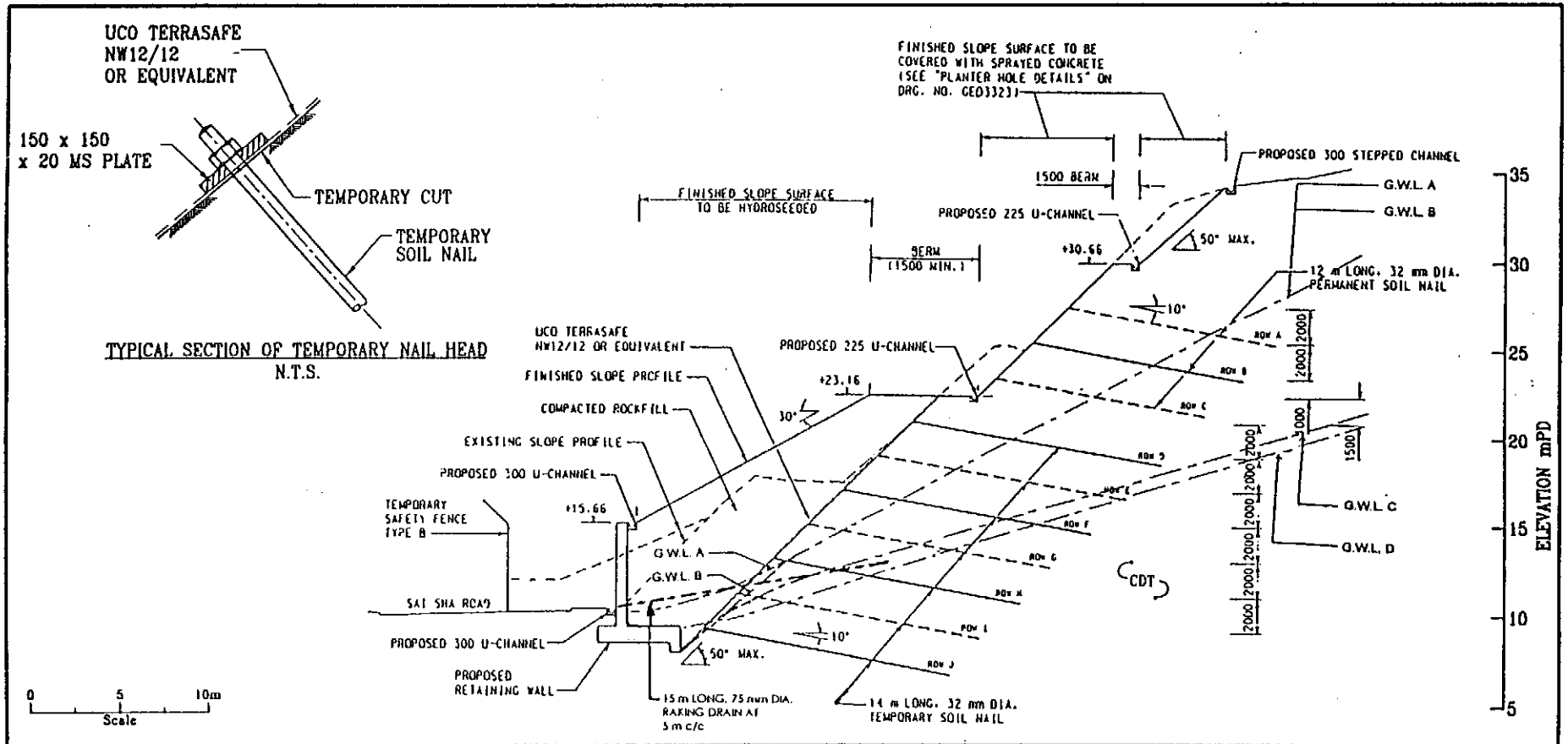


**Legend:** G.W.L.A – Inferred groundwater level corresponding to 2 July 1997 rainstorm
G.W.L.B – Design groundwater level for LPM permanent works
G.W.L.C – Design groundwater level for temporary cut
G.W.L.D – Inferred general groundwater level of 1997 wet season

**Notes:**
1. This section is based on Section 4 – 4 as shown in GEO construction drawing No. GED 3317.
2. The groundwater levels shown in this figure are extracted from GEO stage 3 study report Ref. S3R 152/97.
3. Details of installation of permanent and temporary soil nails were in accordance with GEO standard drawing No. GC 1043C.
4. Nail head details for permanent soil nail Rows A to C were in accordance with GEO standard drawing No. GC 1043/2C.
5. Details of ranking drains were in accordance with CED standard drawing No. C2403.
6. Soil nail drillholes were formed by percussive-rotary drilling with air as the flushing medium.

Figure 6 – Typical Section Showing Details of LPM Works and Ground Conditions Assumed for Design

**Proposed Construction Sequence :**

1. Install soil nail Rows A to F
2. Remove existing rockfill to 900mm below soil nail Row H
3. Install soil nail Rows G and H
4. Remove existing rockfill to ground level
5. Install soil nail Rows I and J
6. Replace existing fence with standard temporary safety fence
7. Excavate to final excavation profile

**Actual Construction Sequence:**

1. Install soil nail Rows A to F on original slope surface during mid Dec. 97 to mid Feb. 98; nail head not yet constructed
2. Remove existing rockfill to level below soil nail Row H during mid Feb. to end Feb. 98
3. Install soil nail Rows G and H during end Feb. 98 to early Mar. 98; nail head not yet constructed
4. Remove existing rockfill to ground level during mid Mar. 98
5. Replace existing fence with standard temporary safety fence during mid Mar. 98 to mid Apr. 98
6. Remove existing chunam on slope face commencing in mid Mar. 98; by end Apr. 98 majority of chunam removed.
7. Excavate to level below soil nail Row I during mid Mar. 98 to early Jun. 98
8. Slope failure occurred on 10 June 1998

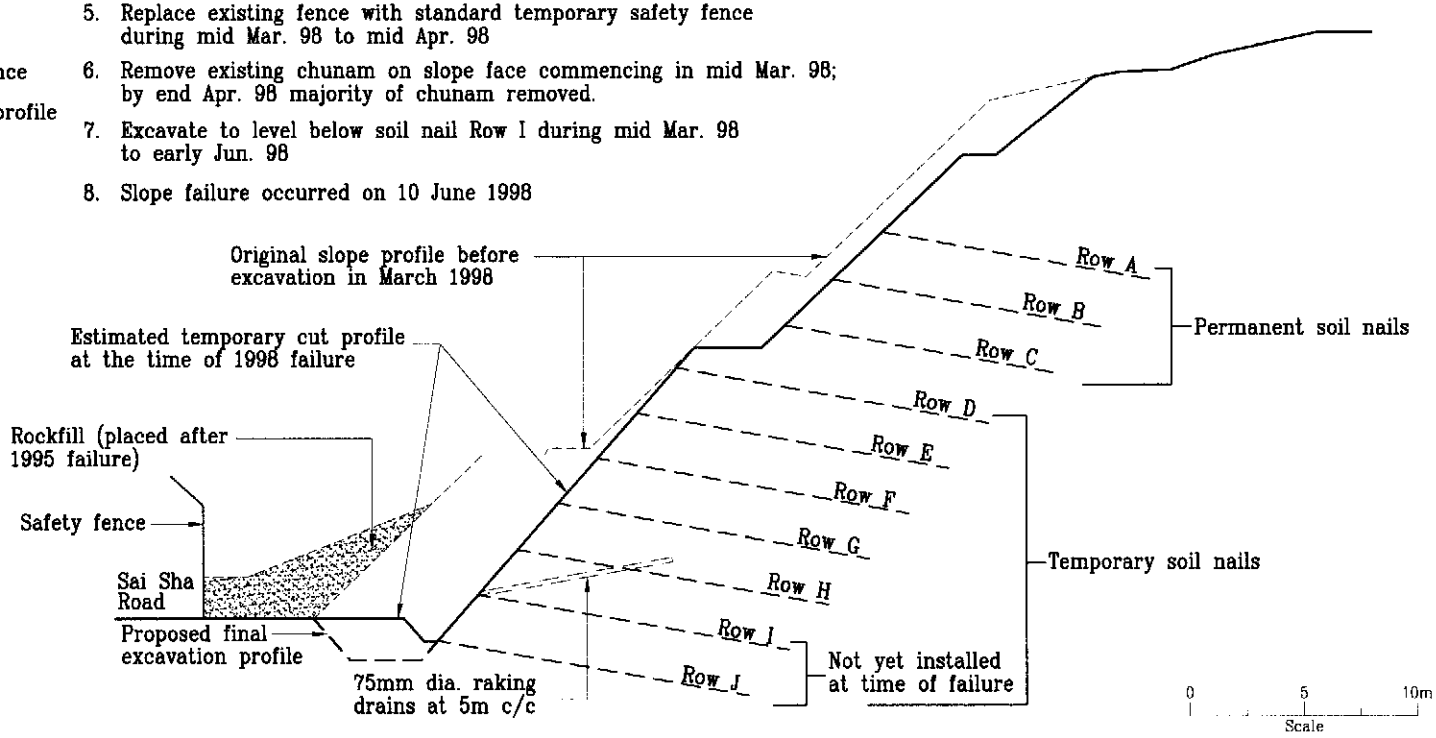


**Notes:** (1) Proposed construction sequence was agreed by the GEO and Contractor on 16 February 1998 on condition that soil nails and raking drains would be installed before the onset of the 1998 wet season.

(2) See Figure 6 for details of proposed LPM works.

Figure 7 - Proposed and Actual Construction Sequence for Temporary Cut at the Southern Landslide Site

**Actual Construction Sequence:**

1. Replace original fence with standard temporary safety fence during mid Feb. 98 to early Mar. 98
2. Remove existing chunam on slope face and excavate to level below soil nail Row G during mid Mar. 98 to end Mar. 98
3. Remove existing rockfill at slope toe and excavate to level below soil nail Row H during end Mar. 98 to end Apr. 98
4. Install soil nail Row D during mid May 98 to end May 98; nail head not yet constructed
5. Construct drillholes for soil nail Row E during end May 98 to early Jun. 98
6. Minor slope failure was noted in the morning on 5 June 1998 which affected some of the drillholes of soil nail Row E (see Figure 2 for locations)
7. Install soil nail Row E which was not affected by the minor failure (5 June 1998) and construct nail heads (150mm square steel plates) for the nails installed, i.e. Rows D and E, in the northern portion of slope (5 June 1998)
8. Major slope failure occurred on 9 June 1998

**Proposed Construction Sequence:**

1. Replace original fence with standard temporary safety fence
2. Excavate to 900mm below soil nail Row G
3. Install soil nail Rows D to G
4. Excavate to final excavation profile
5. Install soil nail Rows H to J

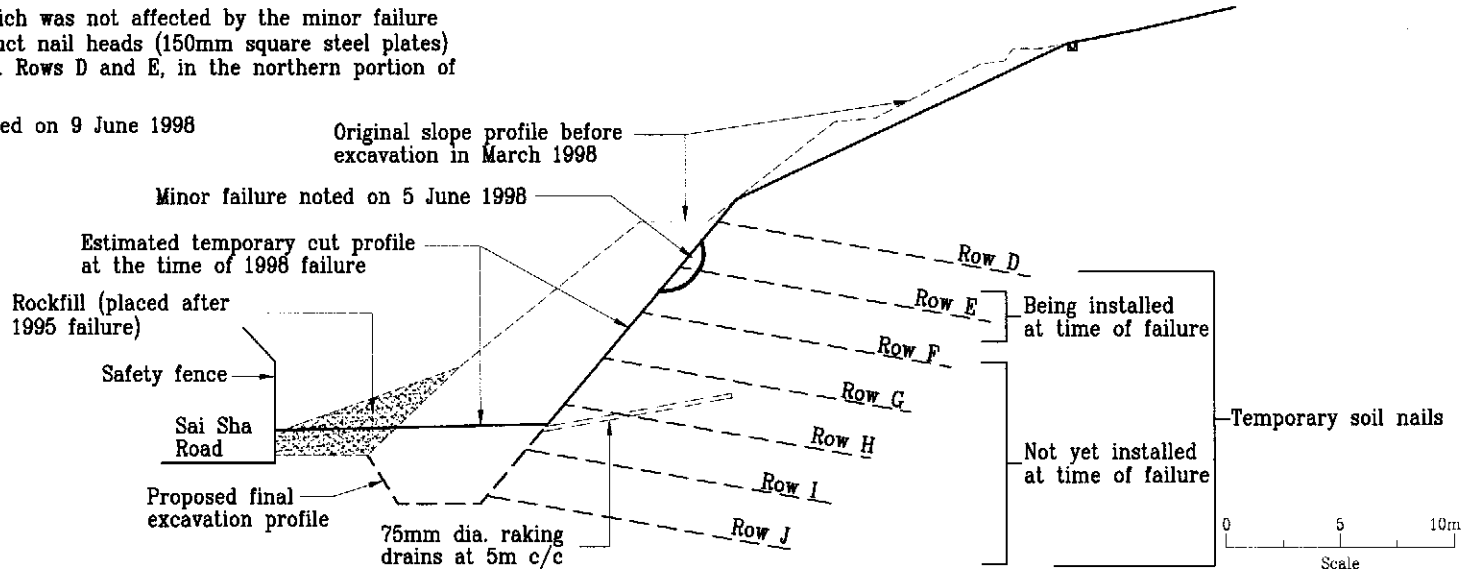


**Notes:** (1) Proposed construction sequence was agreed by the GEO and Contractor on 16 February 1998 on condition that soil nails and raking drains would be installed before the onset of the 1998 wet season.
(2) See Figure 6 for details of proposed LPM works.

Figure 8 - Proposed and Actual Construction Sequence for Temporary Cut at the Northern Landslide Site

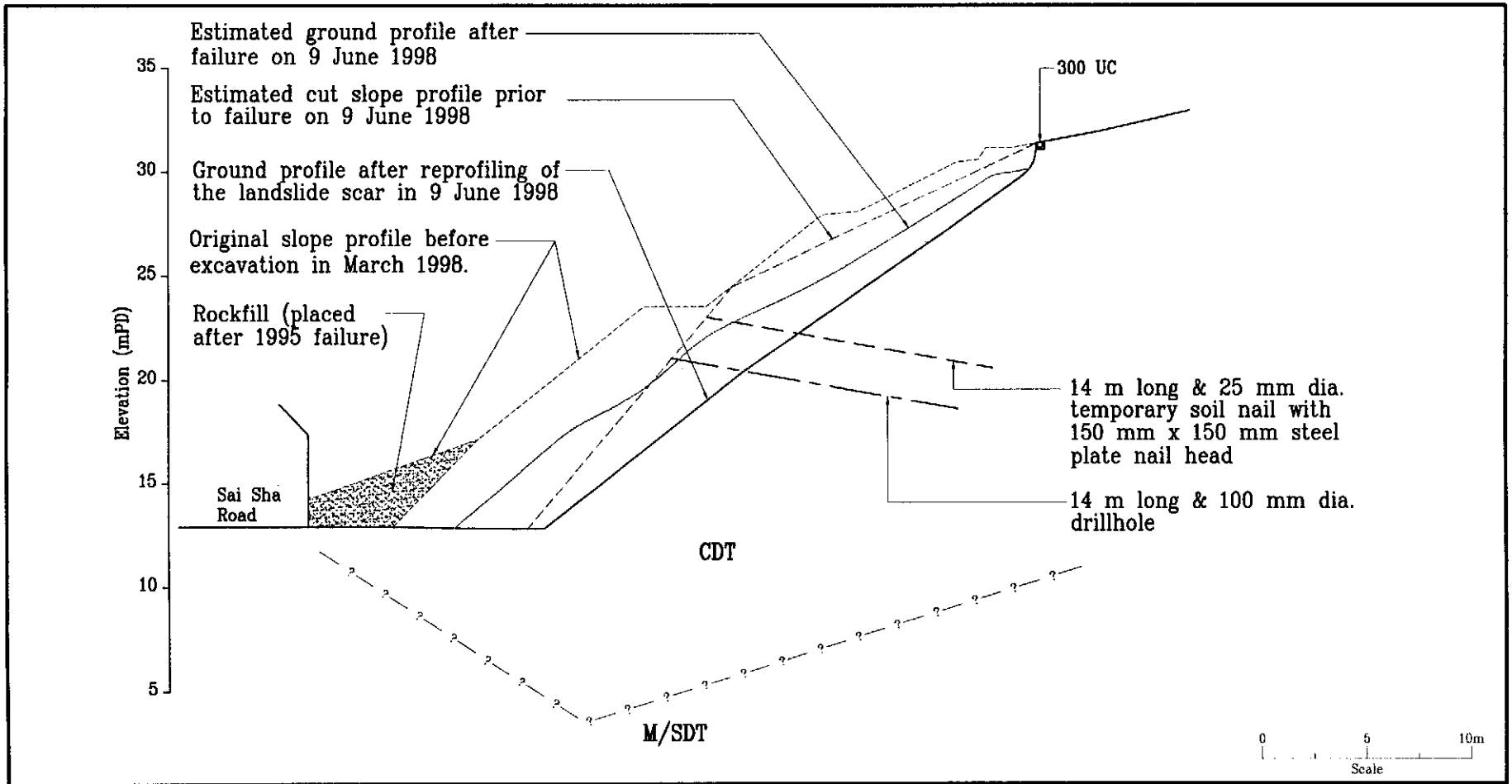


Figure 9 - Section N1 through the Northern Landslide

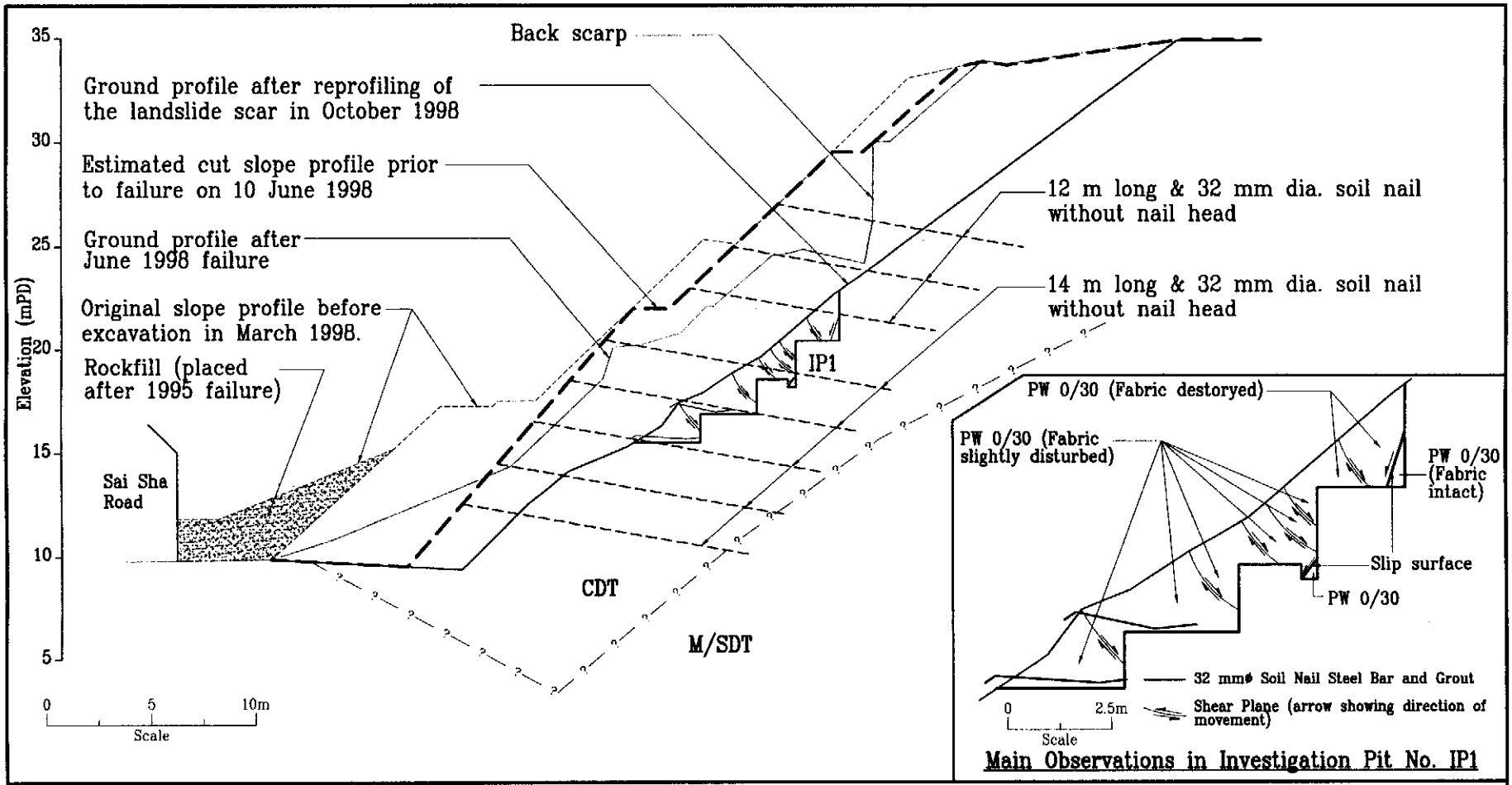


**Legend :** — ? — Inferred Geological Boundary

**Notes :** (1) See Figures 2 and 5 for location of section.
(2) Information shown in this figure is based on topographic survey, geological mapping and documentary records.

Figure 10 - Section S1 through the Southern Landslide

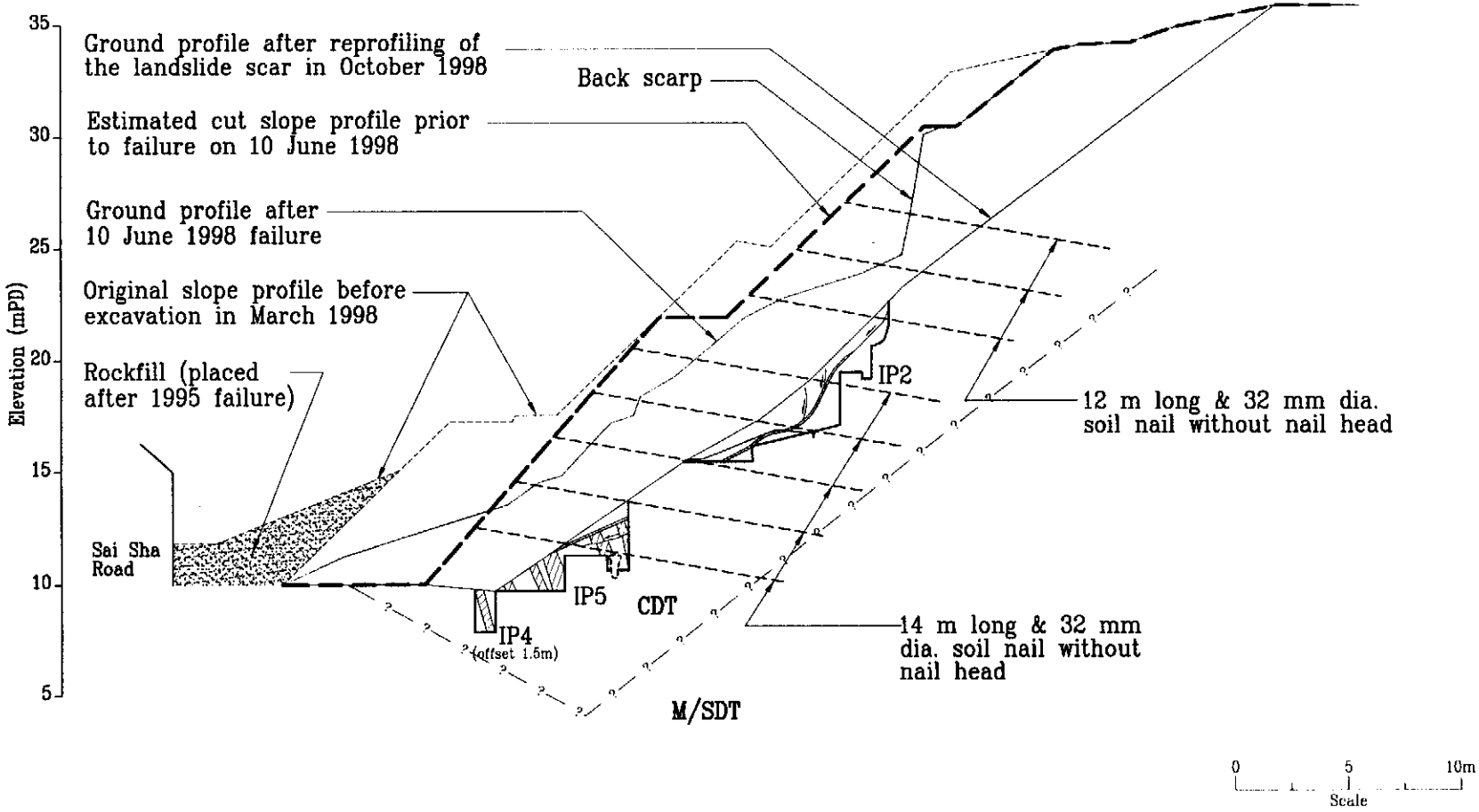


**Legend :** —— ?—— Inferred Geological Boundary

**Notes :** (1) See Figure 2 for location of section and Figure 5 for location of inspection pits on plan.
(2) Details of inspection pit nos. IP2, IP4 and IP5 are shown in Figure 12.
(3) Information shown in this figure is based on topographic survey, geological mapping and documentary records.

Figure 11 - Section S2 through the Southern Landslide

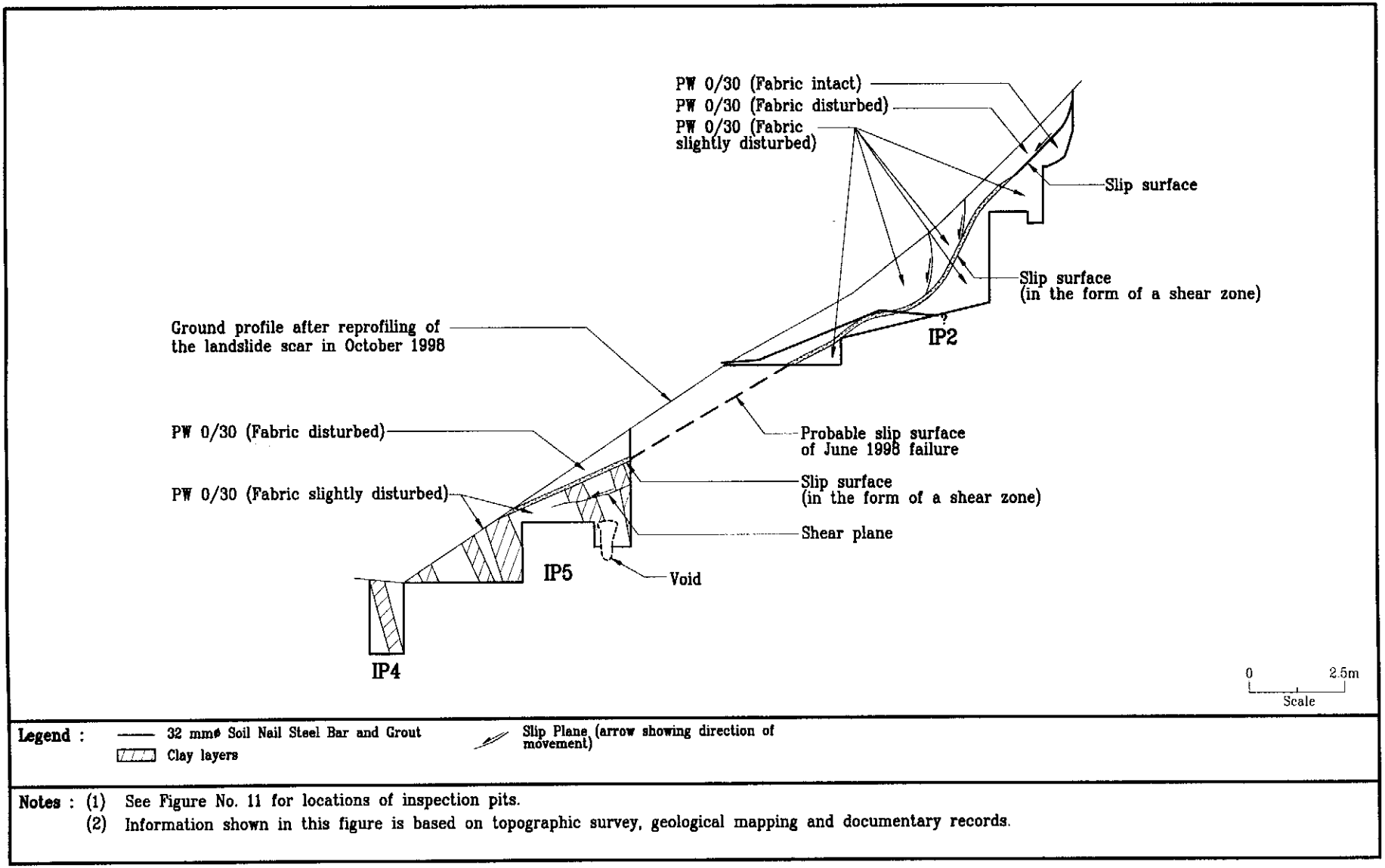


Figure 12 - Main Observations in Inspection Pit Nos. IP2, IP4 and IP5

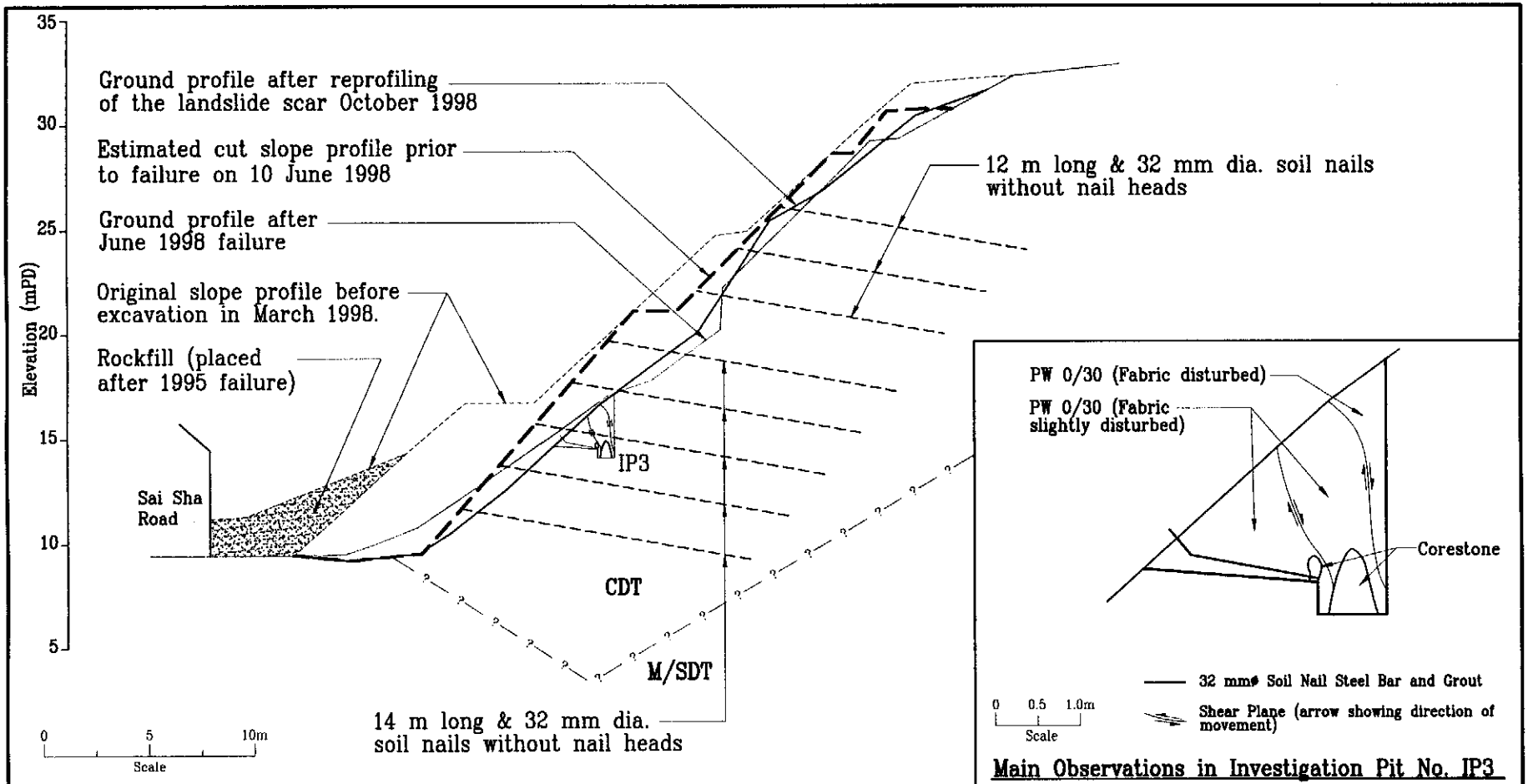


Notes : (1) See Figures 2 and 5 for location of section.
(2) Information shown in this figure is based on topographic survey, geological mapping and documentary records.

Figure 13 - Section S3 through the Southern Landslide

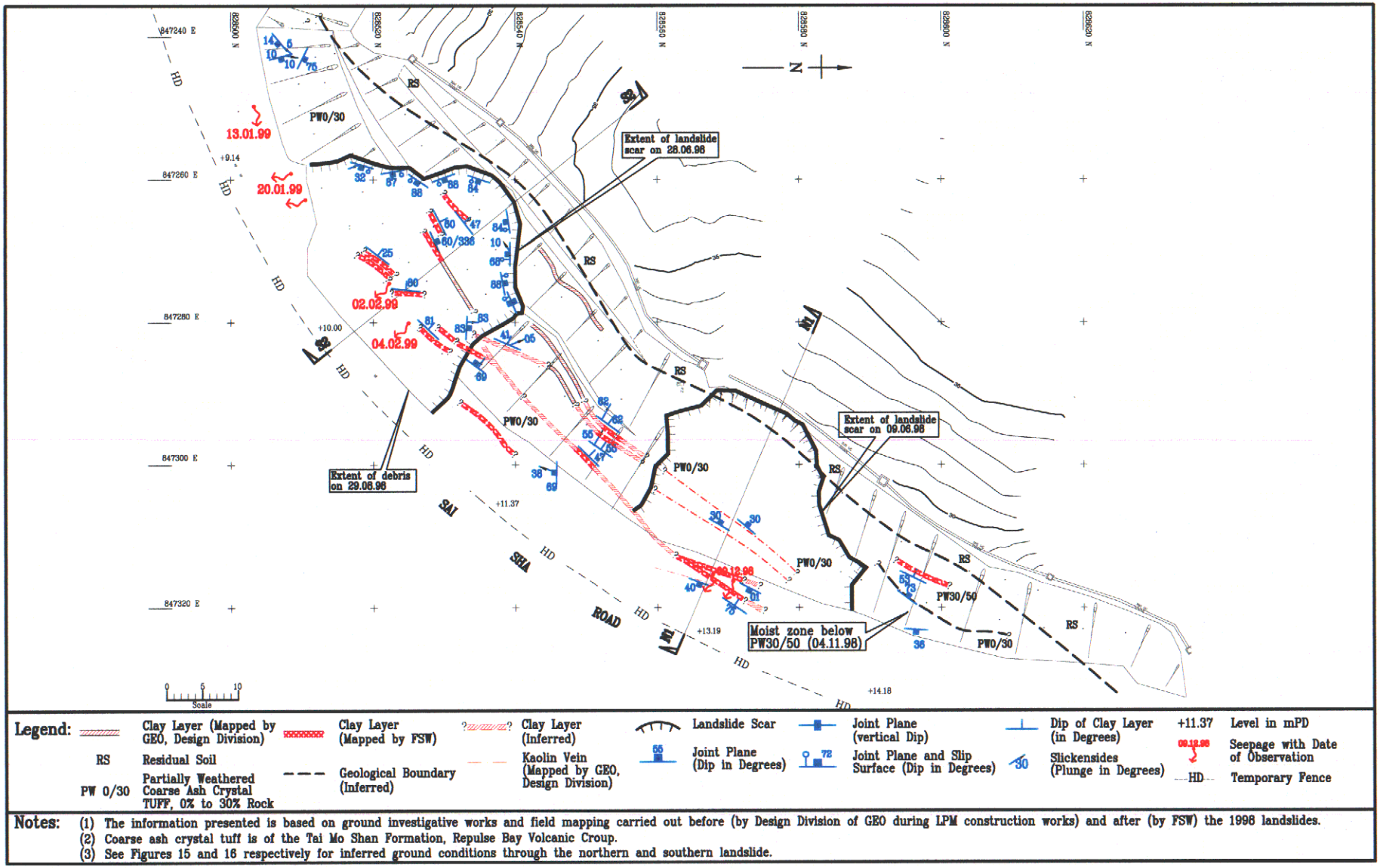


Figure 14 - Geological Features Observed at the Landslide Site

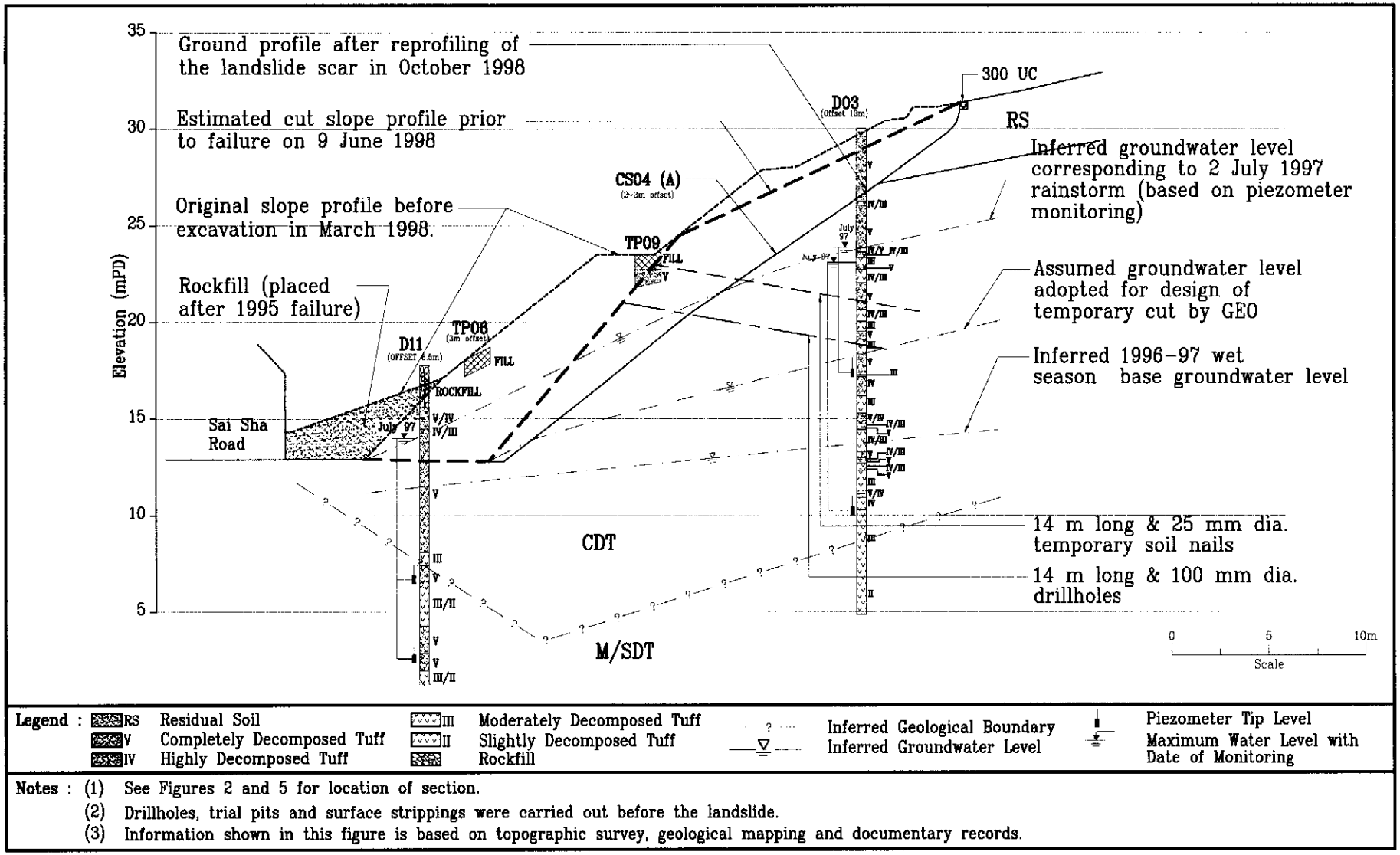


Figure 15 - Section N1 Showing the Inferred Ground Conditions through the Northern Landslide

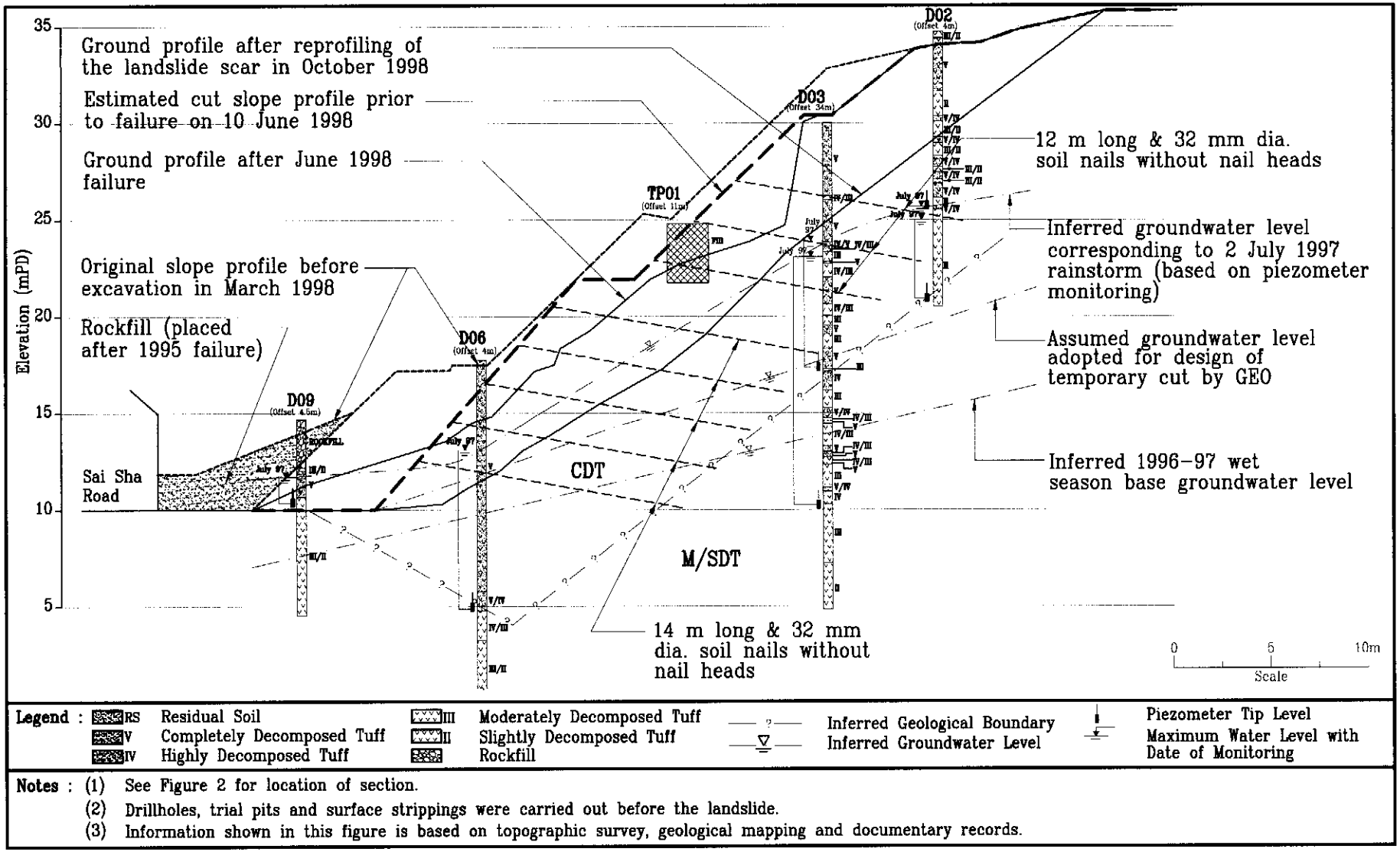


**Notes :** (1) See Figure 2 for location of section.
(2) Drillholes, trial pits and surface strippings were carried out before the landslide.
(3) Information shown in this figure is based on topographic survey, geological mapping and documentary records.

Figure 16 - Section S2 Showing the Inferred Ground Conditions through the Southern Landslide

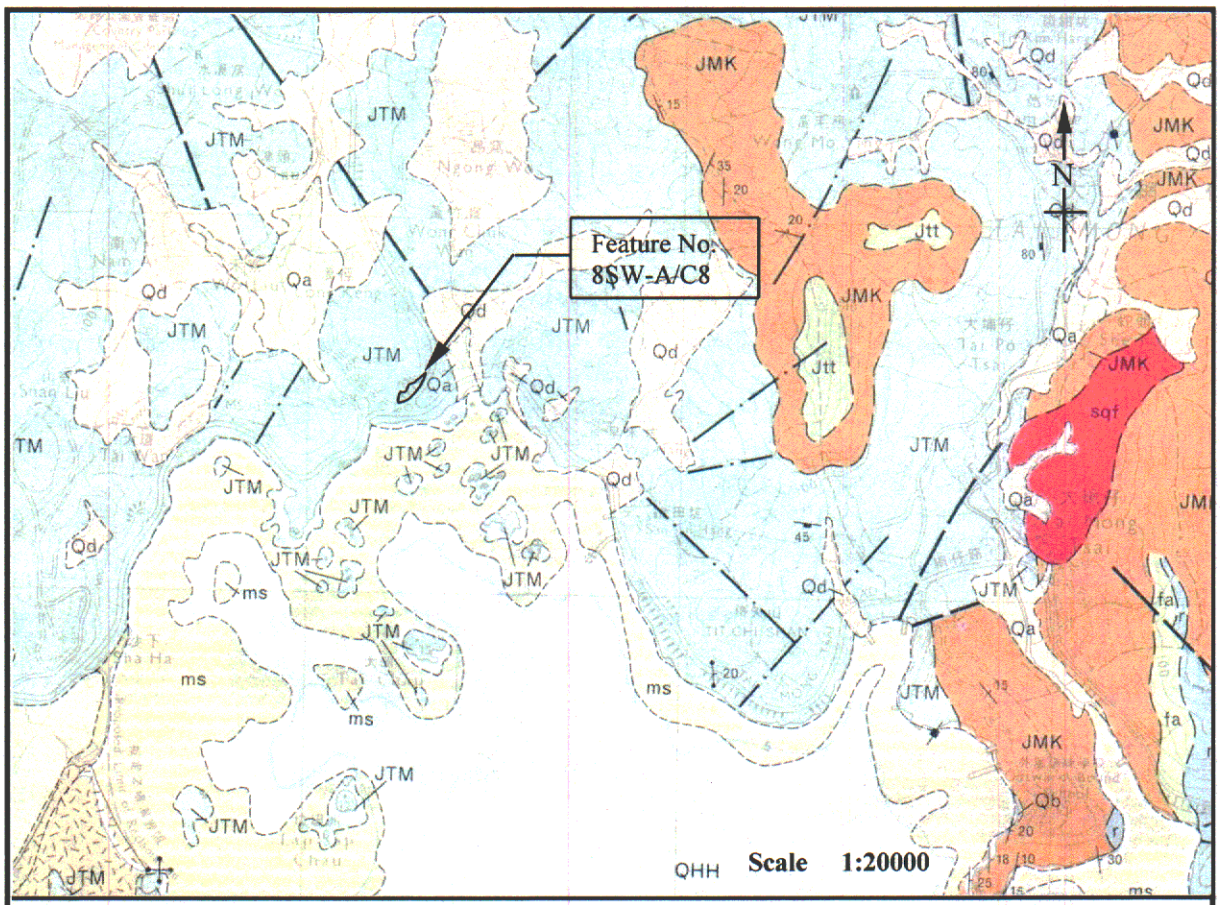


**LEGEND :**

| SUPERFICIAL DEPOSITS | GENETIC CLASSIFICATION | PRINCIPAL MATERIALS |
|---|---|---|
| Qa | Alluvium | Clay/silt, sand and gravel; well-sorted to semi-sorted |
| Qd | Debris flow deposits | Unsorted sand, gravel, cobbles and boulders; clay/siltmatrix |
| QHH | | Undivided, mainly dark grey marine mud |
| ms | | Marine sand, part silty |

**SOLID GEOLOGY**

| | | |
|---|---|---|
| JMK | Repulse Bay Volcanic Group | Undivided, mainly tuffaceous mudstone, siltstone and breccia |
| JTM | Repulse Bay Volcanic Group | Undivided, mainly coarse ash crystal tuff |
| Jtt | Repulse Bay Volcanic Group | Eutaxite |

**GEOLOGICAL LINES**

Geological boundary, superficial deposit
Geological boundary, solid rock
Fault (certain)
Fault (inferred)
Photogeological lineamnet

**STRUCTURAL SYMBOLS**

| | Horizontal | Inclined | Vertical |
|---|---|---|---|
| Bedding | | | |
| Flow fabric | | | |
| Jointing | | | |

Note: Figure is extracted from Hong Kong Geological Survey Sheet 8 (1989) with additional faults and photogeological lineaments from Lai & Langford (1991)

Figure 17 – Regional Geological Plan

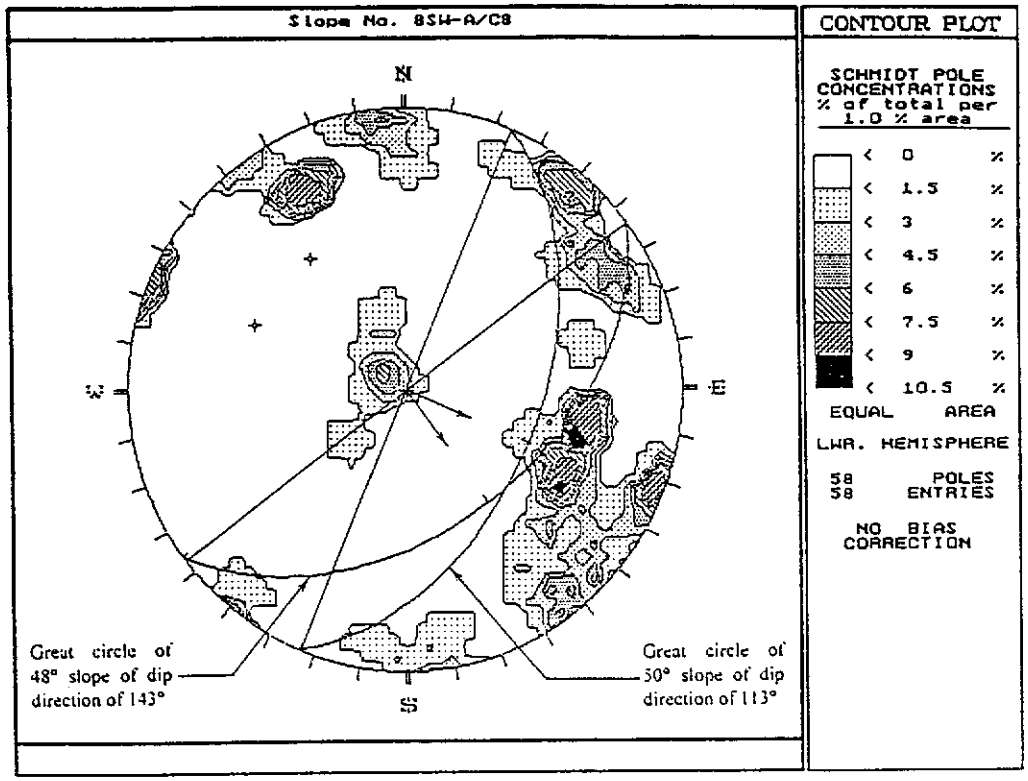


(a) Relict Joints

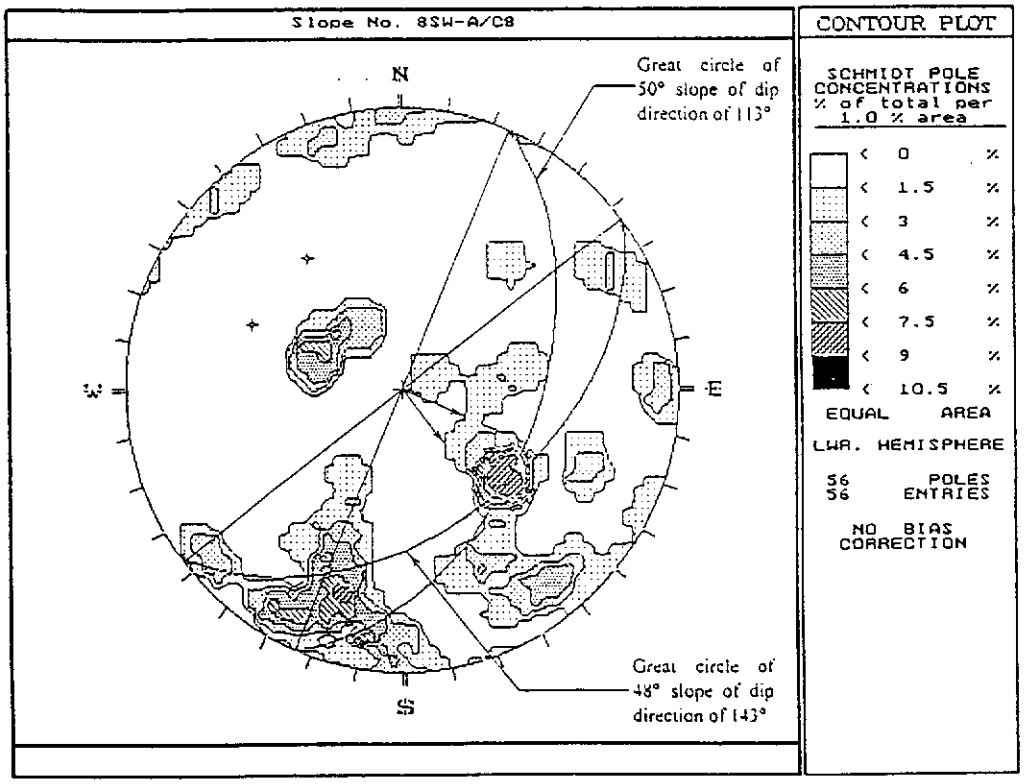


(b) Slickensided Relict Joints

Note: Dip angles and dip directions of the slope profile before the 1998 failures are $50^0/113^0$ and $48^0/143^0$ for the Northern and Southern Landslides, respectively.

Figure 18 – Stereoplots for the Measured Orientations of Relict Joints in Completely Decomposed Tuff

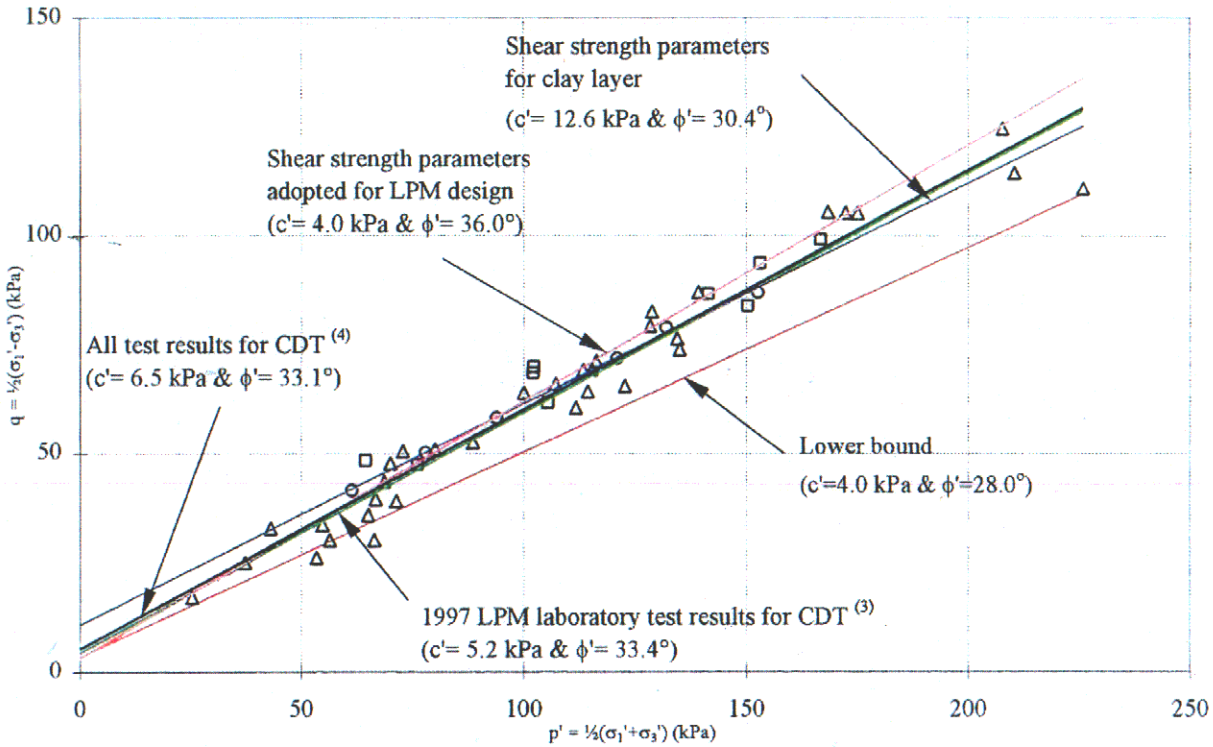


**Legend :** □ Data Points from 1998/99 Laboratory Test Results for CDT ○ Data Points from 1998/99 Laboratory Test Results for Clay Layer
△ Data Points from 1997 LPM Laboratory Test Results for CDT

**Notes :**
(1) Triaxial compression test results correspond to those at the point of maximum stress obliquity, i.e. maximum stress ratio s1'/s3'.
(2) Line of strength parameters are lines of best fit by least square method.
(3) Line of best fit for 1997 LPM laboratory test results for CDT.
(4) Line of best fit for all laboratory test results (i.e. results of 1997 laboratory tests for LPM and 1998/99 laboratory tests for landslide investigation).

Figure 19 – Triaxial Compression Test Results for Completely Decomposed Tuff/Clay Layer

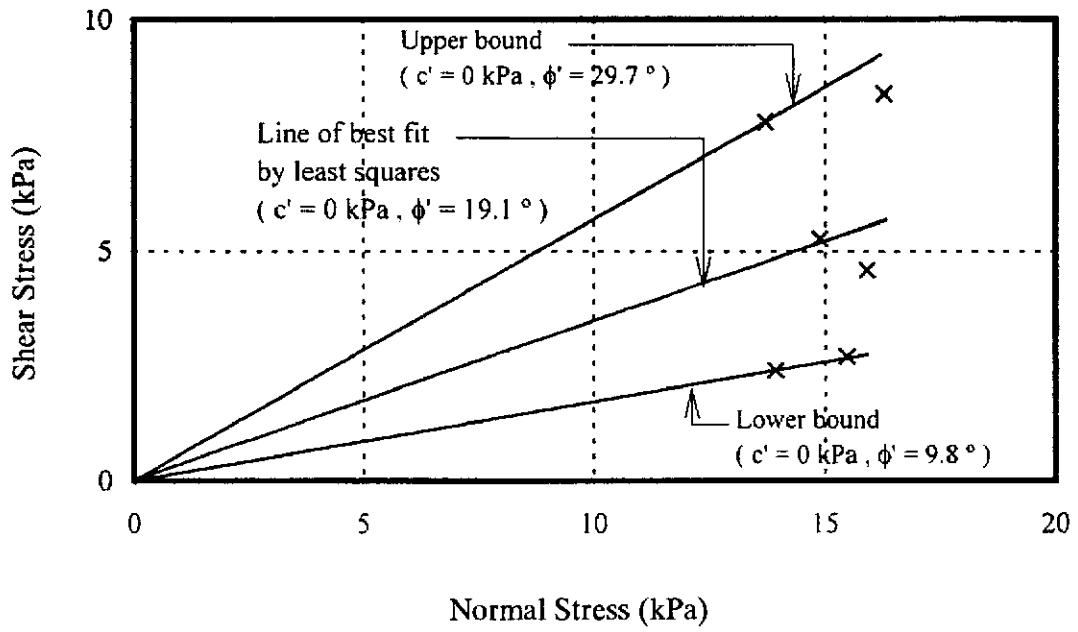


Test Results for Slickensided Relict Joints

**Legend:** c' cohesion ϕ' Angle of shearing resistance

**Notes:**
(1) Specimens were sheared along the joint plane and along the slickensided direction for slickensided joint planes.
(2) Direct shear test results shown in this figure corresppond to those at the point of peak shear stress.
(3) Zero cohesion intercept was assumed in fitting the line of best fit by least square method.

Figure 20 – Direct Shear Box Test Result for Relict Joints in Completely Decomposed Tuff

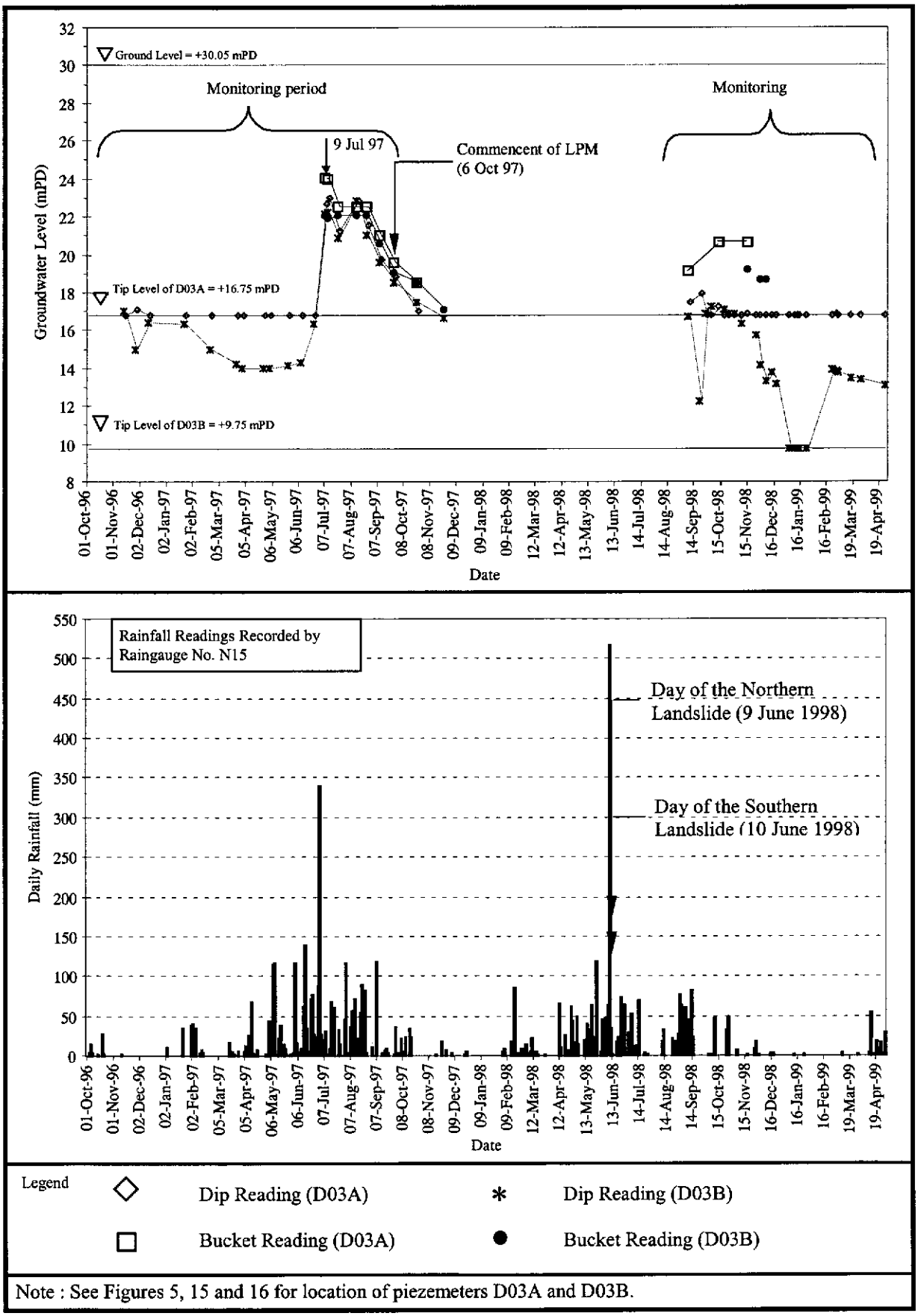


Note : See Figures 5, 15 and 16 for location of piezemeters D03A and D03B.

Figure 21 – Records of Groundwater Monitoring

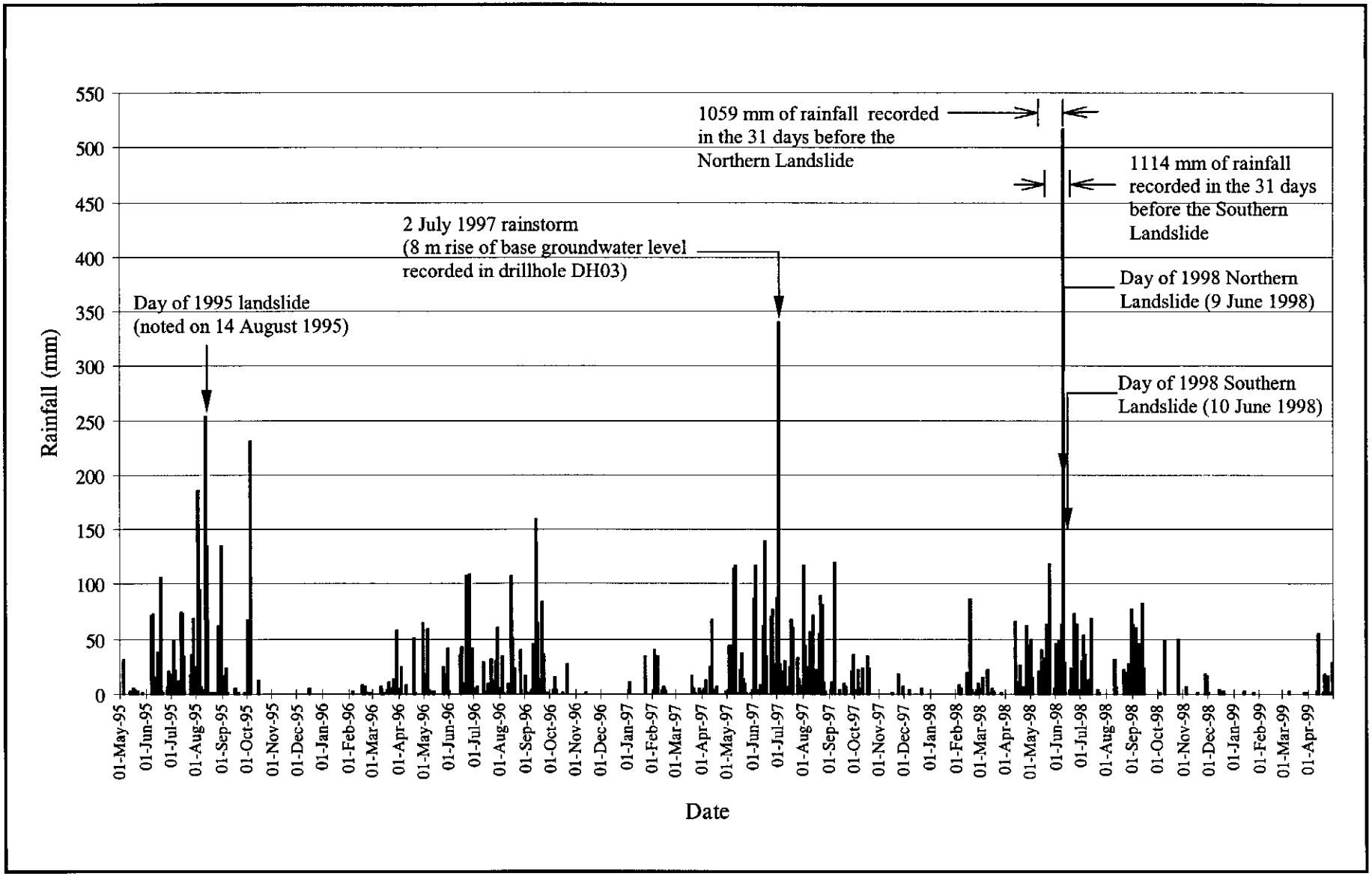


Figure 22 – Daily Rainfall Records of GEO Raingauge No. N15

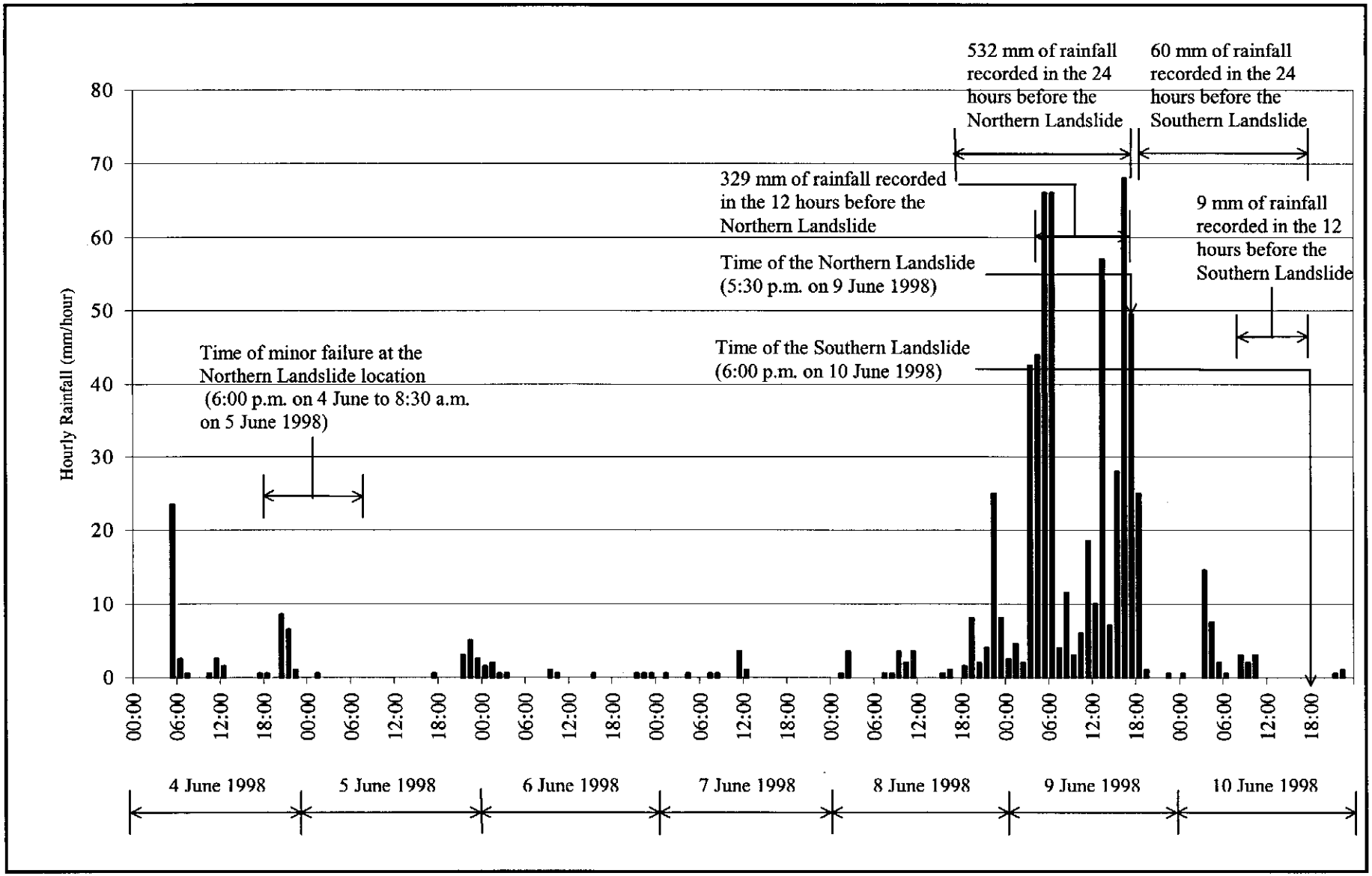


Figure 23 – Hourly Rainfall Records of GEO Raingauge No. N15

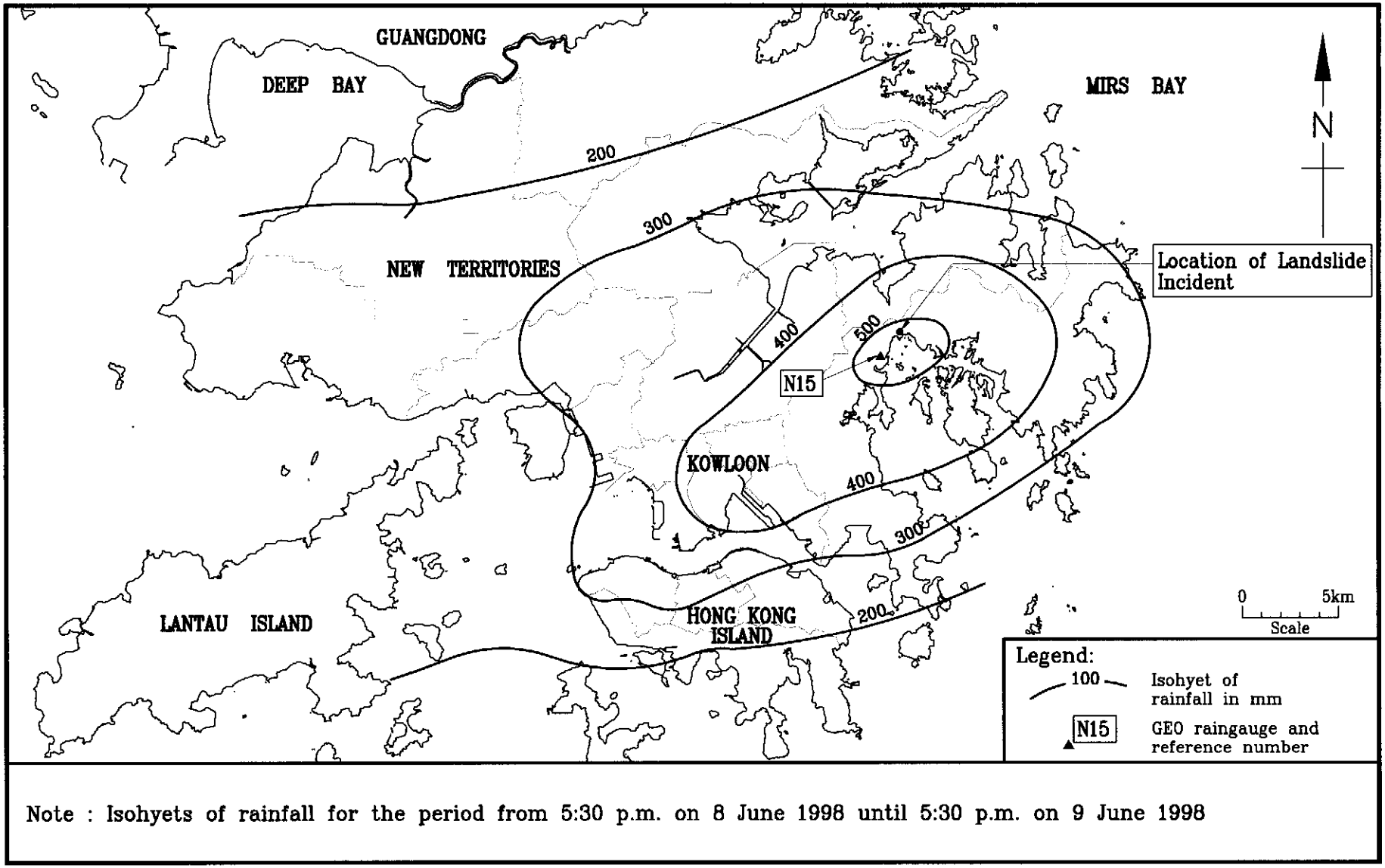


Note : Isohyets of rainfall for the period from 5:30 p.m. on 8 June 1998 until 5:30 p.m. on 9 June 1998

Figure 24 - Rainfall Distribution in the 24 hour Period Preceding the Landslide of 9 June 1998

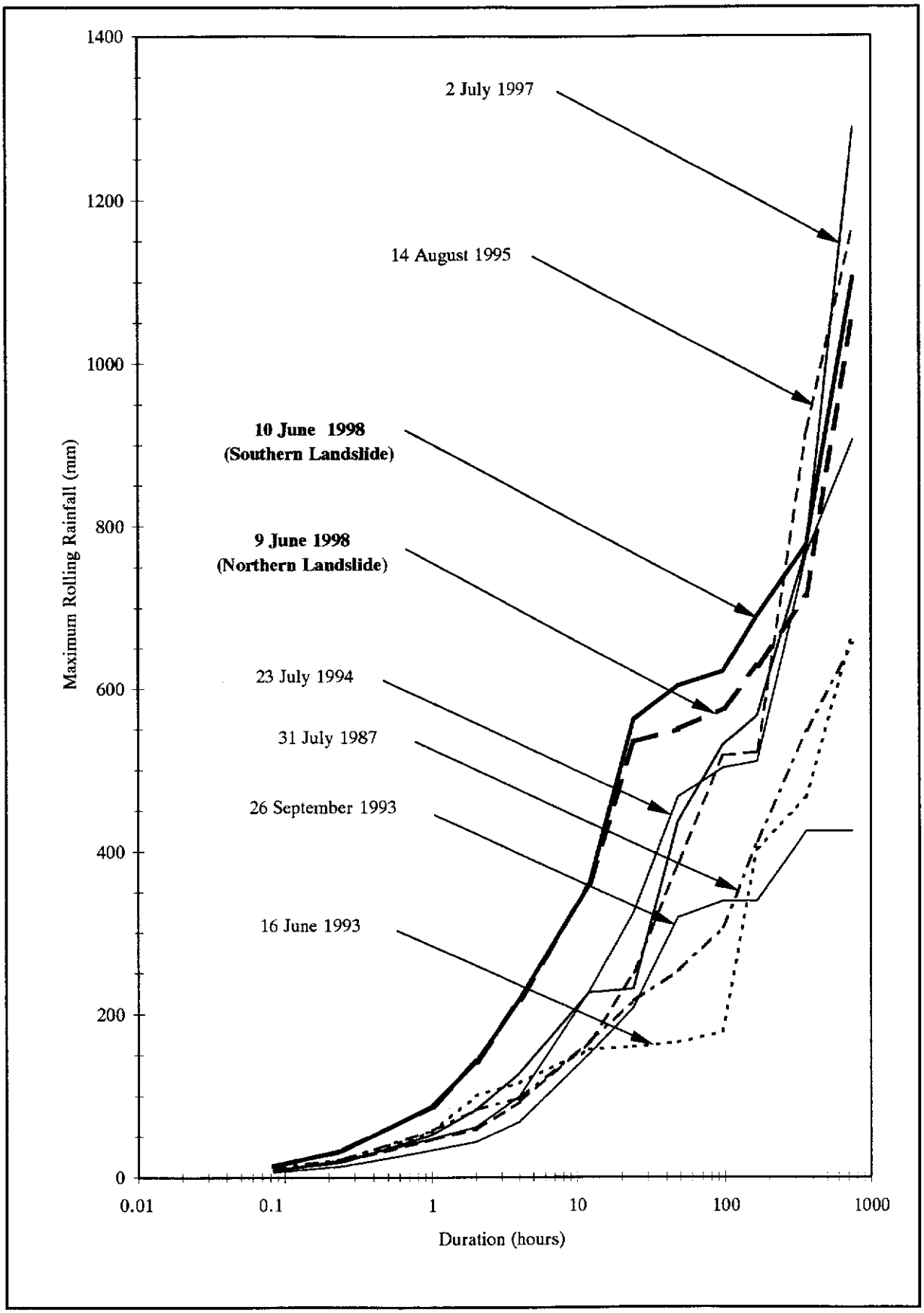


Figure 25 - Maximum Rolling Rainfalls at Raingauge No. N15 for Major Rainstorms

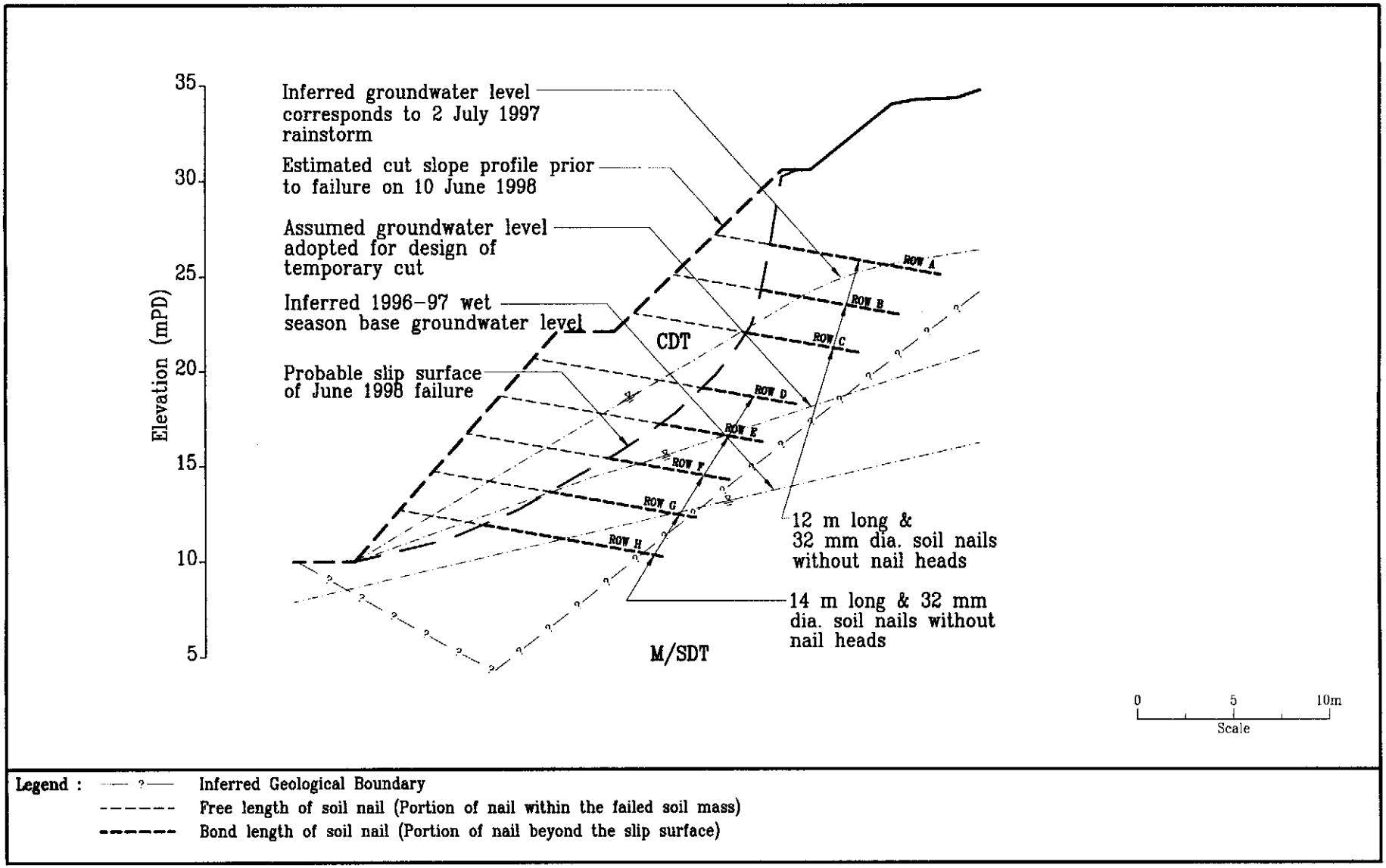


Figure 26 - Cross-section of the Southern Landslide

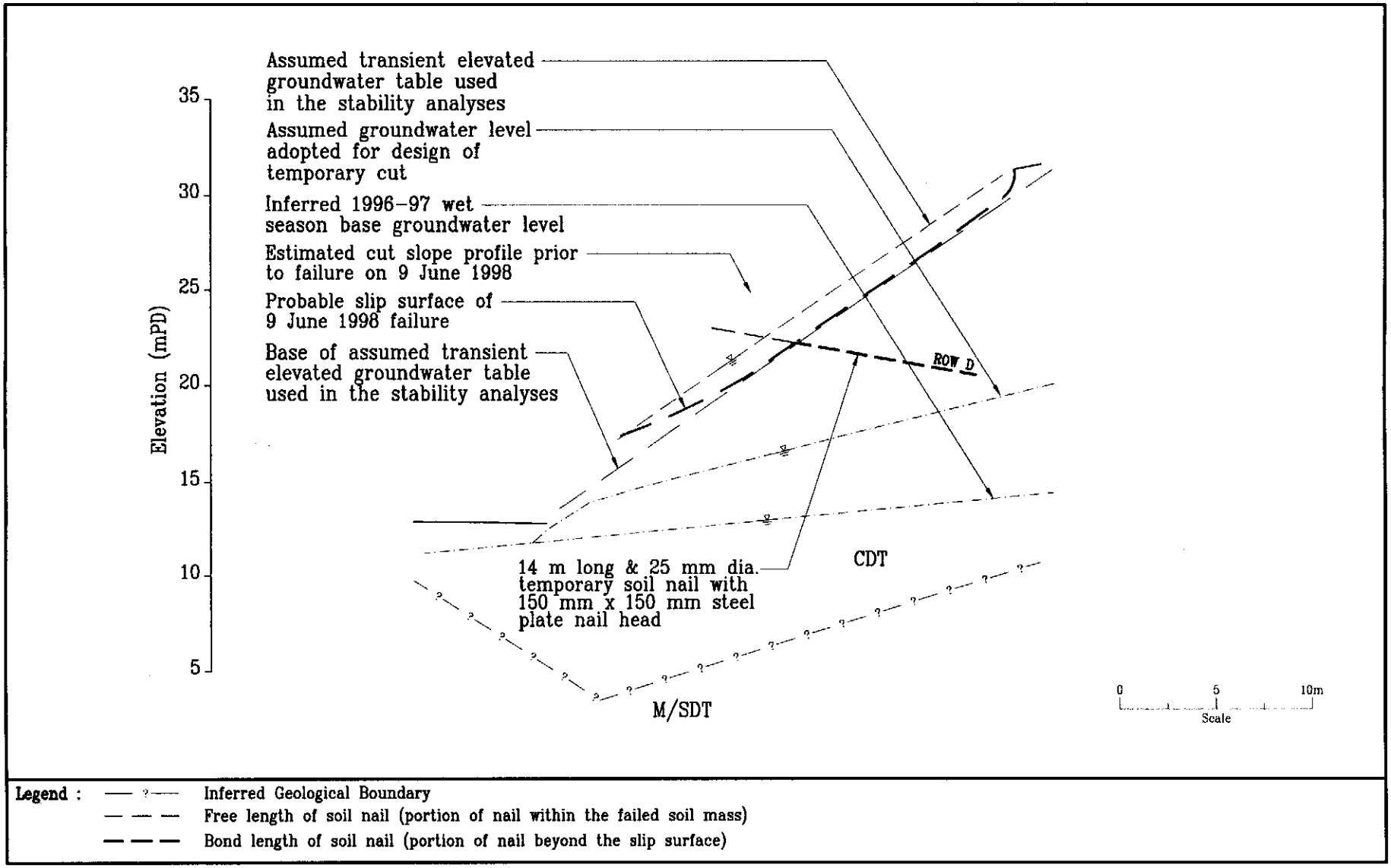


Figure 27 - Cross-section of the Northern Landslide

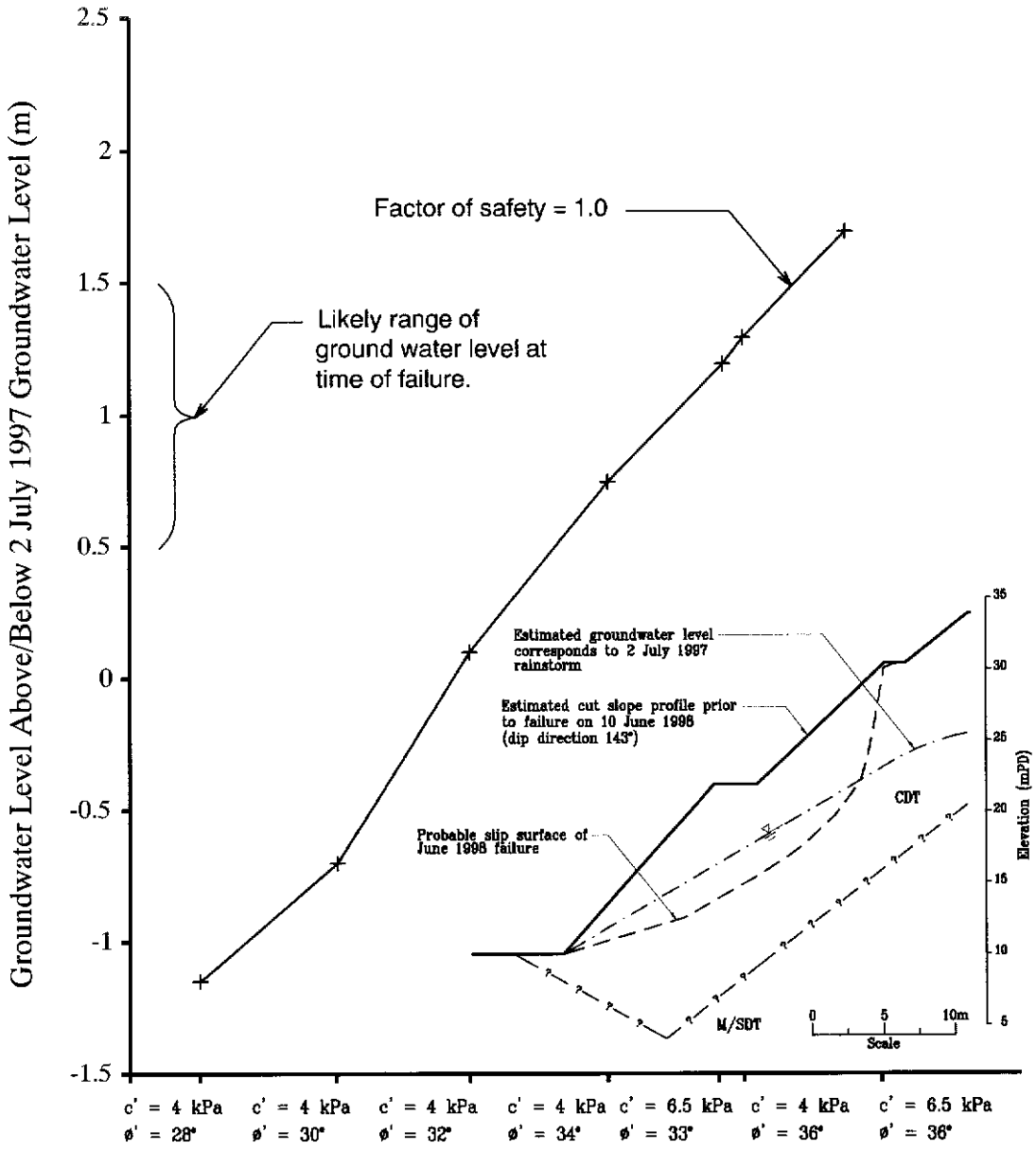


Operational Shear Strength for the Southern Landslide

Note : Heights of groundwater level above/below groundwater level corresponding to 2 July 1997 rainstorm are measured vertically at the slope crest.

Figure 28 - Results of the Stability Analysis for the Southern Landslide

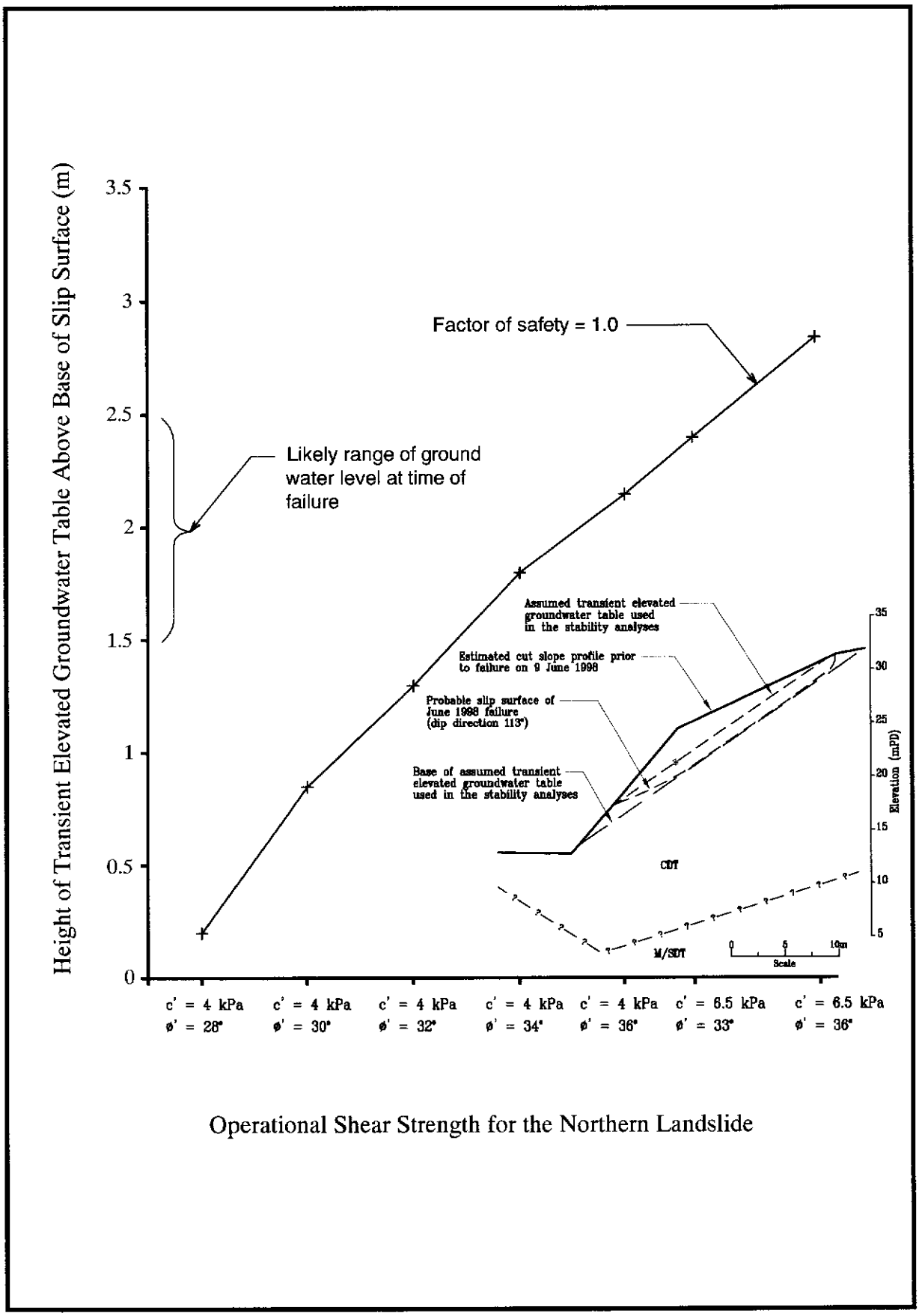


Operational Shear Strength for the Northern Landslide

Figure 29 - Results of the Stability Analysis for the Northern Landslide

| Zone no. | Average inclination of slip surface to the horizonral, ∝ | No. of relict joints within the critical range (1) | Percentage of relict joints within the critical range (%) | Probability of relict joint affecting stability $(P_\theta)_j$ | No. of slickensided relict joints within the critical range | Percentage of slickensided relict joints within the critical range (%) | Probability of slickensided relict joint affecting stability $(P_\theta)_s$ |
|---|---|---|---|---|---|---|---|
| 1 | 79° | 5 | 4.4 | 0.044 | 18 | 15.8 | 0.158 |
| 2 | 54° | 0 | 0 | 0.053 | 6 | 5.3 | 0.053 |
| 3 | 28° | 6 | 5.3 | 0.053 | 1 | 0.9 | 0.009 |
| 4 | 27° | 6 | 5.3 | 0.053 | 3 | 2.6 | 0.026 |
| 5 | 18° | 6 | 5.3 | 0.053 | 5 | 4.4 | 0.044 |
| | | | | Average = 0.041 | | | Average = 0.058 |

| | Inclination of soil nail | No. of relict joints within the critical range (1) | Percentage of relict joints within the critical range (%) | Probability of relict joint affecting stability $(P_\theta)_j$ | No. of slickensided relict joints within the critical range | Percentage of slickensided relict joints within the critical range (%) | Probability of slickensided relict joint affecting stability $(P_\theta)_s$ |
|---|---|---|---|---|---|---|---|
| Soil nail | −10° | 6 | 5.3 | 0.053 | 4 | 3.5 | 0.035 |

Total no. of relict joints = 56(+) ; total no. of slickensided relict joints = 58(◊)

Notes :

1. Critical range is defined as the range of adverse joint orientations affecting the stability of a slip surface. Koo (1982) proposed a critical range of ∝±20 (∝= average inclination of the slip surface) for slope stability analyses. For example, for zone 2 of the slip surface the critical range is defined as the hatched area shown on the equal area stereo projection below:

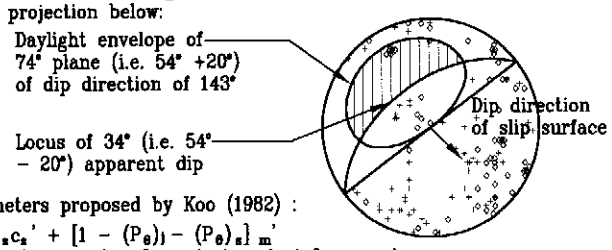


2. Soil mass strength parameters proposed by Koo (1982) :

$c' = (P_\theta)_j c_j' + (P_\theta)_s c_s' + [1 - (P_\theta)_j - (P_\theta)_s] c_m'$

$\tan \phi' = (P_\theta)_j \tan \phi_j' + (P_\theta)_s \tan \phi_s' + [1 - (P_\theta)_j - (P_\theta)_s] \tan \phi'$

where $c_j' = 2$kPa , $\phi_j' = 30°$ are shear strength parameters of relict joint (assumed)
$c_s' = 0$kPa , $\phi_s' = 19.1°$ are shear strength parameters of slickensided relict joint (see Figure 20)
$c_m' = 6.5$kPa , $\phi_m' = 33.1°$ are shear strength parameters of intact CDT (see Figure 19)

(i) For slope stability analyses:

$c' = 0.041 \times 2 + 0.058 \times 0 + (1 - 0.041 - 0.058) \times 6.5 = 5.9$ kPa

$\phi' = \tan^{-1} [0.041 \tan 30° + 0.058 \tan 19.1° + (1 - 0.041 - 0.058) \times \tan 33.1°] = 32.3°$

(ii) For estimate of soil nail forces:

$c' = 0.053 \times 2 + 0.035 \times 0 + (1 - 0.053 - 0.035) \times 6.5 = 6$ kPa

$\phi' = \tan^{-1} [0.053 \tan 30° + 0.035 \times \tan 19.1° + (1 - 0.053 - 0.035) \tan 33.1°] = 32.5°$

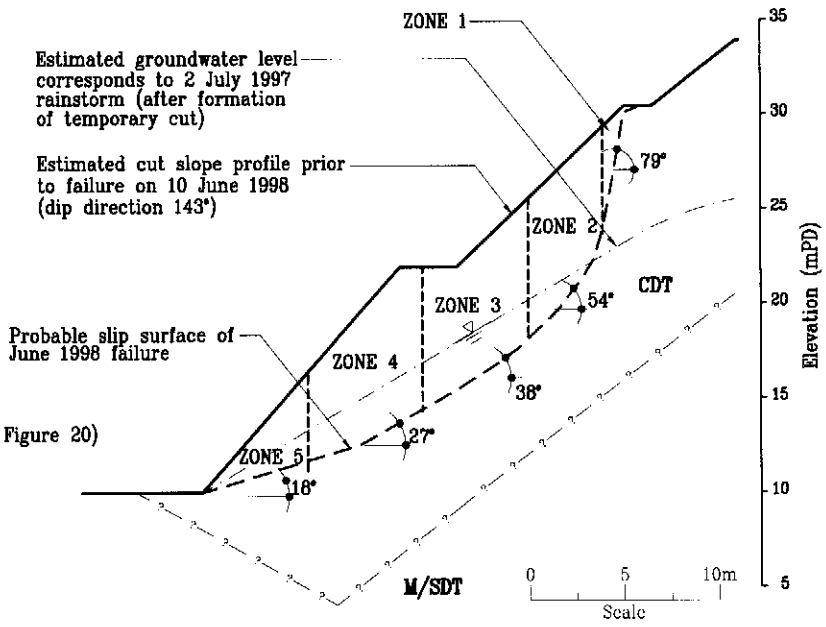


Figure 30 - Representative Cross-section and Soil Mass Strength of the Southern Landslide for Slope Stability Analysis

| Zone no. | Average inclination of slip surface to the horizontal, $\propto$ | No. of relict joints within the critical range (1) | Percentage of relict joints within the critical range (%) | Probability of relict joint affecting stability $(P_\theta)_j$ | No. of slickensided relict joints within the critical range | Percentage of slickensided relict joints within the critical range (%) | Probability of slickensided relict joint affecting stability $(P_\theta)_s$ |
|---|---|---|---|---|---|---|---|
| 1 | 40° | 5 | 4.4 | 0.041 | 0 | 0 | 0 |
| 2 | 34° | 6 | 5.3 | 0.053 | 1 | 0.9 | 0.009 |
| 3 | 34° | 6 | 5.3 | 0.053 | 1 | 0.9 | 0.009 |
| 4 | 22° | 6 | 5.3 | 0.053 | 4 | 3.5 | 0.035 |
| | | | | 0.051 | | | Average = 0.073 |

| | Inclination of soil nail | No. of relict joints within the critical range (1) | Percentage of relict joints within the critical range (%) | Probability of relict joint affecting stability $(P_\theta)_j$ | No. of slickensided relict joints within the critical range | Percentage of slickensided relict joints within the critical range (%) | Probability of slickensided relict joint affecting stability $(P_\theta)_s$ |
|---|---|---|---|---|---|---|---|
| Soil nail | -10° | 3 | 2.6 | 0.026 | 5 | 4.4 | 0.044 |

Total no. of relict joints = 56(+); total no. of slickensided relict joints = 58(◊)

**Notes :**

1. Critical range is defined as the range of adverse joint orientations affecting the stability of a slip surface. Koo (1982) proposed a critical range of $\propto \pm 20$ ($\propto$ = average inclination of the slip surface) for slope stability analyses. For example, for zone 1 of the slip surface the critical range is defined as the hatched area shown on the equal area stereo projection below:

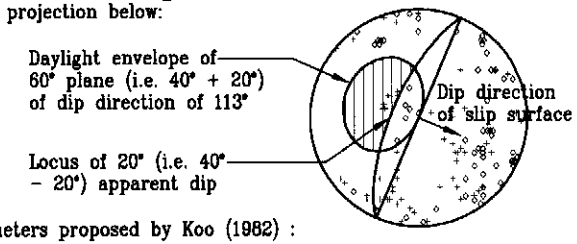


2. Soil mass strength parameters proposed by Koo (1982) :

$c' = (P_\theta)_j c_j' + (P_\theta)_s c_s' + [1 - (P_\theta)_j - (P_\theta)_s] c_m'$

$\tan \phi' = (P_\theta)_j \tan \phi_j' + (P_\theta)_s \tan \phi_s' + [1 - (P_\theta)_j - (P_\theta)_s] \tan \phi_m'$

where $c_j' = 2$kPa , $\phi_j' = 30°$ are shear strength parameters of relict joint (assumed)
$c_s' = 0$kPa , $\phi_s' = 19.1°$ are shear strength parameters of slickensided relict joint (see Figure 20)
$c_m' = 6.5$kPa , $\phi_m' = 33.1°$ are shear strength parameters of intact CDT (see Figure 19)

(i) For slope stability analyses:

$c' = 0.051 \times 2 + 0.013 \times 0 + (1 - 0.051 - 0.013) \times 6.5 = 6.2$ kPa

$\phi' = \tan^{-1} [0.051 \tan 30° + 0.013 \tan 19.1° + (1 - 0.051 - 0.013) \times \tan 33.1°] = 32.6°$

(ii) For estimate of soil nail forces:

$c' = 0.026 \times 2 + 0.044 \times 0 + (1 - 0.026 - 0.044) \times 6.5 = 6.1$ kPa

$\phi' = \tan^{-1} [0.026 \tan 30° + 0.044 \tan 19.1° + (1 - 0.026 - 0.044) \times \tan 33.1°] = 32.5°$

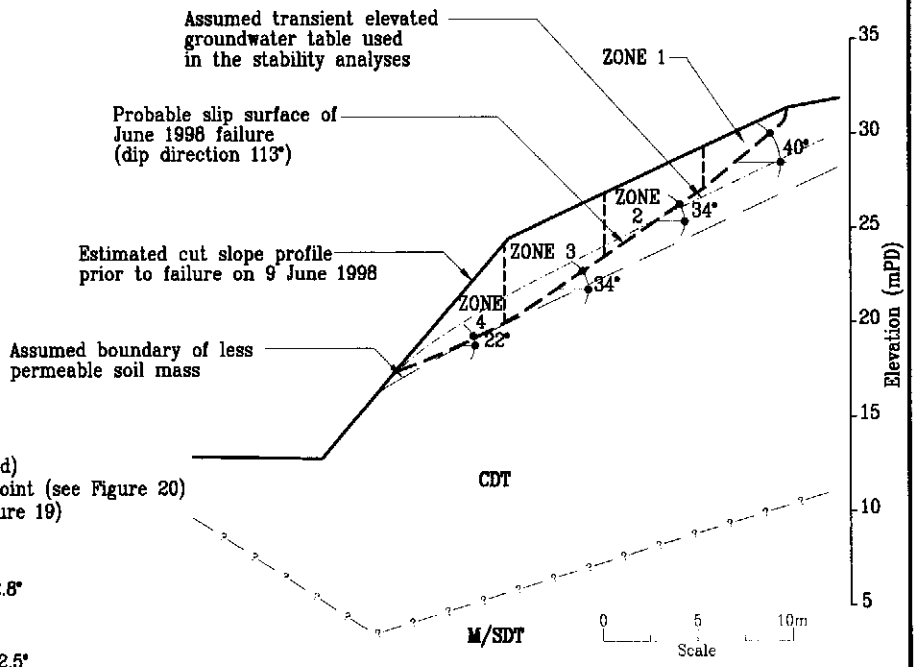


Figure 31 - Representative Cross-section and Soil Mass Strength of the Northern Landslide for Slope Stability Analysis

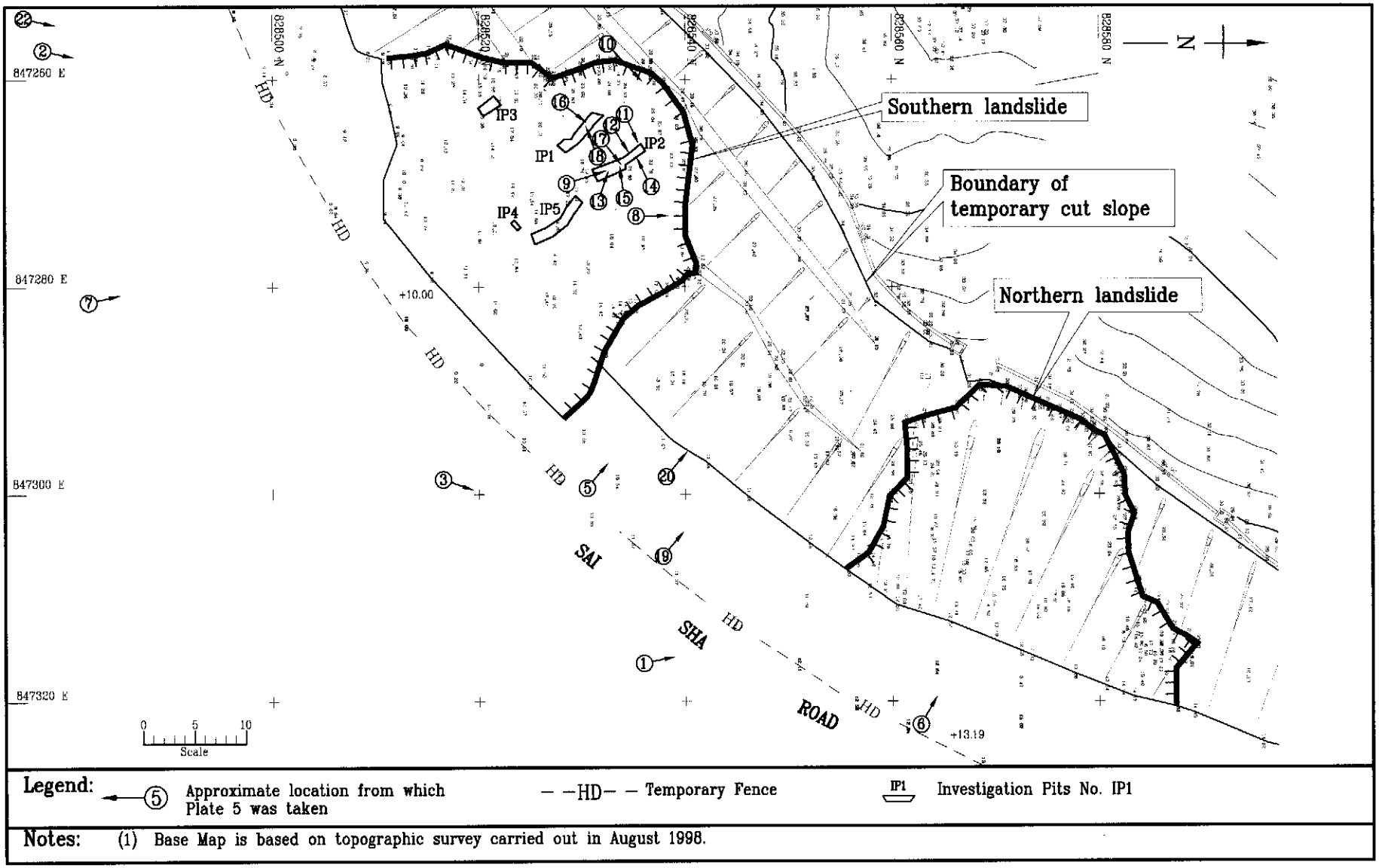


Figure 32 - Location Plan of Photographs Taken

LIST OF PLATES

Plate 1 – General View of the Northern Landslide
(Photograph taken on 22 June 1998 and Reproduced from GEO Site Record. See Figure 32 for Location.)

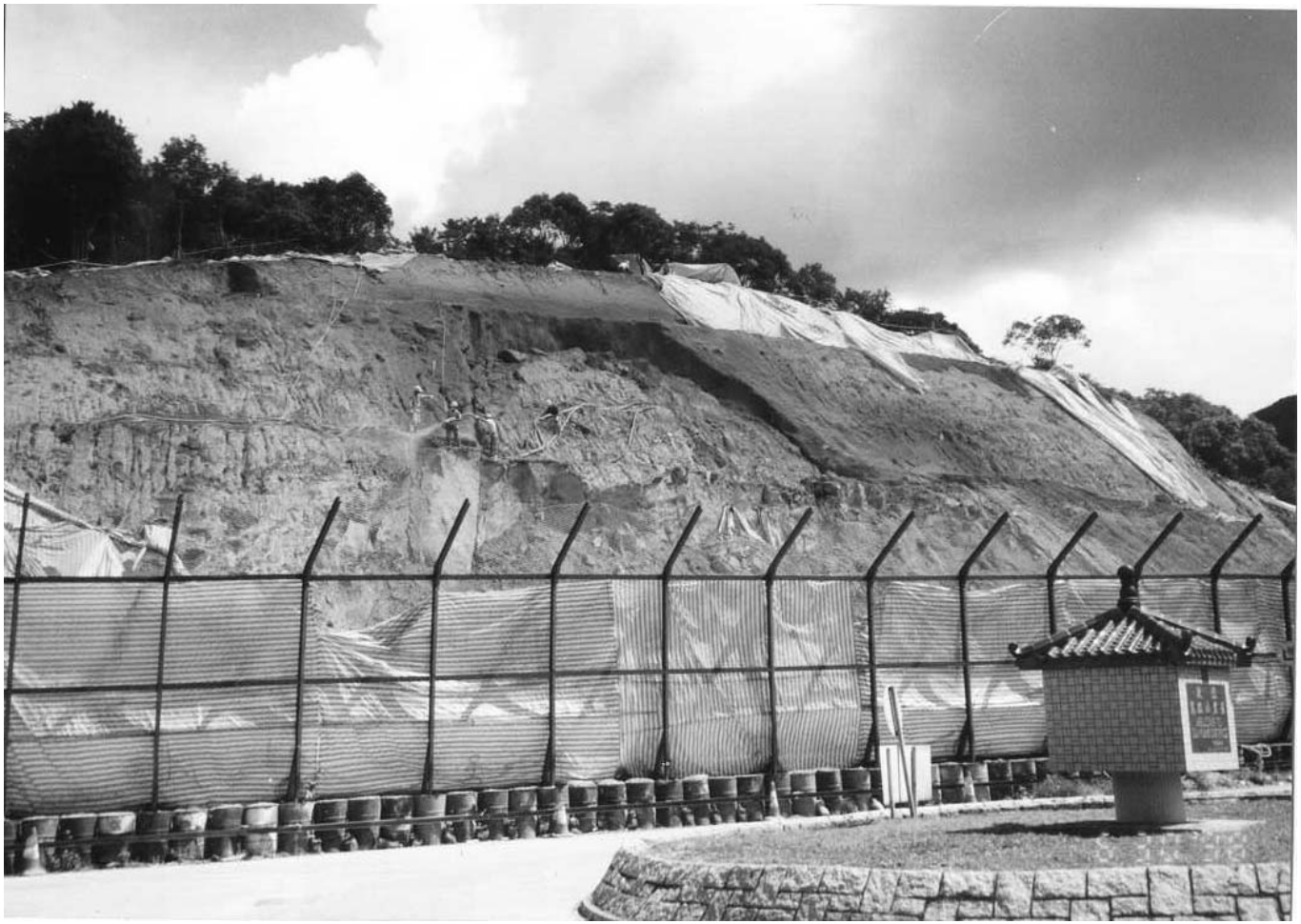

Plate 2 – General View of the Southern Landslide
(Photograph taken on 30 June 1998 and Reproduced
from GEO Site Record. See Figure 32 for Location.)

Plate 3 – General View of the 1995 Landslide in the Northern Portion of the Slope
(Photograph taken on 14 August 1995. See Figure 32 for Location.)

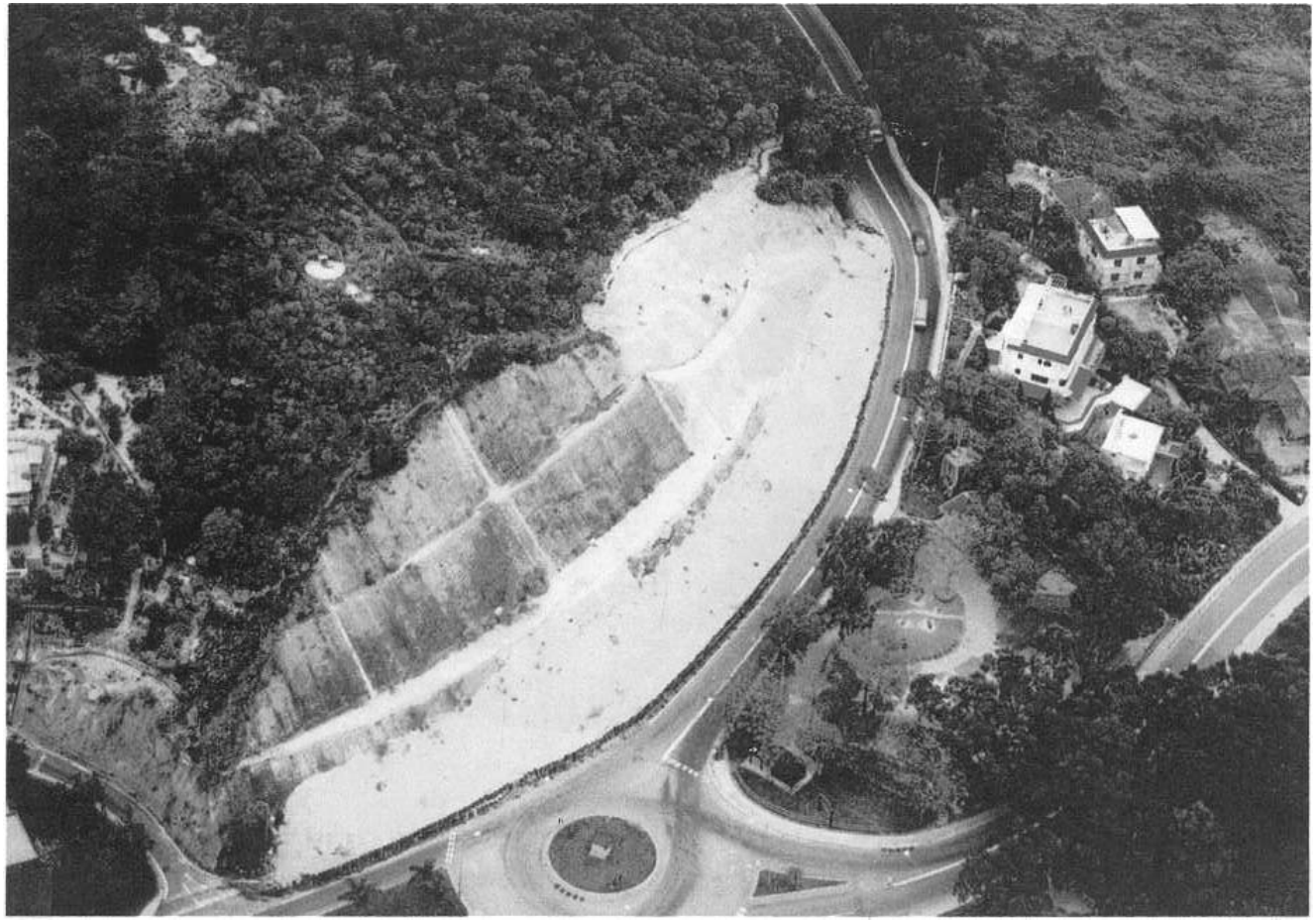

Plate 4 – Aerial View of the Slope after Completion of Emergency Repair Works Subsequent to the 1995 Failure

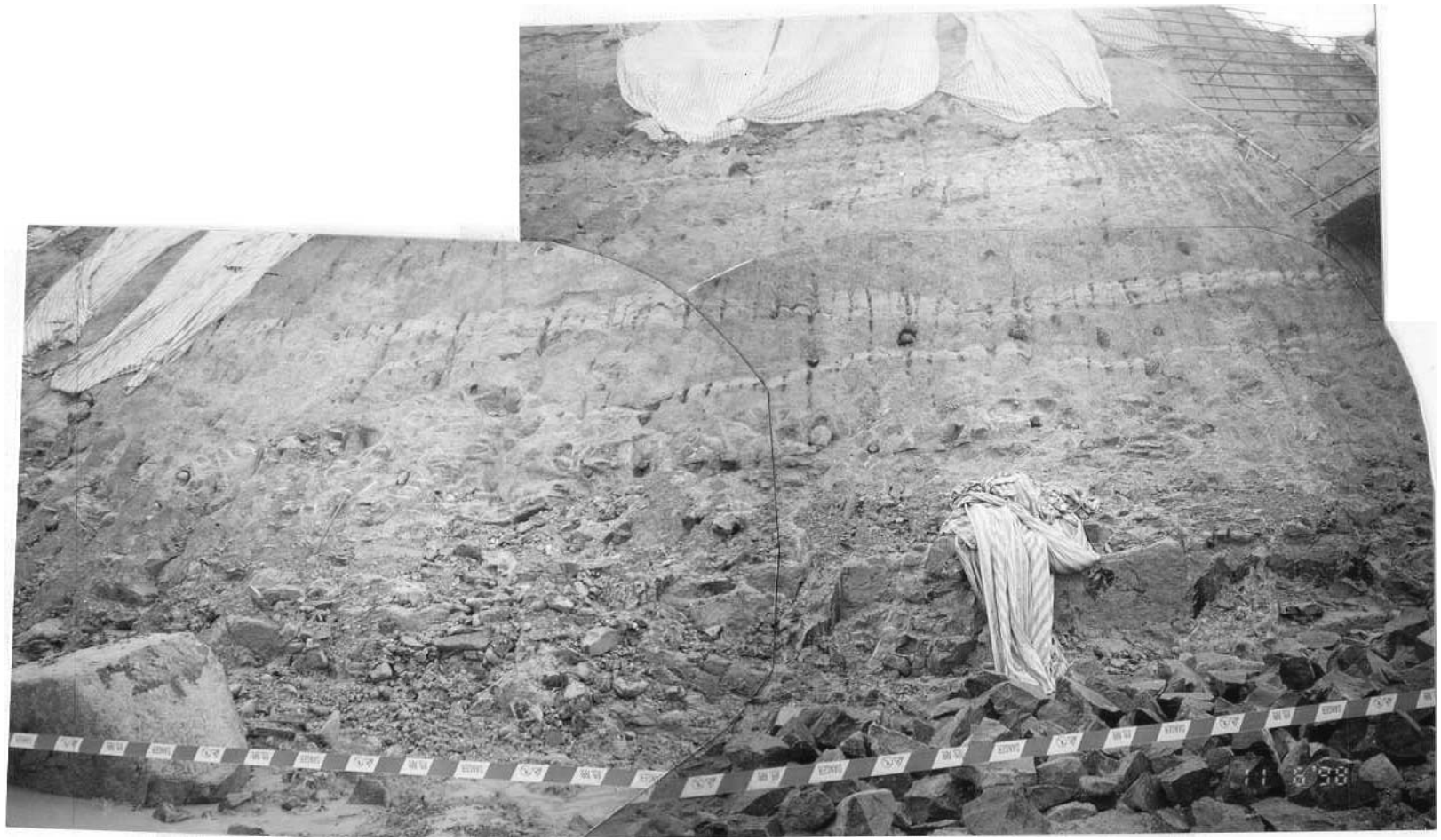

Plate 5 – View of Temporary Cut Slope Surface with Temporary Soil Nails without Nail Head
(Photograph taken on 11 June 1998 and Reproduced from GEO Site Record. See Figure 32 for Location.)

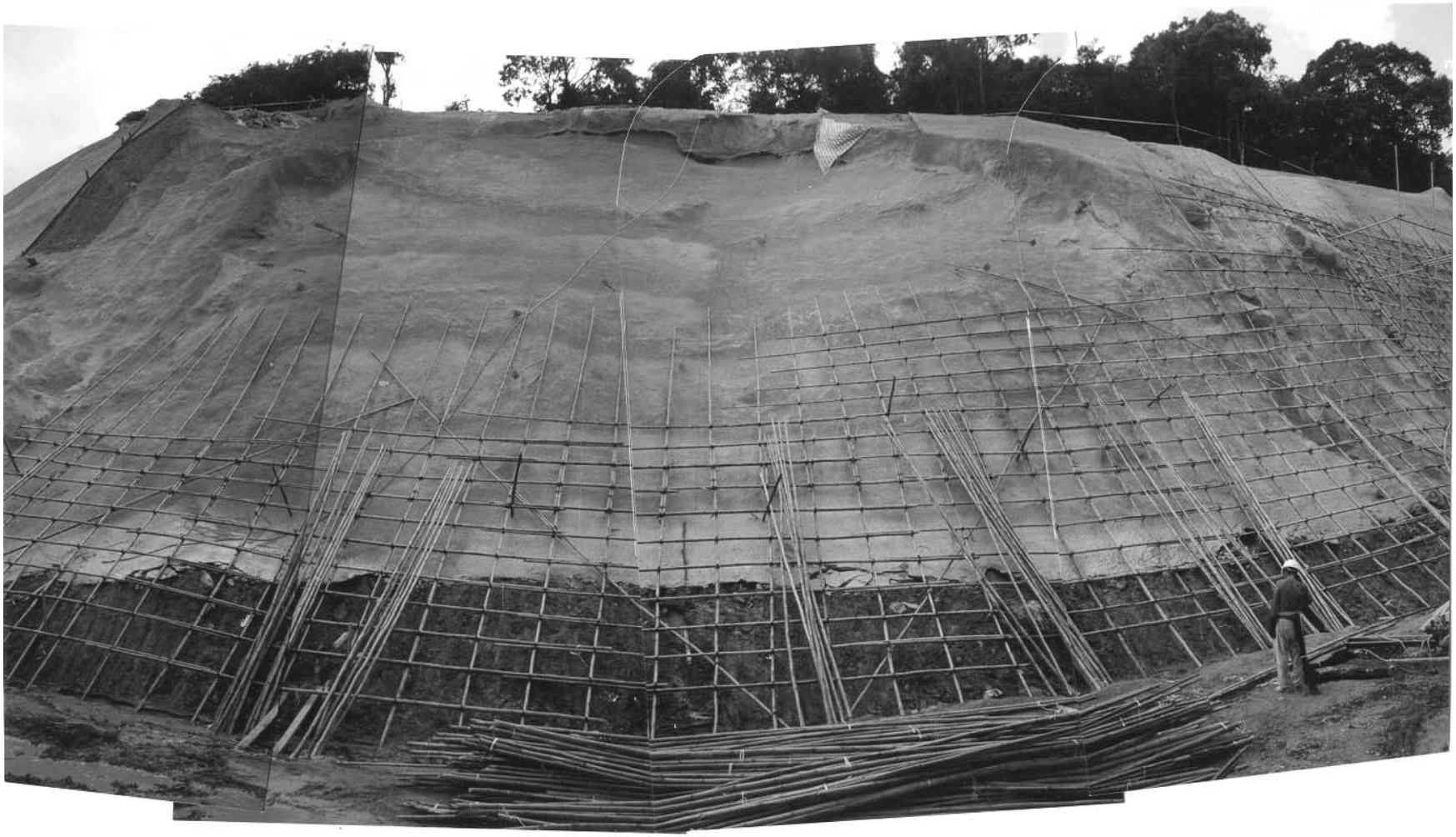

Plate 6 – General View of the Northern Landslide after Removal of Debris and Shotcreting
(Photograph taken on 13 August 1998. See Figure 32 for Location.)

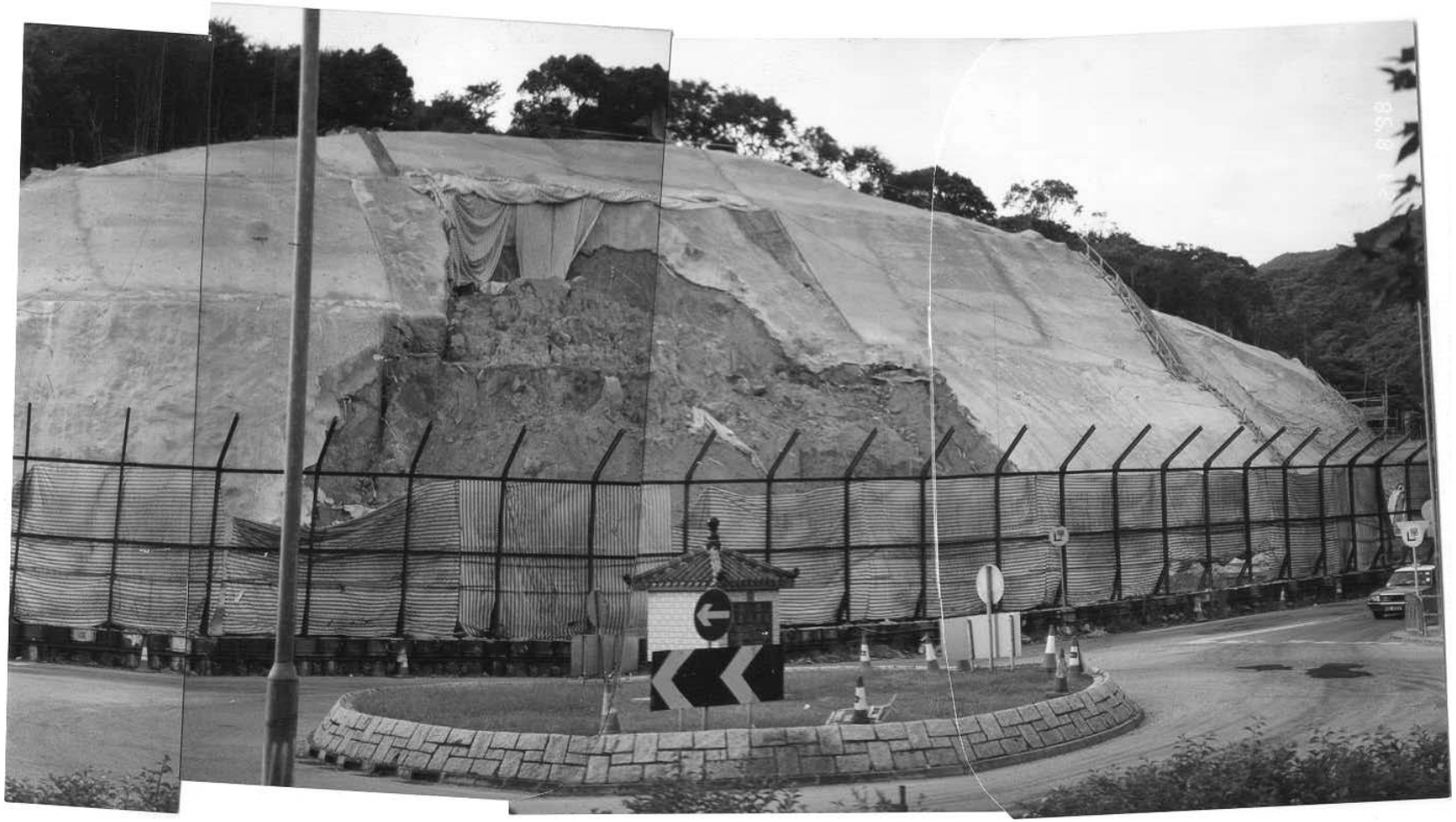

Plate 7 – General View of the Southern Landslide after Shotcreting the Adjacent Areas
(Photograph taken on 27 August 1998. See Figure 32 for Location.)

Plate 8 – Sub-vertical, Slickensided, Manganese Infilled Relict Joints
Forming Part of the Release Plane of the Southern Landslide
(Photograph taken on 12 August 1998. See Figure 32 for Location.)


Plate 9 – Opened Relict Joint (Dipping into the Slope) within the Slipped Mass of Southern Landslide (Photograph taken on 9 February 1999. See Figure 32 for Location.)

Plate 10 – Close-up View of Deformed Soil Nails Protruding from the Main Scarp of Southern Landslide
(Photograph taken on 13 August 1998. See Figure 32 for Location.)

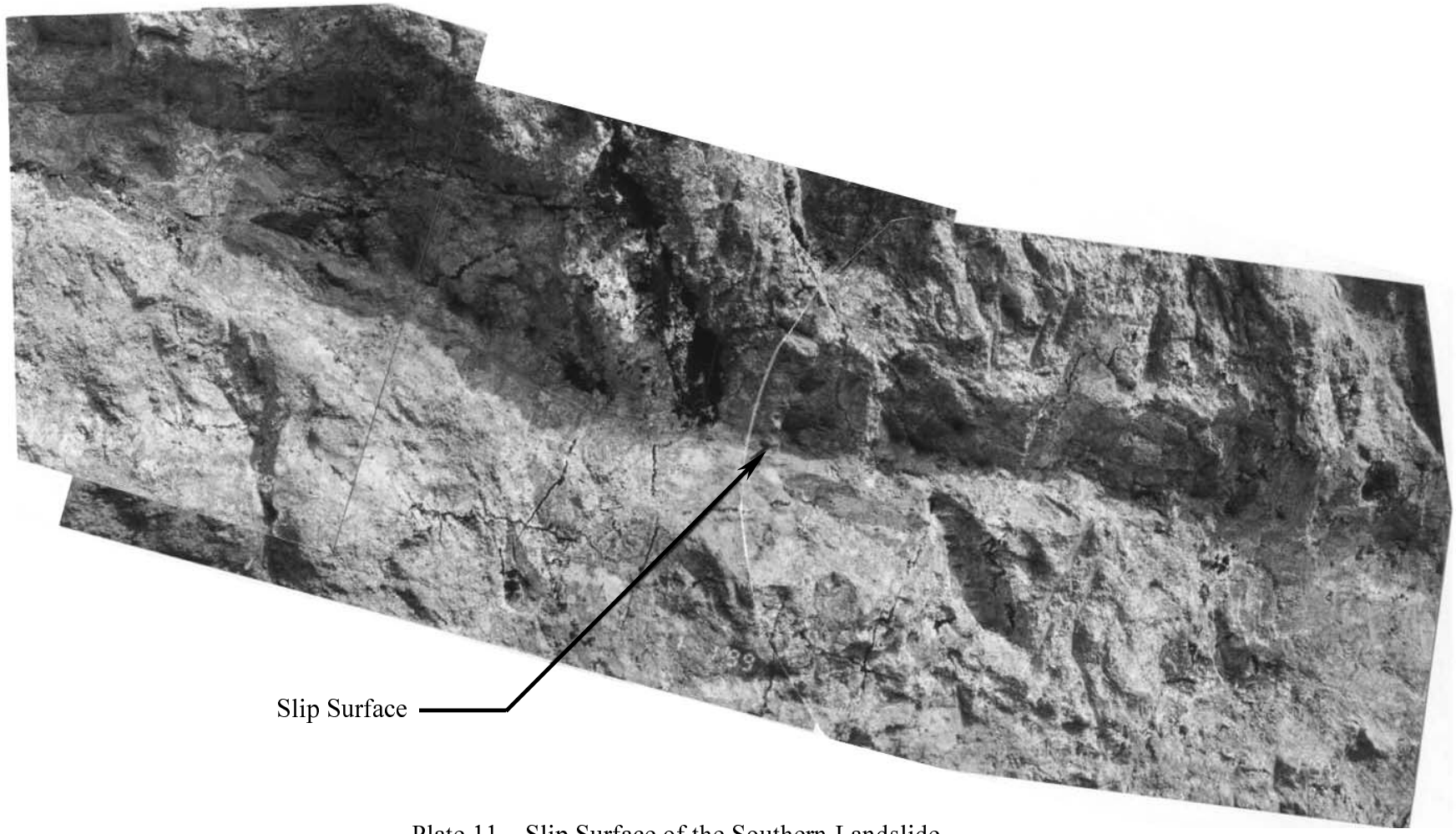


Plate 11 – Slip Surface of the Southern Landslide
(Photograph taken on 31 January 1999.
See Figure 32 for Location.)

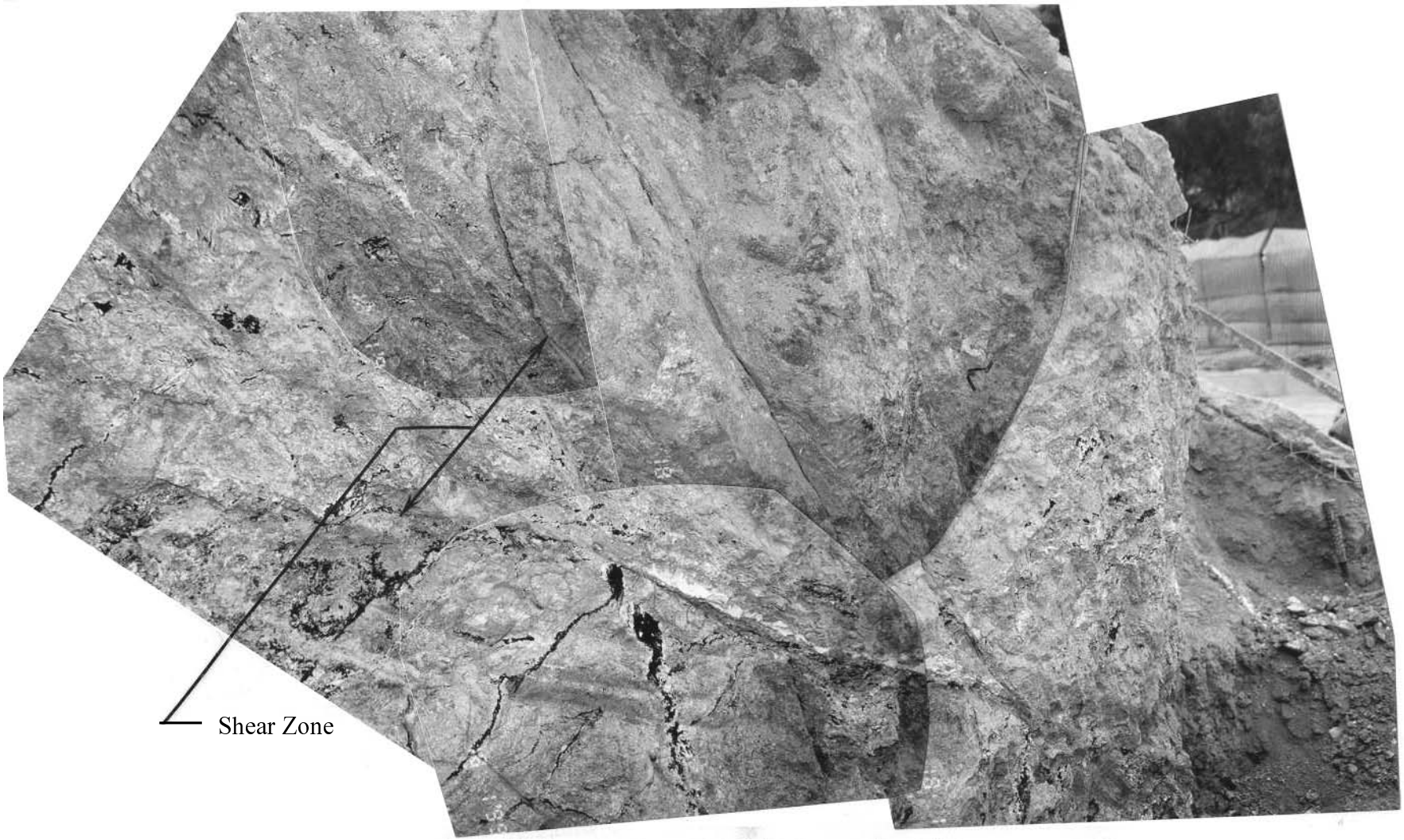


Plate 12 – Slip Surface of the Southern Landslide in the Form of Shear Zone
(Photograph taken on 18 January 1999. See Figure 32 for Location.)

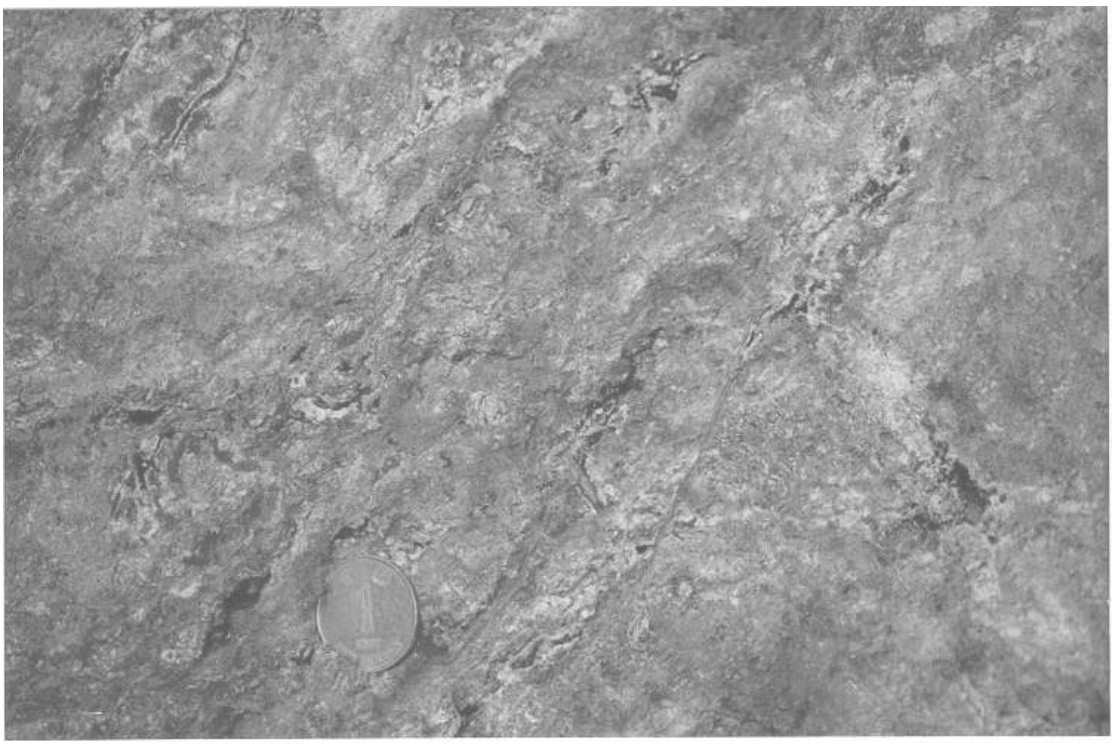

Plate 13 – Close-up View of Sigmodial S-C Fabrics within Shear Zone above the Slip Surface of Southern Landslide (Photograph taken on 9 February 1999. See Figure 32 for Location.)

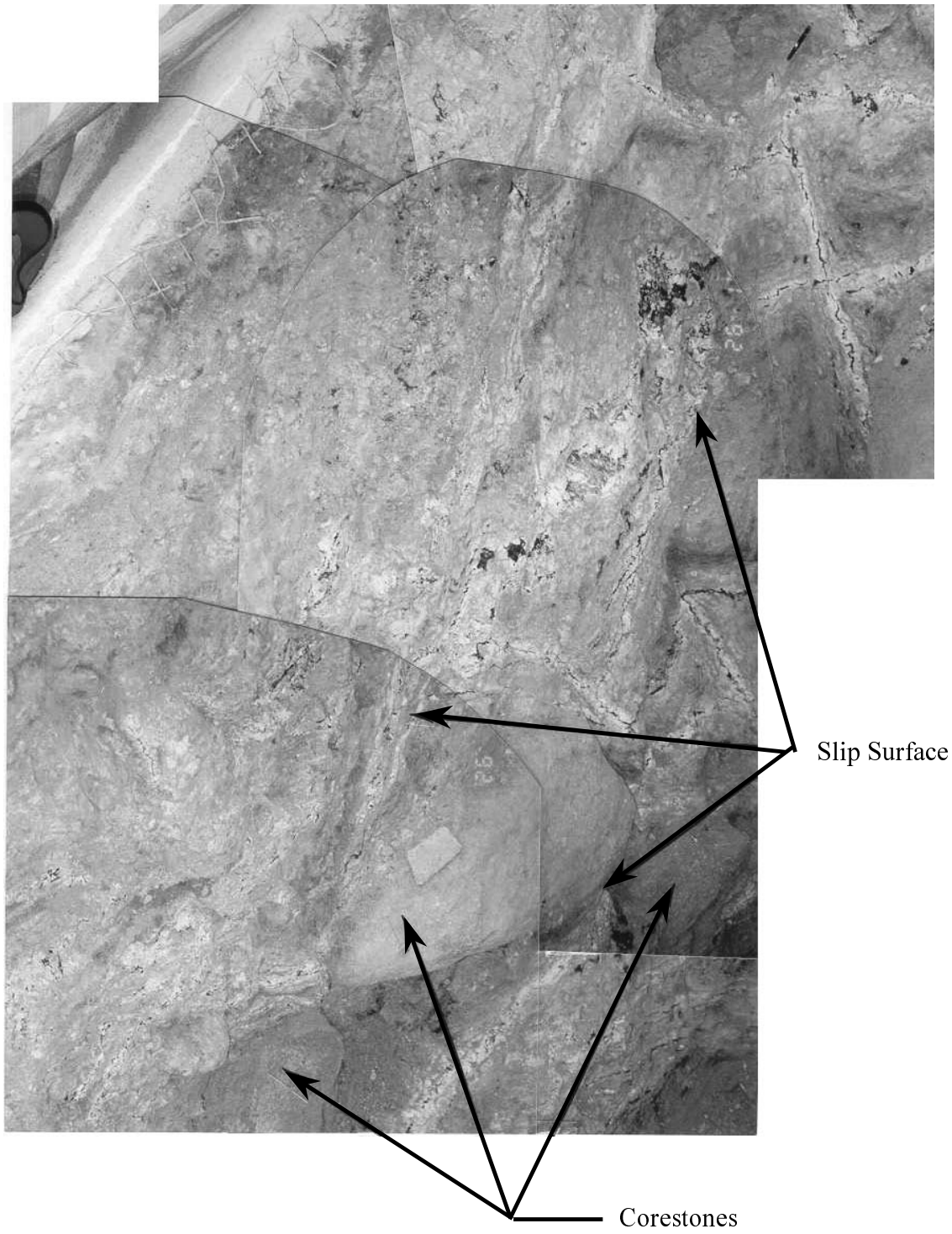


Plate 14 – Slip Surface of the Southern Landslide Deflected around Corestones
(Photograph taken on 31 January 1999. See Figure 32 for Location.)

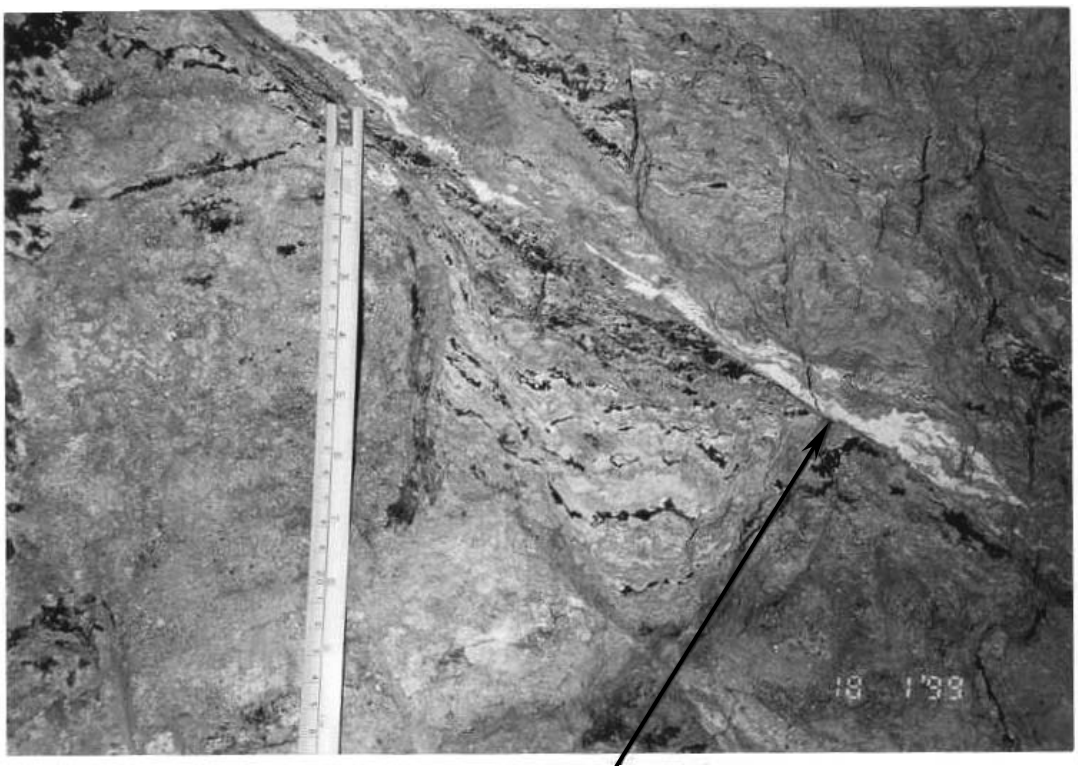


Plate 15 – Slip Surface of the Southern Landslide along Kaolin Infilled and Manganese Oxide Stained Relict Joint. (Photograph taken on 18 January 1999. See Figure 32 for Location.)

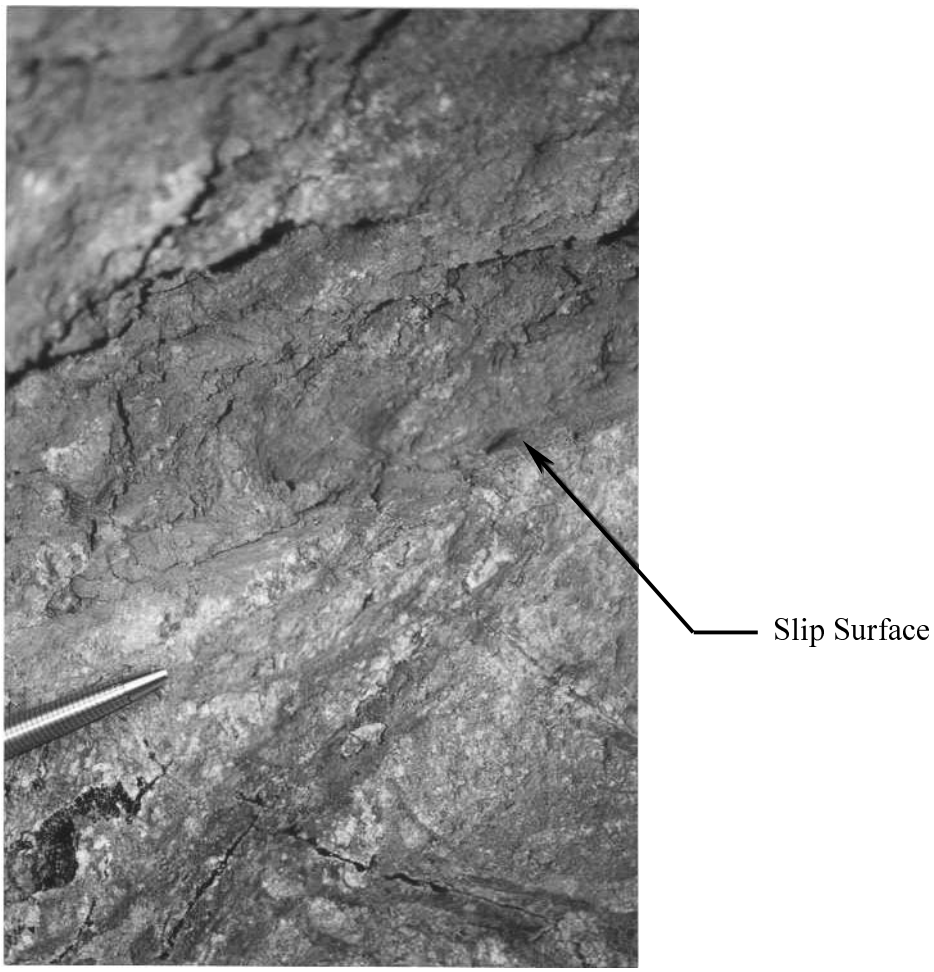


Plate 16 – Close-up View of the Southern Landslide Slip Surface with Destroyed Fabric above and Intact Fabric below the Slip Surface (Photograph taken on 9 February 1999. See Figure 32 for Location.)

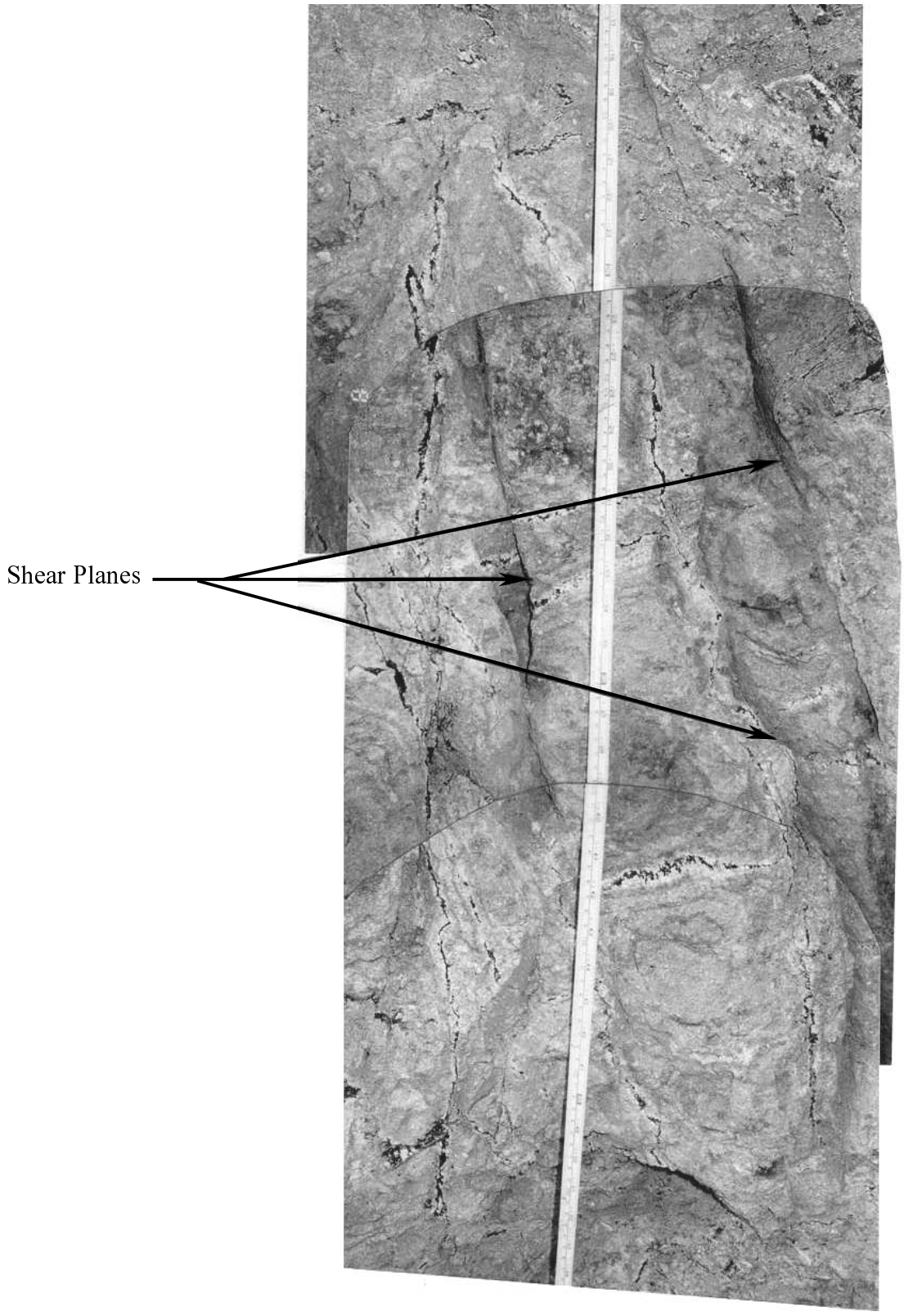


Plate 17 – Localised Sub-vertical Shear Planes within the Slipped Mass of Southern Landslide (Photograph taken on 8 January 1999. See Figure 32 for Location.)

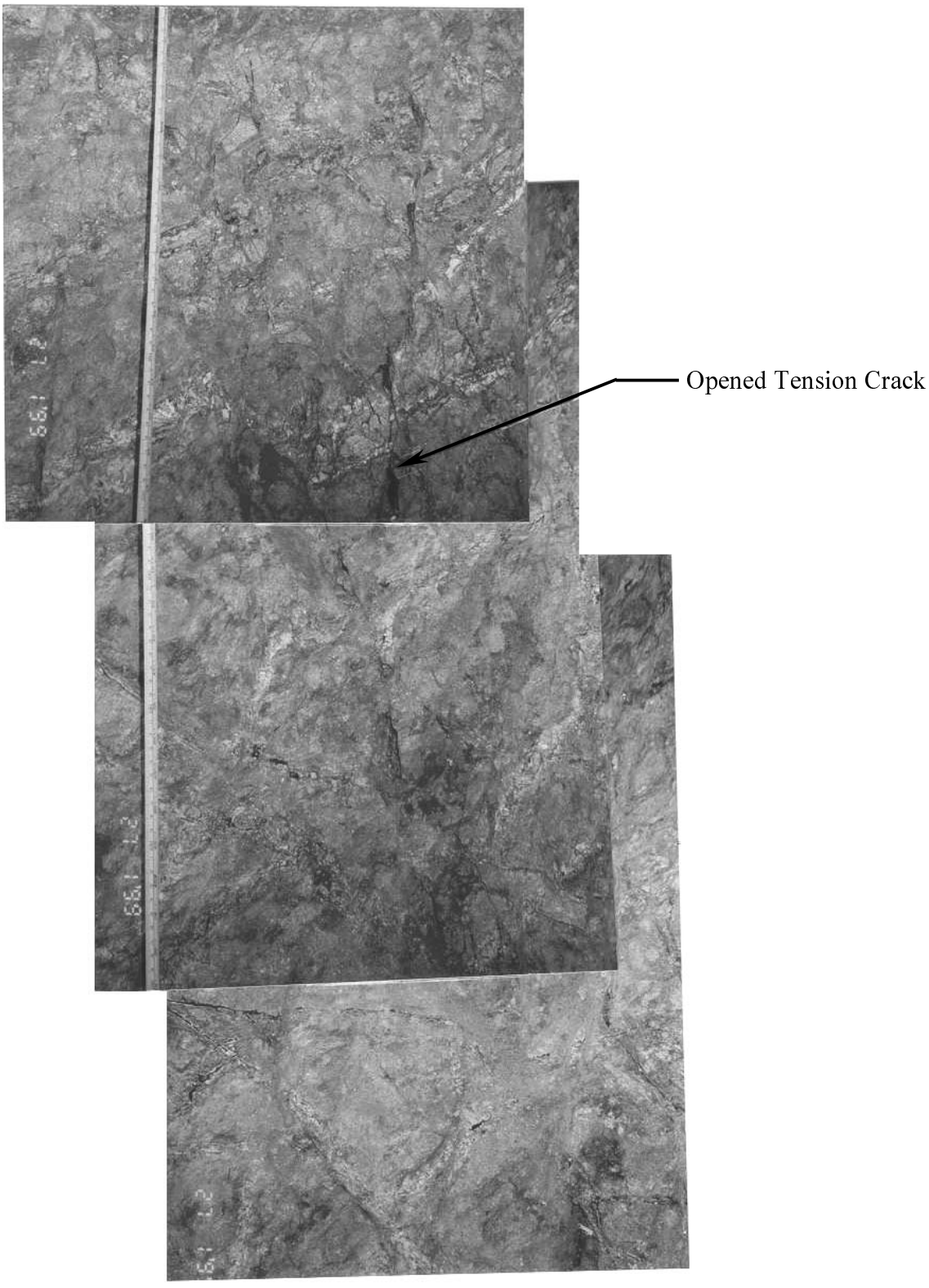


Plate 18 – Opened Tension Cracks within the Slipped Mass of Southern Landslide (Photograph taken on 27 January 1999 See Figure 32 for Location.)

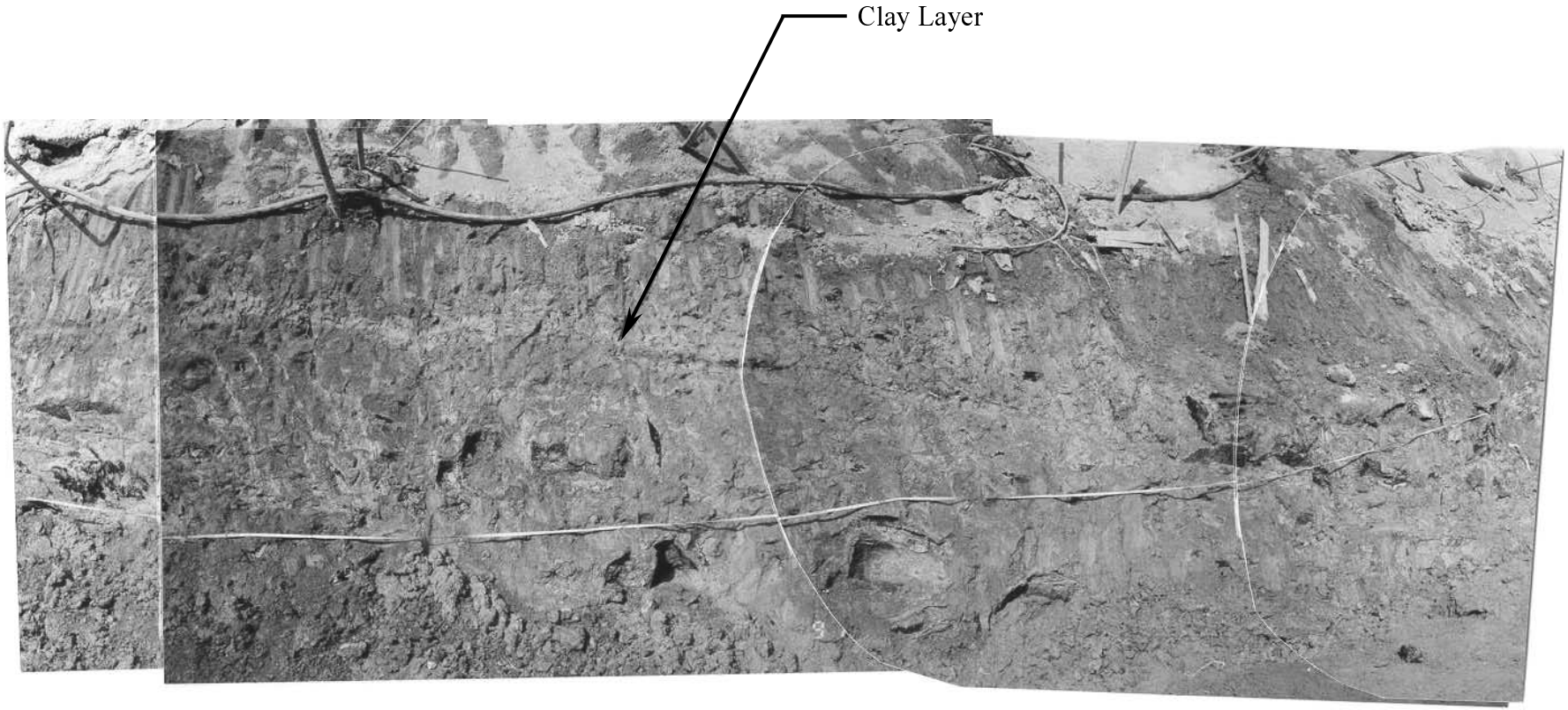


Plate 19 – Clay Layer along the Toe of Temporary Cut Slope
(Photograph taken on 9 December 1998. See Figure 32 for Location.)


Plate 20 – Close-up View of the Clay Layer
(Photograph taken on 9 December 1998.
See Figure 32 for Location.)

Plate 21 – Close-up View of Fractured Soil Nail Bar

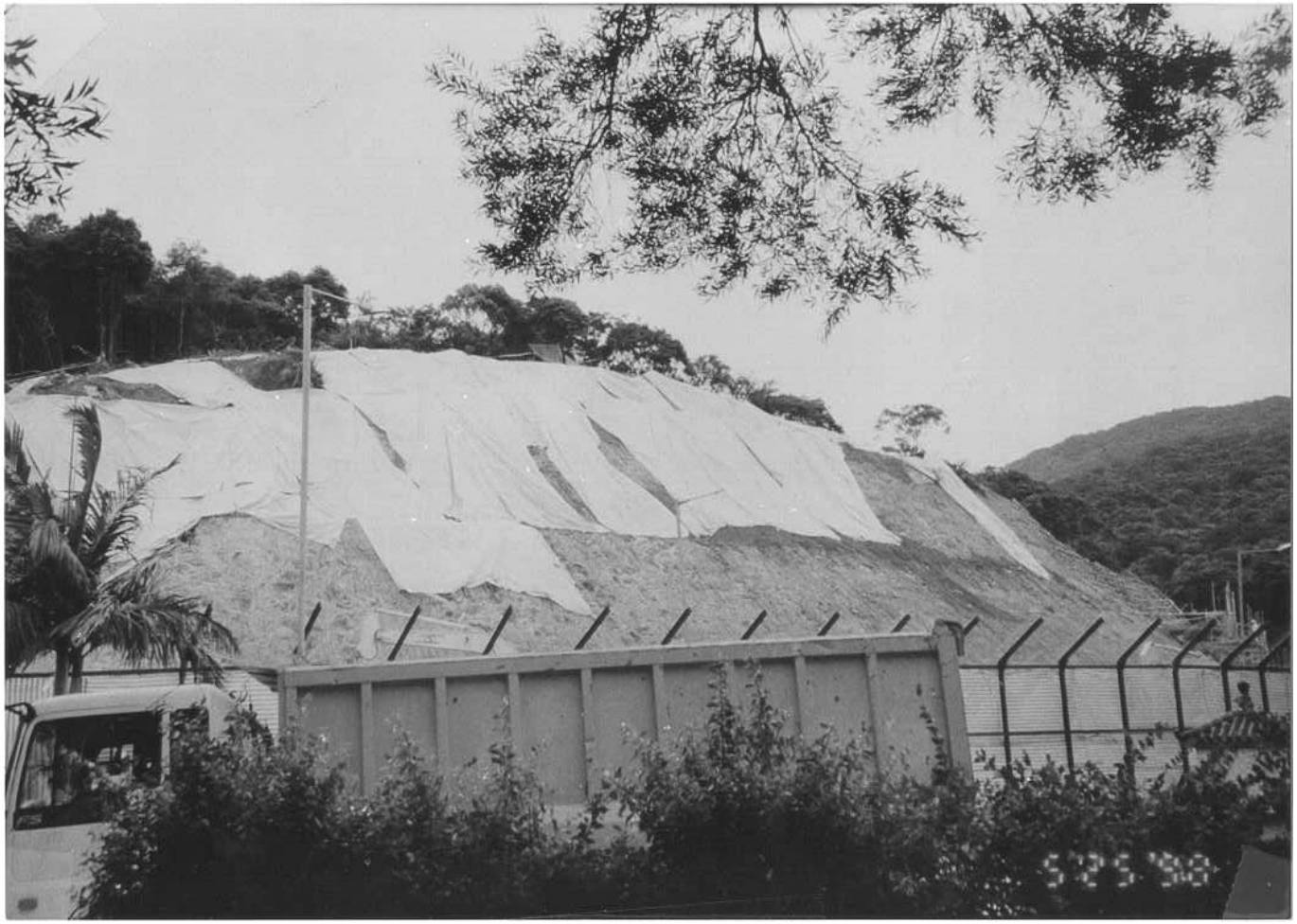

Plate 22 – General View of the Temporary Cut Slope after Removal of Chunam Surface Protection
(Photograph taken on 25 May 1998 and Reproduced from GEO Site Record. See Figure 32 for Location.)

# APPENDIX A

## SUMMARY OF OBSERVATIONS FROM AERIAL PHOTOGRAPH INTEPRETATION

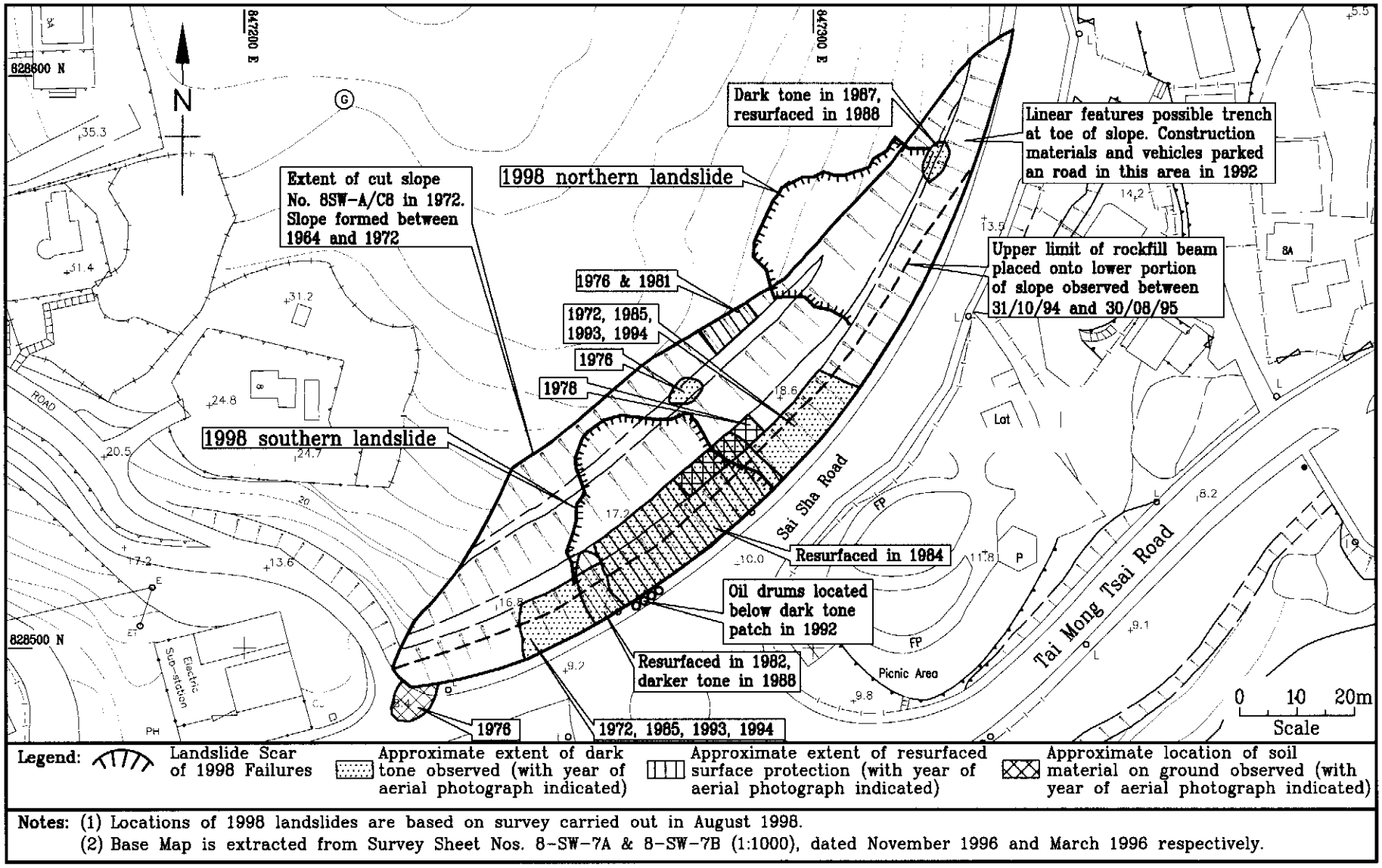


**Notes:** (1) Locations of 1998 landslides are based on survey carried out in August 1998.
(2) Base Map is extracted from Survey Sheet Nos. 8-SW-7A & 8-SW-7B (1:1000), dated November 1996 and March 1996 respectively.

Appendix A - Summary of Observations from Aerial Photograph Interpretation